Robotics: Advanced Concepts & Analysis

Module 8 - Modeling and Control of Flexible Robots

Ashitava Ghosal[1]

[1]Department of Mechanical Engineering
&
Centre for Product Design and Manufacture
Indian Institute of Science
Bangalore 560 012, India
Email: asitava@mecheng.iisc.ernet.in

NPTEL, 2010

Outline

- Introduction to flexible manipulators and mechanisms.
- Characteristic of a rigid link.
- Characteristic's of a flexible joint.
- Characteristic of a flexible link.
  - Euler-Bernoulli model of a beam.
  - Modeling a rotating flexible link.
  - Modeling a translating flexible link.
- Summary

- Introduction to flexible manipulators and mechanisms.
- Characteristic of a rigid link.
- Characteristic's of a flexible joint.
- Characteristic of a flexible link.
  - Euler-Bernoulli model of a beam.
  - Modeling a rotating flexible link.
  - Modeling a translating flexible link.
- Summary

- Introduction to flexible manipulators and mechanisms.
- Characteristic of a rigid link.
- Characteristic's of a flexible joint.
- Characteristic of a flexible link.
  - Euler-Bernoulli model of a beam.
  - Modeling a rotating flexible link.
  - Modeling a translating flexible link.
- Summary

- Introduction to flexible manipulators and mechanisms.
- Characteristic of a rigid link.
- Characteristic's of a flexible joint.
- Characteristic of a flexible link.
    - Euler-Bernoulli model of a beam.
    - Modeling a rotating flexible link.
    - Modeling a translating flexible link.
- Summary

Introduction
Overview

- Introduction to flexible manipulators and mechanisms.
- Characteristic of a rigid link.
- Characteristic's of a flexible joint.
- Characteristic of a flexible link.
  - Euler-Bernoulli model of a beam.
  - Modeling a rotating flexible link.
  - Modeling a translating flexible link.
- Summary

INTRODUCTION

- Industrial robots: Required high accuracy and repeatability $\rightarrow$ Heavy, high stiffness and slow.

Figure 1: PUMA 700 Series Industrial Robot

- PUMA 700 series industrial robot (PUMA 761) – *Arm weight* 580 Kg, *Static payload* 10 kg[a].
- Repeatability $\pm$ 0.2 mm.
- Maximum straight line speed 1.0 $\mathrm{m/sec}$.

[a] Documentation on PUMA 700 series robots available here

INTRODUCTION (CONTD.)

- Robots in aero-space applications → Light-weight and flexible.

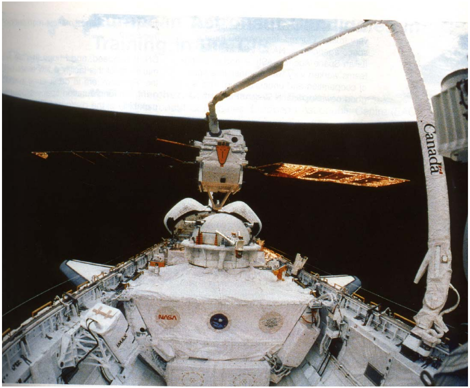

Figure 2: Space Shuttle manipulator system

Figure 3: Solar panels being deployed

- Extreme flexibility in space-shuttle manipulator system → Can be operated safely only in a gravity free environment!!
- Solar panels – light weight and very large!!

Introduction (Contd.)

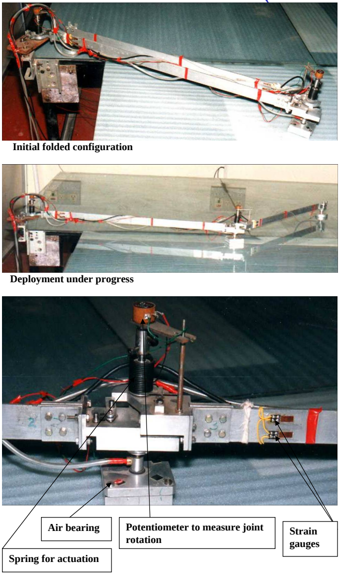

Figure 4: Experimental set-up for solar panel deployment studies

- Two flexible Aluminum beams, initially folded, and floating on air bearings.
- Actuated by two springs at the joints and locking mechanism at joints.
- Final configuration – single cantilever beam.
- See details in Nagaraj et al.(1997) & Nagaraj et al. (2003).

Introduction (Contd.)

Solar panel deployment studies

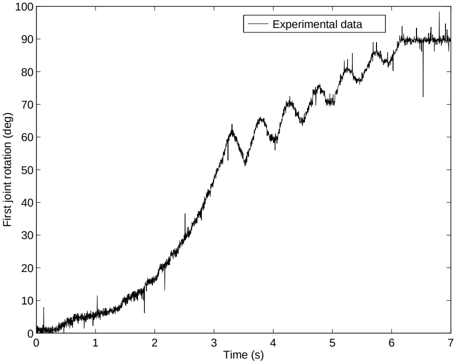

Figure 5: Rotation at joint 1

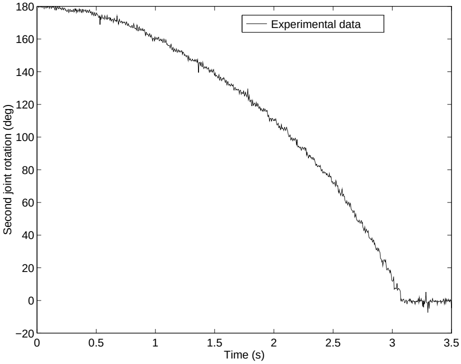

Figure 6: Rotation at joint 2

- Joint 2 lock a little after 3 seconds.
- After joint 2 locks, motion of joint 1 is vibratory → Tip motion is also vibratory!

Introduction (Contd.)

- Light-weight, high speed robots *can no longer* be modeled as ‘rigid’.
- During motion of flexible robots, vibrations are induced in links.
- During locking at joints (in deployable mechanisms) vibrations are set up.
- Control: trajectory following & vibrations must also be *suppressed* in flexible manipulators for tasks such as pick-n-place.
- Accurate modeling of flexibility in links and joints is useful and important to
  - Design ‘model based’ control schemes to damp out vibrations.
  - Reduce expensive experimentations.
  - For *trimmer* designs!

Introduction (Contd.)

- Light-weight, high speed robots *can no longer* be modeled as 'rigid'.
- During motion of flexible robots, vibrations are induced in links.
- During locking at joints (in deployable mechanisms) vibrations are set up.
- Control: trajectory following & vibrations must also be *suppressed* in flexible manipulators for tasks such as pick-n-place.
- Accurate modeling of flexibility in links and joints is useful and important to
  - Design 'model based' control schemes to damp out vibrations.
  - Reduce expensive experimentations.
  - For *trimmer* designs!

Introduction (Contd.)

- Light-weight, high speed robots *can no longer* be modeled as 'rigid'.
- During motion of flexible robots, vibrations are induced in links.
- During locking at joints (in deployable mechanisms) vibrations are set up.
- Control: trajectory following & vibrations must also be *suppressed* in flexible manipulators for tasks such as pick-n-place.
- Accurate modeling of flexibility in links and joints is useful and important to
  - Design 'model based' control schemes to damp out vibrations.
  - Reduce expensive experimentations.
  - For *trimmer* designs!

Introduction (Contd.)

- Light-weight, high speed robots *can no longer* be modeled as ‘rigid’.
- During motion of flexible robots, vibrations are induced in links.
- During locking at joints (in deployable mechanisms) vibrations are set up.
- Control: trajectory following & vibrations must also be *suppressed* in flexible manipulators for tasks such as pick-n-place.
- Accurate modeling of flexibility in links and joints is useful and important to
  - Design ‘model based’ control schemes to damp out vibrations.
  - Reduce expensive experimentations.
  - For *trimmer* designs!

- Light-weight, high speed robots *can no longer* be modeled as ‘rigid’.
- During motion of flexible robots, vibrations are induced in links.
- During locking at joints (in deployable mechanisms) vibrations are set up.
- Control: trajectory following & vibrations must also be *suppressed* in flexible manipulators for tasks such as pick-n-place.
- Accurate modeling of flexibility in links and joints is useful and important to
  - Design ‘model based’ control schemes to damp out vibrations.
  - Reduce expensive experimentations.
  - For *trimmer* designs!

CHARACTERISTIC OF A RIGID LINK

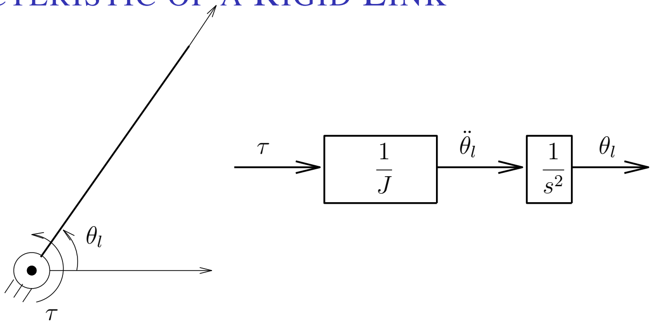

Figure 7: A rigid link with its block diagram representation

- Simple dynamics $\rightarrow$ equation of motion, without friction, is

$$J\ddot{\theta}_l = \tau$$

- One-to-one relationship between τ and θ_l

Characteristic of a Flexible Joint

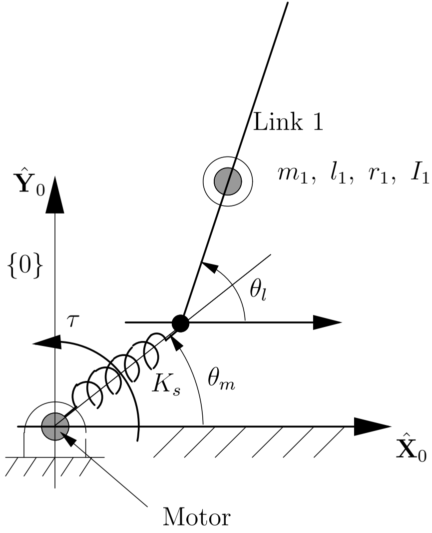

Figure 8: A link of a robot with a flexible joint

- Flexible joint modeled as *torsional spring* with a spring constant K_s.
- Motion in a plane – no out of plane motion!
- Rotation at motor θ_m.
- Rotation of link θ_l.
- Motor torque τ.

- Equation of motion – Two linear coupled ODE's

$$J_m\ddot{\theta}_m + K_s(\theta_m - \theta_l) = \tau, \quad J_l\ddot{\theta}_l + K_s(\theta_l - \theta_m) = 0$$

$J_l = I_1 + m_1 r_1^2$ is the load inertia.

- τ controls two outputs – θ_m and θ_l.
- More complicated than rigid-link case.

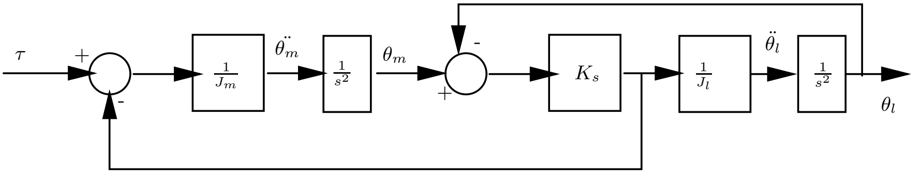

Figure 9: A block diagram of the flexible-joint link

Characteristic of a Flexible Joint (Contd.)

- Test for controllability of θ_m and θ_l by τ
- For state variables $\mathbf{X} = (\theta_m, \theta_l, \dot{\theta}_m, \dot{\theta}_l)^T$, $[F]$ and $[G]$ matrices in $\dot{\mathbf{X}} = [F]\mathbf{X} + [G]u$ are

$$[F] = \begin{pmatrix} 0 & 0 & 1 & 0 \\ 0 & 0 & 0 & 1 \\ -K_s/J_m & K_s/J_m & 0 & 0 \\ K_s/J_l & -K_s/J_l & 0 & 0 \end{pmatrix}, \quad [G] = \begin{pmatrix} 0 \\ 0 \\ \frac{1}{J_m} \\ 0 \end{pmatrix}$$

- Obtain controllability matrix $[Q_c] = [[G] \mid [F][G] \mid [F]^2[G] \mid [F]^3[G]]$
- $\det[Q_c] = -K_s^2/(J_m^4 J_l^2) \neq 0 \rightarrow$ Controllable with τ.
- In presence of gravity, equations of motion are *nonlinear*!

$$J_m\ddot{\theta}_m + K_s(\theta_m - \theta_l) = \tau, \quad J_l\ddot{\theta}_l + K_s(\theta_l - \theta_m) + m_1 g r_1 \sin\theta_l = 0$$

- Model-based controller derived using Lie algebra (Marino and Spong(1986)) for this non-linear system.

Characteristic of a Flexible Joint (Contd.)

- Test for controllability of θ_m and θ_l by τ
- For state variables $\mathbf{X} = (\theta_m, \theta_l, \dot{\theta}_m, \dot{\theta}_l)^T$, $[F]$ and $[G]$ matrices in $\dot{\mathbf{X}} = [F]\mathbf{X} + [G]u$ are

$$[F] = \begin{pmatrix} 0 & 0 & 1 & 0 \\ 0 & 0 & 0 & 1 \\ -K_s/J_m & K_s/J_m & 0 & 0 \\ K_s/J_l & -K_s/J_l & 0 & 0 \end{pmatrix}, \quad [G] = \begin{pmatrix} 0 \\ 0 \\ \frac{1}{J_m} \\ 0 \end{pmatrix}$$

- Obtain controllability matrix $[Q_c] = [[G] \mid [F][G] \mid [F]^2[G] \mid [F]^3[G]]$
- $\det[Q_c] = -K_s^2/(J_m^4 J_l^2) \neq 0 \rightarrow$ Controllable with τ.
- In presence of gravity, equations of motion are *nonlinear*!

$$J_m\ddot{\theta}_m + K_s(\theta_m - \theta_l) = \tau, \quad J_l\ddot{\theta}_l + K_s(\theta_l - \theta_m) + m_1 g r_1 \sin\theta_l = 0$$

- Model-based controller derived using Lie algebra (Marino and Spong(1986)) for this non-linear system.

CHARACTERISTIC OF A FLEXIBLE JOINT (CONTD.)

- Test for controllability of θ_m and θ_l by τ
- For state variables $\mathbf{X} = (\theta_m, \theta_l, \dot{\theta}_m, \dot{\theta}_l)^T$, $[F]$ and $[G]$ matrices in $\dot{\mathbf{X}} = [F]\mathbf{X} + [G]u$ are

$$[F] = \begin{pmatrix} 0 & 0 & 1 & 0 \\ 0 & 0 & 0 & 1 \\ -K_s/J_m & K_s/J_m & 0 & 0 \\ K_s/J_l & -K_s/J_l & 0 & 0 \end{pmatrix}, \quad [G] = \begin{pmatrix} 0 \\ 0 \\ \frac{1}{J_m} \\ 0 \end{pmatrix}$$

- Obtain controllability matrix $[Q_c] = [[G] \mid [F][G] \mid [F]^2[G] \mid [F]^3[G]]$
- $\det[Q_c] = -K_s^2/(J_m^4 J_l^2) \neq 0 \rightarrow$ Controllable with τ.
- In presence of gravity, equations of motion are *nonlinear*!

$$J_m\ddot{\theta}_m + K_s(\theta_m - \theta_l) = \tau, \quad J_l\ddot{\theta}_l + K_s(\theta_l - \theta_m) + m_1 g r_1 \sin\theta_l = 0$$

- Model-based controller derived using Lie algebra (Marino and Spong(1986)) for this non-linear system.

Characteristic of a Flexible Joint (Contd.)

- Test for controllability of θ_m and θ_l by τ
- For state variables $\mathbf{X} = (\theta_m, \theta_l, \dot{\theta}_m, \dot{\theta}_l)^T$, $[F]$ and $[G]$ matrices in $\dot{\mathbf{X}} = [F]\mathbf{X} + [G]u$ are

$$[F] = \begin{pmatrix} 0 & 0 & 1 & 0 \\ 0 & 0 & 0 & 1 \\ -K_s/J_m & K_s/J_m & 0 & 0 \\ K_s/J_l & -K_s/J_l & 0 & 0 \end{pmatrix}, \quad [G] = \begin{pmatrix} 0 \\ 0 \\ \frac{1}{J_m} \\ 0 \end{pmatrix}$$

- Obtain controllability matrix $[Q_c] = [[G] \mid [F][G] \mid [F]^2[G] \mid [F]^3[G]]$
- $\det[Q_c] = -K_s^2/(J_m^4 J_l^2) \neq 0 \rightarrow$ Controllable with τ.
- In presence of gravity, equations of motion are *nonlinear*!

$$J_m\ddot{\theta}_m + K_s(\theta_m - \theta_l) = \tau, \quad J_l\ddot{\theta}_l + K_s(\theta_l - \theta_m) + m_1 g r_1 \sin\theta_l = 0$$

- Model-based controller derived using Lie algebra (Marino and Spong(1986)) for this non-linear system.

Characteristic of a Flexible Joint (Contd.)

- Test for controllability of θ_m and θ_l by τ
- For state variables $\mathbf{X} = (\theta_m, \theta_l, \dot{\theta}_m, \dot{\theta}_l)^T$, $[F]$ and $[G]$ matrices in $\dot{\mathbf{X}} = [F]\mathbf{X} + [G]u$ are

$$[F] = \begin{pmatrix} 0 & 0 & 1 & 0 \\ 0 & 0 & 0 & 1 \\ -K_s/J_m & K_s/J_m & 0 & 0 \\ K_s/J_l & -K_s/J_l & 0 & 0 \end{pmatrix}, \quad [G] = \begin{pmatrix} 0 \\ 0 \\ \frac{1}{J_m} \\ 0 \end{pmatrix}$$

- Obtain controllability matrix $[Q_c] = [[G] \mid [F][G] \mid [F]^2[G] \mid [F]^3[G]]$
- $\det[Q_c] = -K_s^2/(J_m^4 J_l^2) \neq 0 \rightarrow$ Controllable with τ.
- In presence of gravity, equations of motion are *nonlinear*!

$$J_m\ddot{\theta}_m + K_s(\theta_m - \theta_l) = \tau, \quad J_l\ddot{\theta}_l + K_s(\theta_l - \theta_m) + m_1 g r_1 \sin\theta_l = 0$$

- Model-based controller derived using Lie algebra (Marino and Spong(1986)) for this non-linear system.

Characteristic of a Flexible Joint (Contd.)

- Test for controllability of θ_m and θ_l by τ
- For state variables $\mathbf{X} = (\theta_m, \theta_l, \dot{\theta}_m, \dot{\theta}_l)^T$, $[F]$ and $[G]$ matrices in $\dot{\mathbf{X}} = [F]\mathbf{X} + [G]u$ are

$$[F] = \begin{pmatrix} 0 & 0 & 1 & 0 \\ 0 & 0 & 0 & 1 \\ -K_s/J_m & K_s/J_m & 0 & 0 \\ K_s/J_l & -K_s/J_l & 0 & 0 \end{pmatrix}, \quad [G] = \begin{pmatrix} 0 \\ 0 \\ \frac{1}{J_m} \\ 0 \end{pmatrix}$$

- Obtain controllability matrix $[Q_c] = [[G] \mid [F][G] \mid [F]^2[G] \mid [F]^3[G]]$
- $\det[Q_c] = -K_s^2/(J_m^4 J_l^2) \neq 0 \rightarrow$ Controllable with τ.
- In presence of gravity, equations of motion are *nonlinear*!

$$J_m\ddot{\theta}_m + K_s(\theta_m - \theta_l) = \tau, \quad J_l\ddot{\theta}_l + K_s(\theta_l - \theta_m) + m_1 g r_1 \sin\theta_l = 0$$

- Model-based controller derived using Lie algebra (Marino and Spong(1986)) for this non-linear system.

Characteristic of a Flexible Link

- To start with – flexible links undergoing *only* bending vibrations.
- Flexible link modeled as *slender flexible beam*.
- Main assumptions:
  - Small deformations $\rightarrow$ Linear elasticity theory is applicable.
  - Each flexible link is a homogeneous, isotropic and elastic material.
  - Linear stress-strain relationship.
  - Euler-Bernoulli hypothesis for slender beams – Plain sections remain plane etc.
  - Longitudinal deformation is negligible and no torsion due to transverse loads.
- Transverse vibration of a flexible beam $\rightarrow$ Partial differential equation.
- Infinite degrees of freedom – contrast with rigid or flexible joint!!

Characteristic of a Flexible Link

- To start with – flexible links undergoing *only* bending vibrations.
- Flexible link modeled as *slender flexible beam*.
- Main assumptions:
  - Small deformations $\rightarrow$ Linear elasticity theory is applicable.
  - Each flexible link is a homogeneous, isotropic and elastic material.
  - Linear stress-strain relationship.
  - Euler-Bernoulli hypothesis for slender beams – Plain sections remain plane etc.
  - Longitudinal deformation is negligible and no torsion due to transverse loads.
- Transverse vibration of a flexible beam $\rightarrow$ Partial differential equation.
- Infinite degrees of freedom – contrast with rigid or flexible joint!!

Characteristic of a Flexible Link

- To start with – flexible links undergoing *only* bending vibrations.
- Flexible link modeled as *slender flexible beam*.
- Main assumptions:
  - Small deformations $\rightarrow$ Linear elasticity theory is applicable.
  - Each flexible link is a homogeneous, isotropic and elastic material.
  - Linear stress-strain relationship.
  - Euler-Bernoulli hypothesis for slender beams – Plain sections remain plane etc.
  - Longitudinal deformation is negligible and no torsion due to transverse loads.
- Transverse vibration of a flexible beam $\rightarrow$ Partial differential equation.
- Infinite degrees of freedom – contrast with rigid or flexible joint!!

Characteristic of a Flexible Link

- To start with – flexible links undergoing *only* bending vibrations.
- Flexible link modeled as *slender flexible beam*.
- Main assumptions:
  - Small deformations $\rightarrow$ Linear elasticity theory is applicable.
  - Each flexible link is a homogeneous, isotropic and elastic material.
  - Linear stress-strain relationship.
  - Euler-Bernoulli hypothesis for slender beams – Plain sections remain plane etc.
  - Longitudinal deformation is negligible and no torsion due to transverse loads.
- Transverse vibration of a flexible beam $\rightarrow$ Partial differential equation.
- Infinite degrees of freedom – contrast with rigid or flexible joint!!

Characteristic of a Flexible Link

- To start with – flexible links undergoing *only* bending vibrations.
- Flexible link modeled as *slender flexible beam*.
- Main assumptions:
  - Small deformations $\rightarrow$ Linear elasticity theory is applicable.
  - Each flexible link is a homogeneous, isotropic and elastic material.
  - Linear stress-strain relationship.
  - Euler-Bernoulli hypothesis for slender beams – Plain sections remain plane etc.
  - Longitudinal deformation is negligible and no torsion due to transverse loads.
- Transverse vibration of a flexible beam $\rightarrow$ Partial differential equation.
- Infinite degrees of freedom – contrast with rigid or flexible joint!!

Characteristic of a Flexible Link (Contd.)

Euler-Bernoulli beam model

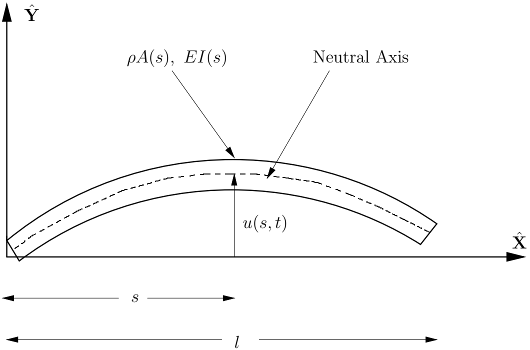

Figure 10: A beam in flexure

- PDE describing the transverse free bending vibration of a beam

$$\frac{\partial^2}{\partial s^2}\left(EI(s)\frac{\partial^2 u(s,t)}{\partial s^2}\right) + \rho A(s)\frac{\partial^2 u(s,t)}{\partial t^2} = 0$$

- $EI(s)$: flexural rigidity & $\rho A(s)$: mass per unit length.

- PDE second order in $t \rightarrow$ Need two initial conditions, $u(s,t)|_{t=0}$ and $\frac{\partial u(s,t)}{\partial t}|_{t=0}$. Since the PDE
- Since PDE is fourth order in $s \rightarrow$ four boundary conditions required.
- *Geometric* boundary conditions – deflection $u(s,t)$ or slope $\frac{\partial u(s,t)}{\partial s}$ at the boundaries.
- *Natural* boundary conditions – moment $\left(EI(s)\frac{\partial^2 u(s,t)}{\partial s^2}\right)$ or shear force $\frac{\partial}{\partial s}\left(EI(s)\frac{\partial^2 u(s,t)}{\partial s^2}\right)$ at the boundaries.
- Boundary conditions at $s=0$ depends on *type of joint*.
- Two common types of joints – Rotary (R) and Prismatic (P) joint.

Characteristic of a Flexible Link (contd.)

Euler-Bernoulli beam model

- PDE second order in $t \rightarrow$ Need two initial conditions, $u(s,t)|_{t=0}$ and $\frac{\partial u(s,t)}{\partial t}|_{t=0}$. Since the PDE
- Since PDE is fourth order in $s \rightarrow$ four boundary conditions required.
- *Geometric* boundary conditions – deflection $u(s,t)$ or slope $\frac{\partial u(s,t)}{\partial s}$ at the boundaries.
- *Natural* boundary conditions – moment $\left(EI(s)\frac{\partial^2 u(s,t)}{\partial s^2}\right)$ or shear force $\frac{\partial}{\partial s}\left(EI(s)\frac{\partial^2 u(s,t)}{\partial s^2}\right)$ at the boundaries.
- Boundary conditions at $s=0$ depends on *type of joint*.
- Two common types of joints – Rotary (R) and Prismatic (P) joint.

Characteristic of a Flexible Link (Contd.)

Euler-Bernoulli beam model

- PDE second order in $t \rightarrow$ Need two initial conditions, $u(s,t)|_{t=0}$ and $\frac{\partial u(s,t)}{\partial t}|_{t=0}$. Since the PDE
- Since PDE is fourth order in $s \rightarrow$ four boundary conditions required.
- *Geometric* boundary conditions – deflection $u(s,t)$ or slope $\frac{\partial u(s,t)}{\partial s}$ at the boundaries.
- *Natural* boundary conditions – moment $\left(EI(s)\frac{\partial^2 u(s,t)}{\partial s^2}\right)$ or shear force $\frac{\partial}{\partial s}\left(EI(s)\frac{\partial^2 u(s,t)}{\partial s^2}\right)$ at the boundaries.
- Boundary conditions at $s=0$ depends on *type of joint.*
- Two common types of joints – Rotary (R) and Prismatic (P) joint.

Characteristic of a Flexible Link (Contd.)

Euler-Bernoulli beam model

- PDE second order in t $\rightarrow$ Need two initial conditions, $u(s,t)|_{t=0}$ and $\frac{\partial u(s,t)}{\partial t}|_{t=0}$. Since the PDE
- Since PDE is fourth order in s $\rightarrow$ four boundary conditions required.
- *Geometric* boundary conditions – deflection $u(s,t)$ or slope $\frac{\partial u(s,t)}{\partial s}$ at the boundaries.
- *Natural* boundary conditions – moment $\left(EI(s)\frac{\partial^2 u(s,t)}{\partial s^2}\right)$ or shear force $\frac{\partial}{\partial s}\left(EI(s)\frac{\partial^2 u(s,t)}{\partial s^2}\right)$ at the boundaries.
- Boundary conditions at $s = 0$ depends on *type of joint*.
- Two common types of joints – Rotary (R) and Prismatic (P) joint.

- PDE second order in $t \rightarrow$ Need two initial conditions, $u(s,t)|_{t=0}$ and $\frac{\partial u(s,t)}{\partial t}|_{t=0}$. Since the PDE
- Since PDE is fourth order in $s \rightarrow$ four boundary conditions required.
- *Geometric* boundary conditions – deflection $u(s,t)$ or slope $\frac{\partial u(s,t)}{\partial s}$ at the boundaries.
- *Natural* boundary conditions – moment $\left(EI(s)\frac{\partial^2 u(s,t)}{\partial s^2}\right)$ or shear force $\frac{\partial}{\partial s}\left(EI(s)\frac{\partial^2 u(s,t)}{\partial s^2}\right)$ at the boundaries.
- Boundary conditions at $s = 0$ depends on *type of joint*.
- Two common types of joints – Rotary (R) and Prismatic (P) joint.

- PDE second order in $t \rightarrow$ Need two initial conditions, $u(s,t)|_{t=0}$ and $\frac{\partial u(s,t)}{\partial t}|_{t=0}$. Since the PDE
- Since PDE is fourth order in $s \rightarrow$ four boundary conditions required.
- *Geometric* boundary conditions – deflection $u(s,t)$ or slope $\frac{\partial u(s,t)}{\partial s}$ at the boundaries.
- *Natural* boundary conditions – moment $\left(EI(s)\frac{\partial^2 u(s,t)}{\partial s^2}\right)$ or shear force $\frac{\partial}{\partial s}\left(EI(s)\frac{\partial^2 u(s,t)}{\partial s^2}\right)$ at the boundaries.
- Boundary conditions at $s = 0$ depends on *type of joint*.
- Two common types of joints – Rotary (R) and Prismatic (P) joint.

Characteristic of a Flexible Link (Contd.)

Rotating Flexible Link

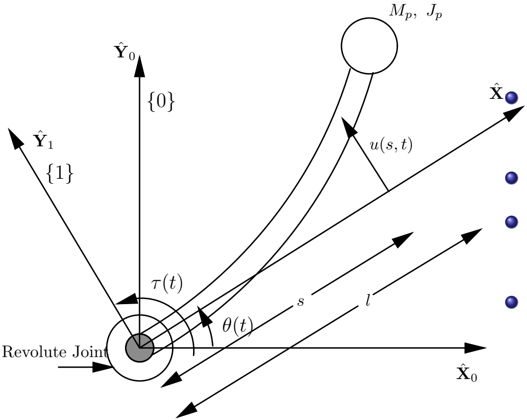

Figure 11: A flexible link with a rotary joint

- Rotation of joint $\theta(t)$.
- $u(s,t)$ deflection at s and time t in addition to rotation $\theta(t)$.
- Motor torque $\tau(t)$.
- Payload of mass M_p and inertia J_p.
- Two possible boundary conditions at $s = 0$ – *clamped* or *pinned*.

- *Clamped* boundary conditions
  - $\hat{\mathbf{X}}_1$ axis of $\{1\}$, rotating with the link, is chosen tangent to the link at the origin $\rightarrow$ Deflection and slope at $s = 0$ is zero

$$[u(s,t)]_{s=0} = 0, \quad \left[\frac{\partial u(s,t)}{\partial s}\right]_{s=0} = 0$$

- *Pinned* boundary conditions
  - $\hat{\mathbf{X}}_1$ axis of $\{1\}$ is chosen such that it passes through the centre of mass of the flexible link at all times $\rightarrow$ Slope at $s = 0$ need not be zero.

$$[u(s,t)]_{s=0} = 0, \quad \left[EI(s)\frac{\partial^2 u(s,t)}{\partial s^2}\right]_{s=0} = J_a\left[\frac{\partial^2}{\partial t^2}\left(\frac{\partial u(s,t)}{\partial s}\right)\right]_{s=0}$$

  J_a is the total inertia as seen by joint actuator.
- Neither clamped nor pinned exactly – not a built in cantilever and motor control torque provide non-zero stiffness!
- If $J_a >>$ flexible beam inertia (greater than 10) $\rightarrow$ *Clamped* boundary conditions more reasonable (Cetinkunt and Yu, 1991).
- We use clamped conditions at motor end.

Characteristic of a Flexible Link (Contd.)

Rotating Flexible Link

- *Clamped* boundary conditions
  - $\hat{\mathbf{X}}_1$ axis of $\{1\}$, rotating with the link, is chosen tangent to the link at the origin $\rightarrow$ Deflection and slope at $s = 0$ is zero

$$[u(s,t)]_{s=0} = 0, \quad \left[\frac{\partial u(s,t)}{\partial s}\right]_{s=0} = 0$$

- *Pinned* boundary conditions
  - $\hat{\mathbf{X}}_1$ axis of $\{1\}$ is chosen such that it passes through the centre of mass of the flexible link at all times $\rightarrow$ Slope at $s = 0$ need not be zero.

$$[u(s,t)]_{s=0} = 0, \quad \left[EI(s)\frac{\partial^2 u(s,t)}{\partial s^2}\right]_{s=0} = J_a \left[\frac{\partial^2}{\partial t^2}\left(\frac{\partial u(s,t)}{\partial s}\right)\right]_{s=0}$$

  J_a is the total inertia as seen by joint actuator.

- Neither clamped nor pinned exactly – not a built in cantilever and motor control torque provide non-zero stiffness!
- If $J_a >>$ flexible beam inertia (greater than 10) $\rightarrow$ *Clamped* boundary conditions more reasonable (Cetinkunt and Yu, 1991).
- We use clamped conditions at motor end.

- *Clamped* boundary conditions
  - $\hat{\mathbf{X}}_1$ axis of $\{1\}$, rotating with the link, is chosen tangent to the link at the origin $\rightarrow$ Deflection and slope at $s = 0$ is zero

$$[u(s,t)]_{s=0} = 0, \quad \left[\frac{\partial u(s,t)}{\partial s}\right]_{s=0} = 0$$

- *Pinned* boundary conditions
  - $\hat{\mathbf{X}}_1$ axis of $\{1\}$ is chosen such that it passes through the centre of mass of the flexible link at all times $\rightarrow$ Slope at $s = 0$ need not be zero.

$$[u(s,t)]_{s=0} = 0, \quad \left[EI(s)\frac{\partial^2 u(s,t)}{\partial s^2}\right]_{s=0} = J_a \left[\frac{\partial^2}{\partial t^2}\left(\frac{\partial u(s,t)}{\partial s}\right)\right]_{s=0}$$

  J_a is the total inertia as seen by joint actuator.
- Neither clamped nor pinned exactly – not a built in cantilever and motor control torque provide non-zero stiffness!
- If $J_a >>$ flexible beam inertia (greater than 10) $\rightarrow$ *Clamped* boundary conditions more reasonable (Cetinkunt and Yu, 1991).
- We use clamped conditions at motor end.

Characteristic of a Flexible Link (Contd.)

Rotating Flexible Link

- *Clamped* boundary conditions
  - $\hat{\mathbf{X}}_1$ axis of $\{1\}$, rotating with the link, is chosen tangent to the link at the origin $\rightarrow$ Deflection and slope at $s = 0$ is zero

$$[u(s,t)]_{s=0} = 0, \quad \left[\frac{\partial u(s,t)}{\partial s}\right]_{s=0} = 0$$

- *Pinned* boundary conditions
  - $\hat{\mathbf{X}}_1$ axis of $\{1\}$ is chosen such that it passes through the centre of mass of the flexible link at all times $\rightarrow$ Slope at $s = 0$ need not be zero.

$$[u(s,t)]_{s=0} = 0, \quad \left[EI(s)\frac{\partial^2 u(s,t)}{\partial s^2}\right]_{s=0} = J_a\left[\frac{\partial^2}{\partial t^2}\left(\frac{\partial u(s,t)}{\partial s}\right)\right]_{s=0}$$

  J_a is the total inertia as seen by joint actuator.
- Neither clamped nor pinned exactly – not a built in cantilever and motor control torque provide non-zero stiffness!
- If $J_a >>$ flexible beam inertia (greater than 10) $\rightarrow$ *Clamped* boundary conditions more reasonable (Cetinkunt and Yu, 1991).
- We use clamped conditions at motor end.

Rotating Flexible Link

- *Clamped* boundary conditions
  - $\hat{\mathbf{X}}_1$ axis of $\{1\}$, rotating with the link, is chosen tangent to the link at the origin $\rightarrow$ Deflection and slope at $s = 0$ is zero

$$[u(s,t)]_{s=0} = 0, \quad \left[\frac{\partial u(s,t)}{\partial s}\right]_{s=0} = 0$$

- *Pinned* boundary conditions
  - $\hat{\mathbf{X}}_1$ axis of $\{1\}$ is chosen such that it passes through the centre of mass of the flexible link at all times $\rightarrow$ Slope at $s = 0$ need not be zero.

$$[u(s,t)]_{s=0} = 0, \quad \left[EI(s)\frac{\partial^2 u(s,t)}{\partial s^2}\right]_{s=0} = J_a\left[\frac{\partial^2}{\partial t^2}\left(\frac{\partial u(s,t)}{\partial s}\right)\right]_{s=0}$$

  J_a is the total inertia as seen by joint actuator.
- Neither clamped nor pinned exactly – not a built in cantilever and motor control torque provide non-zero stiffness!
- If $J_a >>$ flexible beam inertia (greater than 10) $\rightarrow$ *Clamped* boundary conditions more reasonable (Cetinkunt and Yu, 1991).
- We use clamped conditions at motor end.

- Boundary conditions at $s = l$ – *free* or *mass*.
- Free boundary conditions at $s = l$

$$\left[EI(s)\frac{\partial^2 u(s,t)}{\partial s^2} \right]_{s=l} = 0, \quad \left[\frac{\partial}{\partial s}\left(EI(s)\frac{\partial^2 u(s,t)}{\partial s^2} \right) \right]_{s=l} = 0$$

- Multi-link flexible manipulators or single link with payload $\rightarrow$ More accurate to use *mass* boundary conditions.
- Mass boundary conditions require moment and shear force balance.

$$\begin{aligned} \left[EI(s)\frac{\partial^2 u(s,t)}{\partial s^2} \right]_{s=l} &= -J_p \left[\frac{\partial^2}{\partial t^2}\left(\frac{\partial u(s,t)}{\partial s} \right) \right]_{s=l} \\ \left[\frac{\partial}{\partial s}\left(EI(s)\frac{\partial^2 u(s,t)}{\partial s^2} \right) \right]_{s=l} &= M_p \left[\frac{\partial^2 u(s,t)}{\partial t^2} \right]_{s=l} \end{aligned}$$

where M_p and J_p are the mass and rotary inertia of the payload located at $s = l$.

- Boundary conditions at $s = l$ – *free* or *mass*.
- Free boundary conditions at $s = l$

$$\left[EI(s) \frac{\partial^2 u(s,t)}{\partial s^2} \right]_{s=l} = 0, \quad \left[\frac{\partial}{\partial s} \left(EI(s) \frac{\partial^2 u(s,t)}{\partial s^2} \right) \right]_{s=l} = 0$$

- Multi-link flexible manipulators or single link with payload $\rightarrow$ More accurate to use *mass* boundary conditions.
- Mass boundary conditions require moment and shear force balance.

$$\begin{aligned} \left[EI(s) \frac{\partial^2 u(s,t)}{\partial s^2} \right]_{s=l} &= -J_p \left[\frac{\partial^2}{\partial t^2} \left(\frac{\partial u(s,t)}{\partial s} \right) \right]_{s=l} \\ \left[\frac{\partial}{\partial s} \left(EI(s) \frac{\partial^2 u(s,t)}{\partial s^2} \right) \right]_{s=l} &= M_p \left[\frac{\partial^2 u(s,t)}{\partial t^2} \right]_{s=l} \end{aligned}$$

where M_p and J_p are the mass and rotary inertia of the payload located at $s = l$.

ROTATING FLEXIBLE LINK

- Boundary conditions at $s = l$ – *free* or *mass*.
- Free boundary conditions at $s = l$

$$\left[EI(s)\frac{\partial^2 u(s,t)}{\partial s^2}\right]_{s=l} = 0, \quad \left[\frac{\partial}{\partial s}\left(EI(s)\frac{\partial^2 u(s,t)}{\partial s^2}\right)\right]_{s=l} = 0$$

- Multi-link flexible manipulators or single link with payload $\rightarrow$ More accurate to use *mass* boundary conditions.
- Mass boundary conditions require moment and shear force balance.

$$\left[EI(s)\frac{\partial^2 u(s,t)}{\partial s^2}\right]_{s=l} = -J_p\left[\frac{\partial^2}{\partial t^2}\left(\frac{\partial u(s,t)}{\partial s}\right)\right]_{s=l}$$

$$\left[\frac{\partial}{\partial s}\left(EI(s)\frac{\partial^2 u(s,t)}{\partial s^2}\right)\right]_{s=l} = M_p\left[\frac{\partial^2 u(s,t)}{\partial t^2}\right]_{s=l}$$

where M_p and J_p are the mass and rotary inertia of the payload located at $s = l$.

Characteristic of a Flexible Link (Contd.)

Rotating Flexible Link

- Boundary conditions at $s = l$ – *free* or *mass*.
- Free boundary conditions at $s = l$

$$\left[EI(s)\frac{\partial^2 u(s,t)}{\partial s^2}\right]_{s=l} = 0, \quad \left[\frac{\partial}{\partial s}\left(EI(s)\frac{\partial^2 u(s,t)}{\partial s^2}\right)\right]_{s=l} = 0$$

- Multi-link flexible manipulators or single link with payload $\rightarrow$ More accurate to use *mass* boundary conditions.
- Mass boundary conditions require moment and shear force balance.

$$\begin{aligned}\left[EI(s)\frac{\partial^2 u(s,t)}{\partial s^2}\right]_{s=l} &= -J_p\left[\frac{\partial^2}{\partial t^2}\left(\frac{\partial u(s,t)}{\partial s}\right)\right]_{s=l} \\ \left[\frac{\partial}{\partial s}\left(EI(s)\frac{\partial^2 u(s,t)}{\partial s^2}\right)\right]_{s=l} &= M_p\left[\frac{\partial^2 u(s,t)}{\partial t^2}\right]_{s=l}\end{aligned}$$

where M_p and J_p are the mass and rotary inertia of the payload located at $s = l$.

- Non-dimensional variables: $\widetilde{u}(s,t) = u(s,t)/l$, $\eta = s/l$, $\tau = t/(l/U_g)$, with $U_g \stackrel{\Delta}{=} \frac{1}{l}\sqrt{\frac{EI}{\rho A}}$
- U_g has units of speed & l/U_g has units of time.
- $EI \to \infty$ (rigid)– $l/U_g \to 0$ & EI is small (flexible) – l/U_g is large!
- PDE and boundary conditions in terms of non-dimensional variables

$$\frac{\partial^4 \widetilde{u}(\eta,\tau)}{\partial \eta^4} + \frac{\partial^2 \widetilde{u}(\eta,\tau)}{\partial \tau^2} = 0, \qquad 0 < \eta < 1$$

$$[\widetilde{u}(\eta,\tau)]_{\eta=0} = 0, \quad \left[\frac{\partial^2 \widetilde{u}(\eta,\tau)}{\partial \eta^2}\right]_{\eta=1} = -\frac{J_p}{\rho A l^3}\left[\frac{\partial^2}{\partial \tau^2}\left(\frac{\partial \widetilde{u}(\eta,\tau)}{\partial \eta}\right)\right]_{\eta=1}$$

$$\left[\frac{\partial \widetilde{u}(\eta,\tau)}{\partial \eta}\right]_{\eta=0} = 0, \quad \left[\frac{\partial^3 \widetilde{u}(\eta,\tau)}{\partial \eta^3}\right]_{\eta=1} = \frac{M_p}{\rho A l}\left[\frac{\partial^2 \widetilde{u}(\eta,\tau)}{\partial \tau^2}\right]_{\eta=1}$$

- Non-dimensional variables: $\widetilde{u}(s,t) = u(s,t)/l$, $\eta = s/l$, $\tau = t/(l/U_g)$, with $U_g \stackrel{\Delta}{=} \frac{1}{l}\sqrt{\frac{EI}{\rho A}}$
- U_g has units of speed & l/U_g has units of time.
- $EI \to \infty$ (rigid)– $l/U_g \to 0$ & EI is small (flexible) – l/U_g is large!
- PDE and boundary conditions in terms of non-dimensional variables

$$\frac{\partial^4 \widetilde{u}(\eta,\tau)}{\partial \eta^4} + \frac{\partial^2 \widetilde{u}(\eta,\tau)}{\partial \tau^2} = 0, \qquad 0 < \eta < 1$$

$$[\widetilde{u}(\eta,\tau)]_{\eta=0} = 0, \quad \left[\frac{\partial^2 \widetilde{u}(\eta,\tau)}{\partial \eta^2}\right]_{\eta=1} = -\frac{J_p}{\rho A l^3}\left[\frac{\partial^2}{\partial \tau^2}\left(\frac{\partial \widetilde{u}(\eta,\tau)}{\partial \eta}\right)\right]_{\eta=1}$$

$$\left[\frac{\partial \widetilde{u}(\eta,\tau)}{\partial \eta}\right]_{\eta=0} = 0, \quad \left[\frac{\partial^3 \widetilde{u}(\eta,\tau)}{\partial \eta^3}\right]_{\eta=1} = \frac{M_p}{\rho A l}\left[\frac{\partial^2 \widetilde{u}(\eta,\tau)}{\partial \tau^2}\right]_{\eta=1}$$

- Non-dimensional variables: $\widetilde{u}(s,t) = u(s,t)/l$, $\eta = s/l$, $\tau = t/(l/U_g)$, with $U_g \stackrel{\Delta}{=} \frac{1}{l}\sqrt{\frac{EI}{\rho A}}$
- U_g has units of speed & l/U_g has units of time.
- $EI \to \infty$ (rigid)– $l/U_g \to 0$ & EI is small (flexible) – l/U_g is large!
- PDE and boundary conditions in terms of non-dimensional variables

$$\frac{\partial^4 \widetilde{u}(\eta,\tau)}{\partial \eta^4} + \frac{\partial^2 \widetilde{u}(\eta,\tau)}{\partial \tau^2} = 0, \qquad 0 < \eta < 1$$

$$[\widetilde{u}(\eta,\tau)]_{\eta=0} = 0, \quad \left[\frac{\partial^2 \widetilde{u}(\eta,\tau)}{\partial \eta^2}\right]_{\eta=1} = -\frac{J_p}{\rho A l^3}\left[\frac{\partial^2}{\partial \tau^2}\left(\frac{\partial \widetilde{u}(\eta,\tau)}{\partial \eta}\right)\right]_{\eta=1}$$

$$\left[\frac{\partial \widetilde{u}(\eta,\tau)}{\partial \eta}\right]_{\eta=0} = 0, \quad \left[\frac{\partial^3 \widetilde{u}(\eta,\tau)}{\partial \eta^3}\right]_{\eta=1} = \frac{M_p}{\rho A l}\left[\frac{\partial^2 \widetilde{u}(\eta,\tau)}{\partial \tau^2}\right]_{\eta=1}$$

CHARACTERISTIC OF A FLEXIBLE LINK (CONTD.)

ROTATING FLEXIBLE LINK – NON-DIMENSIONAL FORM

- Non-dimensional variables: $\widetilde{u}(s,t) = u(s,t)/l$, $\eta = s/l$, $\tau = t/(l/U_g)$, with $U_g \stackrel{\Delta}{=} \frac{1}{l}\sqrt{\frac{EI}{\rho A}}$
- U_g has units of speed & l/U_g has units of time.
- $EI \rightarrow \infty$ (rigid)– $l/U_g \rightarrow 0$ & EI is small (flexible) – l/U_g is large!
- PDE and boundary conditions in terms of non-dimensional variables

$$\frac{\partial^4 \widetilde{u}(\eta,\tau)}{\partial \eta^4} + \frac{\partial^2 \widetilde{u}(\eta,\tau)}{\partial \tau^2} = 0, \qquad 0 < \eta < 1$$

$$[\widetilde{u}(\eta,\tau)]_{\eta=0} = 0, \quad \left[\frac{\partial^2 \widetilde{u}(\eta,\tau)}{\partial \eta^2}\right]_{\eta=1} = -\frac{J_p}{\rho A l^3}\left[\frac{\partial^2}{\partial \tau^2}\left(\frac{\partial \widetilde{u}(\eta,\tau)}{\partial \eta}\right)\right]_{\eta=1}$$

$$\left[\frac{\partial \widetilde{u}(\eta,\tau)}{\partial \eta}\right]_{\eta=0} = 0, \quad \left[\frac{\partial^3 \widetilde{u}(\eta,\tau)}{\partial \eta^3}\right]_{\eta=1} = \frac{M_p}{\rho A l}\left[\frac{\partial^2 \widetilde{u}(\eta,\tau)}{\partial \tau^2}\right]_{\eta=1}$$

Characteristic of a Flexible Link (Contd.)

Rotating Flexible Link – Non-dimensional form

- In non-dimensional form easier to decide on boundary conditions at $s = l$.
  - Use free end-conditions if J_p and $M_p << $ rotary inertia ($\rho A l^3$) and mass ($\rho A l$) of the flexible link.
  - If J_p and M_p comparable to link quantities $\rightarrow$ Use mass end-conditions.
- In multi-link flexible manipulators, links *after* the flexible link j can be modeled as an effective M_{p_j} and J_{p_j} acting at $s = l \rightarrow$ More appropriate to use mass end-condition.
- PDE with boundary conditions can be solved by the method of *separation of variables*.
- $\tilde{u}(\eta, \tau)$ is separable in space (η) and time (τ)

$$\tilde{u}(\eta, \tau) = \psi(\eta)\mathbf{q}_f(\tau)$$

$\psi(\eta)$ are called *mode shape functions* and $\mathbf{q}_f(t)$ are the flexible generalised coordinates.

- In non-dimensional form easier to decide on boundary conditions at $s = l$.
  - Use free end-conditions if J_p and $M_p << $ rotary inertia $(\rho A l^3)$ and mass $(\rho A l)$ of the flexible link.
  - If J_p and M_p comparable to link quantities $\rightarrow$ Use mass end-conditions.
- In multi-link flexible manipulators, links *after* the flexible link j can be modeled as an effective M_{p_j} and J_{p_j} acting at $s = l \rightarrow$ More appropriate to use mass end-condition.
- PDE with boundary conditions can be solved by the method of *separation of variables.*
- $\widetilde{u}(\eta, \tau)$ is separable in space (η) and time (τ)

$$\widetilde{u}(\eta, \tau) = \psi(\eta)\mathbf{q}_f(\tau)$$

$\psi(\eta)$ are called *mode shape functions* and $\mathbf{q}_f(t)$ are the flexible generalised coordinates.

- In non-dimensional form easier to decide on boundary conditions at $s = l$.
    - Use free end-conditions if J_p and $M_p <<$ rotary inertia ($\rho A l^3$) and mass ($\rho A l$) of the flexible link.
    - If J_p and M_p comparable to link quantities $\rightarrow$ Use mass end-conditions.
- In multi-link flexible manipulators, links *after* the flexible link j can be modeled as an effective M_{p_j} and J_{p_j} acting at $s = l$ $\rightarrow$ More appropriate to use mass end-condition.
- PDE with boundary conditions can be solved by the method of *separation of variables*.
- $\tilde{u}(\eta, \tau)$ is separable in space (η) and time (τ)

$$\tilde{u}(\eta, \tau) = \psi(\eta)\mathbf{q}_f(\tau)$$

$\psi(\eta)$ are called *mode shape functions* and $\mathbf{q}_f(t)$ are the flexible generalised coordinates.

Characteristic of a Flexible Link (Contd.)

Rotating Flexible Link – Non-dimensional form

- In non-dimensional form easier to decide on boundary conditions at $s = l$.
  - Use free end-conditions if J_p and $M_p << $ rotary inertia ($\rho A l^3$) and mass ($\rho A l$) of the flexible link.
  - If J_p and M_p comparable to link quantities $\rightarrow$ Use mass end-conditions.
- In multi-link flexible manipulators, links *after* the flexible link j can be modeled as an effective M_{p_j} and J_{p_j} acting at $s = l \rightarrow$ More appropriate to use mass end-condition.
- PDE with boundary conditions can be solved by the method of *separation of variables*.
- $\widetilde{u}(\eta, \tau)$ is separable in space (η) and time (τ)

$$\widetilde{u}(\eta, \tau) = \psi(\eta)\mathbf{q}_f(\tau)$$

$\psi(\eta)$ are called *mode shape functions* and $\mathbf{q}_f(t)$ are the flexible generalised coordinates.

Characteristic of a Flexible Link (Contd.)

Rotating Flexible Link – Solution of PDE

- Substitute $\widetilde{u}(\eta,\tau) = \psi(\eta)\mathbf{q}_f(\tau)$ in PDE and rearrange

$$\frac{1}{\mathbf{q}_f(\tau)}\frac{d^2\mathbf{q}_f(\tau)}{d\tau^2} = -\frac{1}{\psi(\eta)}\frac{d^4\psi(\eta)}{d\eta^4}$$

- Both terms are equal to a real constant, $-\omega^2$, and

$$\frac{d^2\mathbf{q}_f(\tau)}{d\tau^2} + \omega^2\mathbf{q}_f(\tau) = 0, \quad \frac{d^4\psi(\eta)}{d\eta^4} - \omega^2\psi(\eta) = 0, \quad 0 < \eta < 1$$

Boundary conditions

$$[\psi(\eta)]_{\eta=0} = 0, \ \left[\frac{d^2\psi(\eta)}{d\eta^2}\right]_{\eta=1} = \frac{J_p\omega^2}{\rho A l^3}\left[\frac{d\psi(\eta)}{d\eta}\right]_{\eta=1}$$

$$\left[\frac{d\psi(\eta)}{d\eta}\right]_{\eta=0} = 0, \ \left[\frac{d^3\psi(\eta)}{d\eta^3}\right]_{\eta=1} = -\frac{M_p\omega^2}{\rho A l}[\psi(\eta)]_{\eta=1}$$

- Infinite number of eigenvalues $\omega^2 - \omega_i$ are system *natural frequencies*.
- For each ω_i, an eigenfunction or *natural mode* $\psi_i(\eta)$.

- Substitute $\tilde{u}(\eta,\tau) = \psi(\eta)\mathbf{q}_f(\tau)$ in PDE and rearrange

$$\frac{1}{\mathbf{q}_f(\tau)}\frac{d^2\mathbf{q}_f(\tau)}{d\tau^2} = -\frac{1}{\psi(\eta)}\frac{d^4\psi(\eta)}{d\eta^4}$$

- Both terms are equal to a real constant, $-\omega^2$, and

$$\frac{d^2\mathbf{q}_f(\tau)}{d\tau^2} + \omega^2\mathbf{q}_f(\tau) = 0, \quad \frac{d^4\psi(\eta)}{d\eta^4} - \omega^2\psi(\eta) = 0, \quad 0 < \eta < 1$$

  Boundary conditions

$$[\psi(\eta)]_{\eta=0} = 0, \; \left[\frac{d^2\psi(\eta)}{d\eta^2}\right]_{\eta=1} = \frac{J_p\omega^2}{\rho A l^3}\left[\frac{d\psi(\eta)}{d\eta}\right]_{\eta=1}$$

$$\left[\frac{d\psi(\eta)}{d\eta}\right]_{\eta=0} = 0, \; \left[\frac{d^3\psi(\eta)}{d\eta^3}\right]_{\eta=1} = -\frac{M_p\omega^2}{\rho A l}[\psi(\eta)]_{\eta=1}$$

- Infinite number of eigenvalues ω^2 – ω_i are system *natural frequencies*.
- For each ω_i, an eigenfunction or *natural mode* $\psi_i(\eta)$.

Characteristic of a Flexible Link (Contd.)

Rotating Flexible Link – Solution of PDE

- Substitute $\widetilde{u}(\eta,\tau) = \psi(\eta)\mathbf{q}_f(\tau)$ in PDE and rearrange

$$\frac{1}{\mathbf{q}_f(\tau)}\frac{d^2\mathbf{q}_f(\tau)}{d\tau^2} = -\frac{1}{\psi(\eta)}\frac{d^4\psi(\eta)}{d\eta^4}$$

- Both terms are equal to a real constant, $-\omega^2$, and

$$\frac{d^2\mathbf{q}_f(\tau)}{d\tau^2} + \omega^2\mathbf{q}_f(\tau) = 0, \quad \frac{d^4\psi(\eta)}{d\eta^4} - \omega^2\psi(\eta) = 0, \quad 0 < \eta < 1$$

Boundary conditions

$$[\psi(\eta)]_{\eta=0} = 0, \; \left[\frac{d^2\psi(\eta)}{d\eta^2}\right]_{\eta=1} = \frac{J_p\omega^2}{\rho A l^3}\left[\frac{d\psi(\eta)}{d\eta}\right]_{\eta=1}$$

$$\left[\frac{d\psi(\eta)}{d\eta}\right]_{\eta=0} = 0, \; \left[\frac{d^3\psi(\eta)}{d\eta^3}\right]_{\eta=1} = -\frac{M_p\omega^2}{\rho A l}[\psi(\eta)]_{\eta=1}$$

- Infinite number of eigenvalues ω^2 – ω_i are system *natural frequencies*.
- For each ω_i, an eigenfunction or *natural mode* $\psi_i(\eta)$.

Characteristic of a Flexible Link (contd.)

Rotating Flexible Link – Solution of PDE

- Substitute $\widetilde{u}(\eta,\tau) = \psi(\eta)\mathbf{q}_f(\tau)$ in PDE and rearrange

$$\frac{1}{\mathbf{q}_f(\tau)}\frac{d^2\mathbf{q}_f(\tau)}{d\tau^2} = -\frac{1}{\psi(\eta)}\frac{d^4\psi(\eta)}{d\eta^4}$$

- Both terms are equal to a real constant, $-\omega^2$, and

$$\frac{d^2\mathbf{q}_f(\tau)}{d\tau^2} + \omega^2\mathbf{q}_f(\tau) = 0, \quad \frac{d^4\psi(\eta)}{d\eta^4} - \omega^2\psi(\eta) = 0, \quad 0 < \eta < 1$$

  Boundary conditions

$$[\psi(\eta)]_{\eta=0} = 0, \; \left[\frac{d^2\psi(\eta)}{d\eta^2}\right]_{\eta=1} = \frac{J_p\omega^2}{\rho A l^3}\left[\frac{d\psi(\eta)}{d\eta}\right]_{\eta=1}$$

$$\left[\frac{d\psi(\eta)}{d\eta}\right]_{\eta=0} = 0, \; \left[\frac{d^3\psi(\eta)}{d\eta^3}\right]_{\eta=1} = -\frac{M_p\omega^2}{\rho A l}[\psi(\eta)]_{\eta=1}$$

- Infinite number of eigenvalues ω^2 – ω_i are system *natural frequencies*.
- For each ω_i, an eigenfunction or *natural mode* $\psi_i(\eta)$.

Characteristic of a Flexible Link (Contd.)

Translating Flexible Link

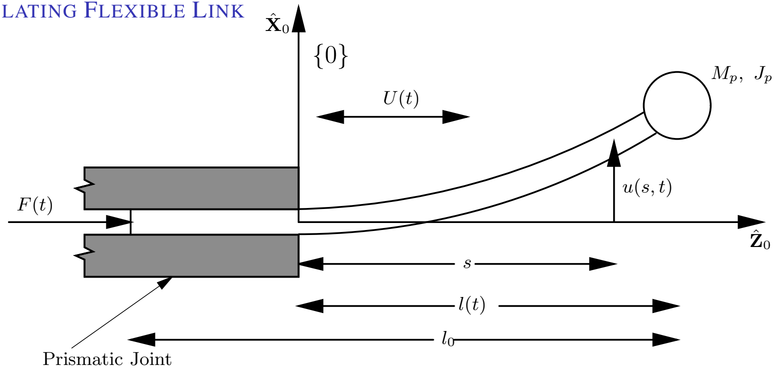

Figure 12: A flexible link with a prismatic joint

- Vibration in the horizontal plane spanned by $\hat{\mathbf{X}}_0$ and $\hat{\mathbf{Z}}_0$.
- Prismatic joint axis along $\hat{\mathbf{Z}}_0$, Total length of link l_0.
- $l(t)$ *vibrating* length outside the *rigid joint hub* at time t.
- The beam inside the hub, $(l_0 - l(t))$, is assumed not to be vibrating.
- The axial velocity $U(t)$ is assumed to be independent of s.

- Free bending vibration of a translating beam with Euler-Bernoulli assumptions

$$\frac{\partial^2}{\partial s^2}\left(EI\frac{\partial^2 u(s,t)}{\partial s^2}\right) + \rho A\left(\frac{\partial^2 u(s,t)}{\partial t^2} + 2U\frac{\partial^2 u(s,t)}{\partial s \partial t} + U^2\frac{\partial^2 u(s,t)}{\partial s^2} + \frac{dU}{dt}\frac{\partial u(s,t)}{\partial s}\right) = 0$$

where $0 < s < l(t)$.

- Clamped-mass boundary conditions are

$$[u(s,t)]_{s=0} = 0, \ EI\left[\frac{\partial^2 u(s,t)}{\partial s^2}\right]_{s=l(t)} = -J_p\left[\frac{\partial^2}{\partial t^2}\left(\frac{\partial u(s,t)}{\partial s}\right)\right]_{s=l(t)}$$

$$\left[\frac{\partial u(s,t)}{\partial s}\right]_{s=0} = 0, \ EI\left[\frac{\partial^3 u(s,t)}{\partial s^3}\right]_{s=l(t)} = M_p\left[\frac{\partial^2 u(s,t)}{\partial t^2}\right]_{s=l(t)}$$

- Free bending vibration of a translating beam with Euler-Bernoulli assumptions

$$\frac{\partial^2}{\partial s^2}\left(EI\frac{\partial^2 u(s,t)}{\partial s^2}\right) + \rho A\left(\frac{\partial^2 u(s,t)}{\partial t^2} + 2U\frac{\partial^2 u(s,t)}{\partial s \partial t} + U^2\frac{\partial^2 u(s,t)}{\partial s^2} + \frac{dU}{dt}\frac{\partial u(s,t)}{\partial s}\right) = 0$$

where $0 < s < l(t)$.

- Clamped-mass boundary conditions are

$$[u(s,t)]_{s=0} = 0,\;\; EI\left[\frac{\partial^2 u(s,t)}{\partial s^2}\right]_{s=l(t)} = -J_p\left[\frac{\partial^2}{\partial t^2}\left(\frac{\partial u(s,t)}{\partial s}\right)\right]_{s=l(t)}$$

$$\left[\frac{\partial u(s,t)}{\partial s}\right]_{s=0} = 0,\;\; EI\left[\frac{\partial^3 u(s,t)}{\partial s^3}\right]_{s=l(t)} = M_p\left[\frac{\partial^2 u(s,t)}{\partial t^2}\right]_{s=l(t)}$$

- Length of beam, $l(t)$, is a function of time – *moving boundary value* problem.
- Presence of *convective* terms $2\rho AU\frac{\partial^2 u(s,t)}{\partial s \partial t}$, $\rho AU^2\frac{\partial^2 u(s,t)}{\partial s^2}$, and $\rho A\frac{dU}{dt}\frac{\partial u(s,t)}{\partial s}$ due to the coupling of axial rigid-body and transverse vibratory motions.
- The centripetal term $\rho AU^2\frac{\partial^2 u(s,t)}{\partial s^2}$ will alter the the 'stiffness' of the system.
- For large U, the centripetal force may overcome the flexural restoring force and the system's oscillatory frequencies would decrease with increasing U (Stylianou and Tabarrok, 1994).
- Much more complicated that rotating link → General analytical solution not known!

Characteristic of a Flexible Link (Contd.)

Translating Flexible Link (Contd.)

- Length of beam, $l(t)$, is a function of time – *moving boundary value* problem.
- Presence of *convective* terms $2\rho AU\frac{\partial^2 u(s,t)}{\partial s \partial t}$, $\rho AU^2\frac{\partial^2 u(s,t)}{\partial s^2}$, and $\rho A\frac{dU}{dt}\frac{\partial u(s,t)}{\partial s}$ due to the coupling of axial rigid-body and transverse vibratory motions.
- The centripetal term $\rho AU^2\frac{\partial^2 u(s,t)}{\partial s^2}$ will alter the the 'stiffness' of the system.
- For large U, the centripetal force may overcome the flexural restoring force and the system's oscillatory frequencies would decrease with increasing U (Stylianou and Tabarrok, 1994).
- Much more complicated that rotating link $\rightarrow$ General analytical solution not known!

- Length of beam, $l(t)$, is a function of time – *moving boundary value* problem.
- Presence of *convective* terms $2\rho AU\frac{\partial^2 u(s,t)}{\partial s \partial t}$, $\rho AU^2\frac{\partial^2 u(s,t)}{\partial s^2}$, and $\rho A\frac{dU}{dt}\frac{\partial u(s,t)}{\partial s}$ due to the coupling of axial rigid-body and transverse vibratory motions.
- The centripetal term $\rho AU^2\frac{\partial^2 u(s,t)}{\partial s^2}$ will alter the the 'stiffness' of the system.
- For large U, the centripetal force may overcome the flexural restoring force and the system's oscillatory frequencies would decrease with increasing U (Stylianou and Tabarrok, 1994).
- Much more complicated that rotating link $\rightarrow$ General analytical solution not known!

Characteristic of a Flexible Link (Contd.)

Translating Flexible Link (Contd.)

- Length of beam, $l(t)$, is a function of time – *moving boundary value* problem.
- Presence of *convective* terms $2\rho AU \frac{\partial^2 u(s,t)}{\partial s \partial t}$, $\rho AU^2 \frac{\partial^2 u(s,t)}{\partial s^2}$, and $\rho A \frac{dU}{dt} \frac{\partial u(s,t)}{\partial s}$ due to the coupling of axial rigid-body and transverse vibratory motions.
- The centripetal term $\rho AU^2 \frac{\partial^2 u(s,t)}{\partial s^2}$ will alter the the 'stiffness' of the system.
- For large U, the centripetal force may overcome the flexural restoring force and the system's oscillatory frequencies would decrease with increasing U (Stylianou and Tabarrok, 1994).
- Much more complicated that rotating link $\rightarrow$ General analytical solution not known!

Characteristic of a Flexible Link (Contd.)

Translating Flexible Link (Contd.)

- Length of beam, $l(t)$, is a function of time – *moving boundary value* problem.
- Presence of *convective* terms $2\rho AU\frac{\partial^2 u(s,t)}{\partial s \partial t}$, $\rho AU^2\frac{\partial^2 u(s,t)}{\partial s^2}$, and $\rho A\frac{dU}{dt}\frac{\partial u(s,t)}{\partial s}$ due to the coupling of axial rigid-body and transverse vibratory motions.
- The centripetal term $\rho AU^2\frac{\partial^2 u(s,t)}{\partial s^2}$ will alter the the 'stiffness' of the system.
- For large U, the centripetal force may overcome the flexural restoring force and the system's oscillatory frequencies would decrease with increasing U (Stylianou and Tabarrok, 1994).
- Much more complicated that rotating link $\rightarrow$ General analytical solution not known!

- Using $\widetilde{u}(s,t) = u(s,t)/l_0$, $\eta = s/l_0$, $\tau = t/(l_0/U_g)$, and $U_g \triangleq \frac{1}{l_0}\sqrt{\frac{EI}{\rho A}}$ PDE is[1],

$$\frac{\partial^4 \widetilde{u}(\eta,\tau)}{\partial \eta^4} + \frac{\partial^2 \widetilde{u}(\eta,\tau)}{\partial \tau^2} + 2\left(\frac{U}{U_g}\right)\frac{\partial^2 \widetilde{u}(\eta,\tau)}{\partial \eta \partial \tau} + \left(\frac{U}{U_g}\right)^2 \frac{\partial^2 \widetilde{u}(\eta,\tau)}{\partial \eta^2} + \left(\frac{d}{d\tau}\left(\frac{U}{U_g}\right)\right)\frac{\partial \widetilde{u}(\eta,\tau)}{\partial \eta} = 0$$

- Boundary conditions

$$[\widetilde{u}(\eta,\tau)]_{\eta=0} = 0, \quad \left[\frac{\partial^2 \widetilde{u}(\eta,\tau)}{\partial \eta^2}\right]_{\eta=\frac{l(t)}{l_0}} = -\frac{J_p}{\rho A l^3}\left[\frac{\partial^2}{\partial \tau^2}\left(\frac{\partial \widetilde{u}(\eta,\tau)}{\partial \eta}\right)\right]_{\eta=\frac{l(t)}{l_0}}$$

$$\left[\frac{\partial \widetilde{u}(\eta,\tau)}{\partial \eta}\right]_{\eta=0} = 0, \quad \left[\frac{\partial^3 \widetilde{u}(\eta,\tau)}{\partial \eta^3}\right]_{\eta=\frac{l(t)}{l_0}} = \frac{M_p}{\rho A l}\left[\frac{\partial^2 \widetilde{u}(\eta,\tau)}{\partial \tau^2}\right]_{\eta=\frac{l(t)}{l_0}}$$

[1] U_g is based on l_0 or the smallest U_g value is used.

Translating Flexible Link (Contd.)

- Using $\tilde{u}(s,t) = u(s,t)/l_0$, $\eta = s/l_0$, $\tau = t/(l_0/U_g)$, and $U_g \triangleq \frac{1}{l_0}\sqrt{\frac{EI}{\rho A}}$

  PDE is[1],

$$\frac{\partial^4 \tilde{u}(\eta,\tau)}{\partial \eta^4} + \frac{\partial^2 \tilde{u}(\eta,\tau)}{\partial \tau^2} + 2\left(\frac{U}{U_g}\right)\frac{\partial^2 \tilde{u}(\eta,\tau)}{\partial \eta \partial \tau}$$
$$+\left(\frac{U}{U_g}\right)^2 \frac{\partial^2 \tilde{u}(\eta,\tau)}{\partial \eta^2} + \left(\frac{d}{d\tau}\left(\frac{U}{U_g}\right)\right)\frac{\partial \tilde{u}(\eta,\tau)}{\partial \eta} = 0$$

- Boundary conditions

$$[\tilde{u}(\eta,\tau)]_{\eta=0} = 0, \ \left[\frac{\partial^2 \tilde{u}(\eta,\tau)}{\partial \eta^2}\right]_{\eta=\frac{l(t)}{l_0}} = -\frac{J_p}{\rho A l^3}\left[\frac{\partial^2}{\partial \tau^2}\left(\frac{\partial \tilde{u}(\eta,\tau)}{\partial \eta}\right)\right]_{\eta=\frac{l(t)}{l_0}}$$

$$\left[\frac{\partial \tilde{u}(\eta,\tau)}{\partial \eta}\right]_{\eta=0} = 0, \ \left[\frac{\partial^3 \tilde{u}(\eta,\tau)}{\partial \eta^3}\right]_{\eta=\frac{l(t)}{l_0}} = \frac{M_p}{\rho A l}\left[\frac{\partial^2 \tilde{u}(\eta,\tau)}{\partial \tau^2}\right]_{\eta=\frac{l(t)}{l_0}}$$

[1] U_g is based on l_0 or the smallest U_g value is used.

Characteristic of a Flexible Link (Contd.)

Translating Flexible Link (Contd.)

- Using $\widetilde{u}(\eta,\tau) = \psi(\eta)\mathbf{q}_f(\tau)$, PDE can be written as

$$\psi(\eta)\frac{d^2\mathbf{q}_f(\tau)}{d\tau^2} + 2\frac{U}{U_g}\frac{d\psi(\eta)}{d\eta}\frac{d\mathbf{q}_f(\tau)}{d\tau}$$
$$= -\left(\frac{d^4\psi(\eta)}{d\eta^4} + \left(\frac{U}{U_g}\right)^2\frac{d^2\psi(\eta)}{d\eta^2} + \frac{d}{d\tau}\left(\frac{U}{U_g}\right)\frac{d\psi(\eta)}{d\eta}\right)\mathbf{q}_f(\tau)$$

- Above equation not separable in η and τ!!
- If $U \ll U_g$ and constant $\left(\frac{d}{d\tau}\left(\frac{U}{U_g}\right) = 0\right)$, the convective terms can be dropped and one can *approximately* use separation of variables.
- Mode shape functions $\psi_i(\eta)$ and the natural frequencies ω_i *time dependent*.
- Time varying boundary conditions solved using an ODE (Theodore and Ghosal, 1995 – See Lecture 2).

Characteristic of a Flexible Link (contd.)

Translating Flexible Link (contd.)

- Using $\tilde{u}(\eta,\tau) = \psi(\eta)\mathbf{q}_f(\tau)$, PDE can be written as

$$\psi(\eta)\frac{d^2\mathbf{q}_f(\tau)}{d\tau^2} + 2\frac{U}{U_g}\frac{d\psi(\eta)}{d\eta}\frac{d\mathbf{q}_f(\tau)}{d\tau}$$
$$= -\left(\frac{d^4\psi(\eta)}{d\eta^4} + \left(\frac{U}{U_g}\right)^2\frac{d^2\psi(\eta)}{d\eta^2} + \frac{d}{d\tau}\left(\frac{U}{U_g}\right)\frac{d\psi(\eta)}{d\eta}\right)\mathbf{q}_f(\tau)$$

- Above equation not separable in η and τ!!
- If $U \ll U_g$ and constant ($\frac{d}{d\tau}\left(\frac{U}{U_g}\right) = 0$), the convective terms can be dropped and one can *approximately* use separation of variables.
- Mode shape functions $\psi_i(\eta)$ and the natural frequencies ω_i *time dependent*.
- Time varying boundary conditions solved using an ODE (Theodore and Ghosal, 1995 – See Lecture 2).

Characteristic of a Flexible Link (contd.)

Translating Flexible Link (contd.)

- Using $\tilde{u}(\eta,\tau) = \psi(\eta)\mathbf{q}_f(\tau)$, PDE can be written as

$$\psi(\eta)\frac{d^2\mathbf{q}_f(\tau)}{d\tau^2} + 2\frac{U}{U_g}\frac{d\psi(\eta)}{d\eta}\frac{d\mathbf{q}_f(\tau)}{d\tau}$$
$$= -\left(\frac{d^4\psi(\eta)}{d\eta^4} + \left(\frac{U}{U_g}\right)^2\frac{d^2\psi(\eta)}{d\eta^2} + \frac{d}{d\tau}\left(\frac{U}{U_g}\right)\frac{d\psi(\eta)}{d\eta}\right)\mathbf{q}_f(\tau)$$

- Above equation not separable in η and τ!!
- If $U \ll U_g$ and constant ($\frac{d}{d\tau}\left(\frac{U}{U_g}\right) = 0$), the convective terms can be dropped and one can *approximately* use separation of variables.
- Mode shape functions $\psi_i(\eta)$ and the natural frequencies ω_i *time dependent*.
- Time varying boundary conditions solved using an ODE (Theodore and Ghosal, 1995 – See Lecture 2).

- Using $\widetilde{u}(\eta,\tau) = \psi(\eta)\mathbf{q}_f(\tau)$, PDE can be written as

$$\psi(\eta)\frac{d^2\mathbf{q}_f(\tau)}{d\tau^2} + 2\frac{U}{U_g}\frac{d\psi(\eta)}{d\eta}\frac{d\mathbf{q}_f(\tau)}{d\tau}$$
$$= -\left(\frac{d^4\psi(\eta)}{d\eta^4} + \left(\frac{U}{U_g}\right)^2\frac{d^2\psi(\eta)}{d\eta^2} + \frac{d}{d\tau}\left(\frac{U}{U_g}\right)\frac{d\psi(\eta)}{d\eta}\right)\mathbf{q}_f(\tau)$$

- Above equation not separable in η and τ!!
- If $U \ll U_g$ and constant $(\frac{d}{d\tau}\left(\frac{U}{U_g}\right) = 0)$, the convective terms can be dropped and one can *approximately* use separation of variables.
- Mode shape functions $\psi_i(\eta)$ and the natural frequencies ω_i *time dependent*.
- Time varying boundary conditions solved using an ODE (Theodore and Ghosal, 1995 – See Lecture 2).

Characteristic of a Flexible Link (Contd.)

Translating Flexible Link (Contd.)

- Using $\tilde{u}(\eta,\tau) = \psi(\eta)\mathbf{q}_f(\tau)$, PDE can be written as

$$\psi(\eta)\frac{d^2\mathbf{q}_f(\tau)}{d\tau^2} + 2\frac{U}{U_g}\frac{d\psi(\eta)}{d\eta}\frac{d\mathbf{q}_f(\tau)}{d\tau}$$
$$= -\left(\frac{d^4\psi(\eta)}{d\eta^4} + \left(\frac{U}{U_g}\right)^2\frac{d^2\psi(\eta)}{d\eta^2} + \frac{d}{d\tau}\left(\frac{U}{U_g}\right)\frac{d\psi(\eta)}{d\eta}\right)\mathbf{q}_f(\tau)$$

- Above equation not separable in η and τ!!
- If $U \ll U_g$ and constant ($\frac{d}{d\tau}\left(\frac{U}{U_g}\right) = 0$), the convective terms can be dropped and one can *approximately* use separation of variables.
- Mode shape functions $\psi_i(\eta)$ and the natural frequencies ω_i *time dependent*.
- Time varying boundary conditions solved using an ODE (Theodore and Ghosal, 1995 – See Lecture 2).

Summary

- Flexibility of links and joints important for aero-space, high-speed application and for "trimmer" design of all manipulators.
- Rigid link $\rightarrow$ Simple ODE model & one-to-one relationship between joint torque and link rotation.
- Flexible joint
  - Modeled as torsional spring.
  - Coupled ODE model $\rightarrow$ one input and two outputs.
  - Motor torque can control both rotation of joint and link.
- Flexible link
  - Partial differential equation for bending vibration $\rightarrow$ infinite dimensional system.
  - Boundary conditions depend on rotary (R) or prismatic (P) joint $\rightarrow$ Clamped-mass boundary conditions more reasonable.
  - Separation of variables can be used for rotary joints and under simplifying assumptions for prismatic joint.

SUMMARY

- Flexibility of links and joints important for aero-space, high-speed application and for "trimmer" design of all manipulators.
- Rigid link $\rightarrow$ Simple ODE model & one-to-one relationship between joint torque and link rotation.
- Flexible joint
  - Modeled as torsional spring.
  - Coupled ODE model $\rightarrow$ one input and two outputs.
  - Motor torque can control both rotation of joint and link.
- Flexible link
  - Partial differential equation for bending vibration $\rightarrow$ infinite dimensional system.
  - Boundary conditions depend on rotary (R) or prismatic (P) joint $\rightarrow$ Clamped-mass boundary conditions more reasonable.
  - Separation of variables can be used for rotary joints and under simplifying assumptions for prismatic joint.

Summary

- Flexibility of links and joints important for aero-space, high-speed application and for "trimmer" design of all manipulators.
- Rigid link $\rightarrow$ Simple ODE model & one-to-one relationship between joint torque and link rotation.
- Flexible joint
  - Modeled as torsional spring.
  - Coupled ODE model $\rightarrow$ one input and two outputs.
  - Motor torque can control both rotation of joint and link.
- Flexible link
  - Partial differential equation for bending vibration $\rightarrow$ infinite dimensional system.
  - Boundary conditions depend on rotary (R) or prismatic (P) joint $\rightarrow$ Clamped-mass boundary conditions more reasonable.
  - Separation of variables can be used for rotary joints and under simplifying assumptions for prismatic joint.

Summary

- Flexibility of links and joints important for aero-space, high-speed application and for "trimmer" design of all manipulators.
- Rigid link $\rightarrow$ Simple ODE model & one-to-one relationship between joint torque and link rotation.
- Flexible joint
  - Modeled as torsional spring.
  - Coupled ODE model $\rightarrow$ one input and two outputs.
  - Motor torque can control both rotation of joint and link.
- Flexible link
  - Partial differential equation for bending vibration $\rightarrow$ infinite dimensional system.
  - Boundary conditions depend on rotary (R) or prismatic (P) joint $\rightarrow$ Clamped-mass boundary conditions more reasonable.
  - Separation of variables can be used for rotary joints and under simplifying assumptions for prismatic joint.

OUTLINE

- Extension of Denavit-Hartenberg convention to flexible link manipulators.
- Discretisation of PDE for finite dimensional model.
  - Assumed modes method (AMM).
  - Frequency equation as ODE for translating link.
  - Finite element method (FEM).
- Position vector of a point on a flexible link and its velocity.
- Comparison of AMM and FEM.

- Extension of Denavit-Hartenberg convention to flexible link manipulators.
- Discretisation of PDE for finite dimensional model.
  - Assumed modes method (AMM).
  - Frequency equation as ODE for translating link.
  - Finite element method (FEM).
- Position vector of a point on a flexible link and its velocity.
- Comparison of AMM and FEM.

Introduction

Overview

- Extension of Denavit-Hartenberg convention to flexible link manipulators.
- Discretisation of PDE for finite dimensional model.
  - Assumed modes method (AMM).
  - Frequency equation as ODE for translating link.
  - Finite element method (FEM).
- Position vector of a point on a flexible link and its velocity.
- Comparison of AMM and FEM.

- Extension of Denavit-Hartenberg convention to flexible link manipulators.
- Discretisation of PDE for finite dimensional model.
  - Assumed modes method (AMM).
  - Frequency equation as ODE for translating link.
  - Finite element method (FEM).
- Position vector of a point on a flexible link and its velocity.
- Comparison of AMM and FEM.

- Multi-link manipulator with flexible links connected by rotary (R) or prismatic (P) joints.
- Links undergoing *only* transverse bending vibration – axial and torsional deformation not considered.
- Links satisfy Euler-Bernoulli beam assumptions.
- Similar to Denavit-Hartenberg convention for rigid links (see Module 2, Lecture 2)
  - Assign coordinate system $\{j\}$ to link j with $\{0\}$ as the fixed link and $\{n\}$ as the last link.
  - The coordinate axes $(\hat{\mathbf{X}}_j, \hat{\mathbf{Y}}_j, \hat{\mathbf{Z}}_j)$ are assigned to link j and the origin O_j is on the joint axis j.
  - Axis $\hat{\mathbf{Z}}_j$ is along the axis of joint j.
- Define a coordinate system $\{j_*\}$ in such a way that when the link $j-1$ is in its *undeformed* configuration, the $\{j\}$ and $\{j_*\}$ are *coincident* (see figure next page).

EXTENSION OF D-H CONVENTION TO FLEXIBLE LINKS

- Multi-link manipulator with flexible links connected by rotary (R) or prismatic (P) joints.
- Links undergoing *only* transverse bending vibration – axial and torsional deformation not considered.
- Links satisfy Euler-Bernoulli beam assumptions.
- Similar to Denavit-Hartenberg convention for rigid links (see Module 2, Lecture 2)
  - Assign coordinate system $\{j\}$ to link j with $\{0\}$ as the fixed link and $\{n\}$ as the last link.
  - The coordinate axes $(\hat{\mathbf{X}}_j, \hat{\mathbf{Y}}_j, \hat{\mathbf{Z}}_j)$ are assigned to link j and the origin O_j is on the joint axis j.
  - Axis $\hat{\mathbf{Z}}_j$ is along the axis of joint j.
- Define a coordinate system $\{j_*\}$ in such a way that when the link $j-1$ is in its *undeformed* configuration, the $\{j\}$ and $\{j_*\}$ are *coincident* (see figure next page).

- Multi-link manipulator with flexible links connected by rotary (R) or prismatic (P) joints.
- Links undergoing *only* transverse bending vibration – axial and torsional deformation not considered.
- Links satisfy Euler-Bernoulli beam assumptions.
- Similar to Denavit-Hartenberg convention for rigid links (see Module 2, Lecture 2)
  - Assign coordinate system $\{j\}$ to link j with $\{0\}$ as the fixed link and $\{n\}$ as the last link.
  - The coordinate axes $(\hat{\mathbf{X}}_j, \hat{\mathbf{Y}}_j, \hat{\mathbf{Z}}_j)$ are assigned to link j and the origin O_j is on the joint axis j.
  - Axis $\hat{\mathbf{Z}}_j$ is along the axis of joint j.
- Define a coordinate system $\{j_*\}$ in such a way that when the link $j-1$ is in its *undeformed* configuration, the $\{j\}$ and $\{j_*\}$ are *coincident* (see figure next page).

- Multi-link manipulator with flexible links connected by rotary (R) or prismatic (P) joints.
- Links undergoing *only* transverse bending vibration – axial and torsional deformation not considered.
- Links satisfy Euler-Bernoulli beam assumptions.
- Similar to Denavit-Hartenberg convention for rigid links (see Module 2, Lecture 2)
  - Assign coordinate system $\{j\}$ to link j with $\{0\}$ as the fixed link and $\{n\}$ as the last link.
  - The coordinate axes $(\hat{\mathbf{X}}_j, \hat{\mathbf{Y}}_j, \hat{\mathbf{Z}}_j)$ are assigned to link j and the origin O_j is on the joint axis j.
  - Axis $\hat{\mathbf{Z}}_j$ is along the axis of joint j.
- Define a coordinate system $\{j_*\}$ in such a way that when the link $j-1$ is in its *undeformed* configuration, the $\{j\}$ and $\{j_*\}$ are *coincident* (see figure next page).

- Multi-link manipulator with flexible links connected by rotary (R) or prismatic (P) joints.
- Links undergoing *only* transverse bending vibration – axial and torsional deformation not considered.
- Links satisfy Euler-Bernoulli beam assumptions.
- Similar to Denavit-Hartenberg convention for rigid links (see Module 2, Lecture 2)
  - Assign coordinate system $\{j\}$ to link j with $\{0\}$ as the fixed link and $\{n\}$ as the last link.
  - The coordinate axes $(\hat{\mathbf{X}}_j, \hat{\mathbf{Y}}_j, \hat{\mathbf{Z}}_j)$ are assigned to link j and the origin O_j is on the joint axis j.
  - Axis $\hat{\mathbf{Z}}_j$ is along the axis of joint j.
- Define a coordinate system $\{j_*\}$ in such a way that when the link $j-1$ is in its *undeformed* configuration, the $\{j\}$ and $\{j_*\}$ are *coincident* (see figure next page).

D-H Convention for Flexible Links (Contd.)

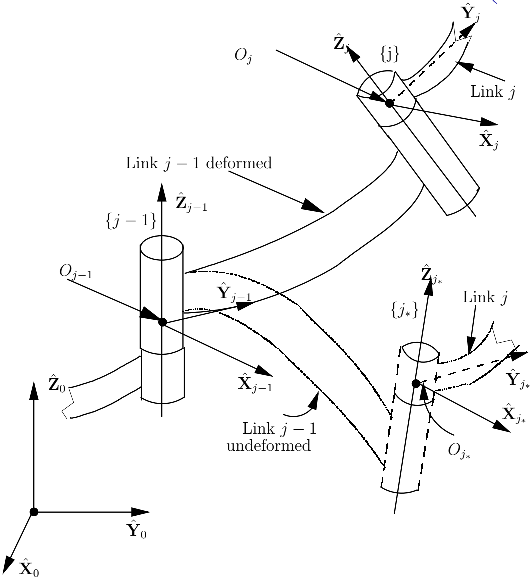

Figure 13: Assignment of frames for the flexible links

- The 4×4 homogeneous transformation matrix relating $\{j_*\}$ to $\{j-1\}$ same as for a rigid manipulator (see Module 2, Lecture 2)

$$ {}^{j-1}_{j_*}[T_r] = \begin{pmatrix} c_{\theta_j} & -s_{\theta_j} & 0 & a_{j-1} \\ s_{\theta_j} c_{\alpha_{j-1}} & c_{\theta_j} c_{\alpha_{j-1}} & -s_{\alpha_{j-1}} & -s_{\alpha_{j-1}} d_j \\ s_{\theta_j} s_{\alpha_{j-1}} & c_{\theta_j} s_{\alpha_{j-1}} & c_{\alpha_{j-1}} & c_{\alpha_{j-1}} d_j \\ 0 & 0 & 0 & 1 \end{pmatrix} $$

  α_{j-1}, a_{j-1}, d_j, and θ_j are the D-H parameters which describe $\{j_*\}$ with respect to $\{j-1\}$.
- q_{j_r} is the joint variable – either θ_j or d_j.
- $n \times 1$ vector $\mathbf{q}_r$ denote rigid joint variables and the flexibility in the link j will be denoted by $\mathbf{q}_{f_j}$.

- The 4×4 homogeneous transformation matrix relating $\{j_*\}$ to $\{j-1\}$ same as for a rigid manipulator (see Module 2, Lecture 2)

$$ {}^{j-1}_{j_*}[T_r] = \begin{pmatrix} c_{\theta_j} & -s_{\theta_j} & 0 & a_{j-1} \\ s_{\theta_j} c_{\alpha_{j-1}} & c_{\theta_j} c_{\alpha_{j-1}} & -s_{\alpha_{j-1}} & -s_{\alpha_{j-1}} d_j \\ s_{\theta_j} s_{\alpha_{j-1}} & c_{\theta_j} s_{\alpha_{j-1}} & c_{\alpha_{j-1}} & c_{\alpha_{j-1}} d_j \\ 0 & 0 & 0 & 1 \end{pmatrix} $$

  α_{j-1}, a_{j-1}, d_j, and θ_j are the D-H parameters which describe $\{j_*\}$ with respect to $\{j-1\}$.

- q_{j_r} is the joint variable – either θ_j or d_j.
- $n \times 1$ vector $\mathbf{q}_r$ denote rigid joint variables and the flexibility in the link j will be denoted by $\mathbf{q}_{f_j}$.

- The 4×4 homogeneous transformation matrix relating $\{j_*\}$ to $\{j-1\}$ same as for a rigid manipulator (see Module 2, Lecture 2)

$$
{}^{j-1}_{j_*}[T_r] = \begin{pmatrix} c_{\theta_j} & -s_{\theta_j} & 0 & a_{j-1} \\ s_{\theta_j} c_{\alpha_{j-1}} & c_{\theta_j} c_{\alpha_{j-1}} & -s_{\alpha_{j-1}} & -s_{\alpha_{j-1}} d_j \\ s_{\theta_j} s_{\alpha_{j-1}} & c_{\theta_j} s_{\alpha_{j-1}} & c_{\alpha_{j-1}} & c_{\alpha_{j-1}} d_j \\ 0 & 0 & 0 & 1 \end{pmatrix}
$$

  α_{j-1}, a_{j-1}, d_j, and θ_j are the D-H parameters which describe $\{j_*\}$ with respect to $\{j-1\}$.

- q_{j_r} is the joint variable – either θ_j or d_j.
- $n \times 1$ vector $\mathbf{q}_r$ denote rigid joint variables and the flexibility in the link j will be denoted by $\mathbf{q}_{f_j}$.

D-H Convention for Flexible Links (Contd.)

4×4 Transformation Matrix (Contd.)

- Any 3D spatial transformation $\rightarrow$ three rotations and three translations.
- $\{j_*\}$ can be taken to $\{j\}$ by

$$\mathrm{Rot}(\hat{Z}, \phi_{z_{j-1}})\mathrm{Trans}(\hat{Z}, \delta_{z_{j-1}})\mathrm{Rot}(\hat{Y}, \phi_{y_{j-1}})\mathrm{Trans}(\hat{Y}, \delta_{y_{j-1}})$$
$$\mathrm{Rot}(\hat{X}, \phi_{x_{j-1}})\mathrm{Trans}(\hat{X}, \delta_{x_{j-1}})$$

- Assuming *small elastic deformation*, sequence becomes (Book 1984)

$$^{j_*}_{j}[T_e] = \begin{pmatrix} 1 & -\phi_{z_{j-1}} & \phi_{y_{j-1}} & \delta_{x_{j-1}} \\ \phi_{z_{j-1}} & 1 & -\phi_{x_{j-1}} & \delta_{y_{j-1}} \\ -\phi_{y_{j-1}} & \phi_{x_{j-1}} & 1 & \delta_{z_{j-1}} \\ 0 & 0 & 0 & 1 \end{pmatrix}$$

Note: If link $j-1$ is rigid, $^{j_*}_{j}[T]$ is a 4×4 identity matrix.

- 4×4 homogeneous transformation matrix relating $\{j\}$ to $\{j-1\}$ is

$$^{j-1}_{j}[T] = {}^{j-1}_{j_*}[T_r]^{j_*}_{j}[T_e]$$

D-H Convention for Flexible Links (Contd.)

4×4 Transformation Matrix (Contd.)

- Any 3D spatial transformation $\rightarrow$ three rotations and three translations.
- $\{j_*\}$ can be taken to $\{j\}$ by

$$\mathrm{Rot}(\hat{Z}, \phi_{z_{j-1}})\mathrm{Trans}(\hat{Z}, \delta_{z_{j-1}})\mathrm{Rot}(\hat{Y}, \phi_{y_{j-1}})\mathrm{Trans}(\hat{Y}, \delta_{y_{j-1}})$$
$$\mathrm{Rot}(\hat{X}, \phi_{x_{j-1}})\mathrm{Trans}(\hat{X}, \delta_{x_{j-1}})$$

- Assuming *small elastic deformation*, sequence becomes (Book 1984)

$$^{j_*}_{j}[T_e] = \begin{pmatrix} 1 & -\phi_{z_{j-1}} & \phi_{y_{j-1}} & \delta_{x_{j-1}} \\ \phi_{z_{j-1}} & 1 & -\phi_{x_{j-1}} & \delta_{y_{j-1}} \\ -\phi_{y_{j-1}} & \phi_{x_{j-1}} & 1 & \delta_{z_{j-1}} \\ 0 & 0 & 0 & 1 \end{pmatrix}$$

  Note: If link $j-1$ is rigid, $^{j_*}_{j}[T]$ is a 4×4 identity matrix.
- 4×4 homogeneous transformation matrix relating $\{j\}$ to $\{j-1\}$ is

$$^{j-1}_{j}[T] = {}^{j-1}_{j_*}[T_r]^{j_*}_{j}[T_e]$$

D-H Convention for Flexible Links (Contd.)

4×4 Transformation Matrix (Contd.)

- Any 3D spatial transformation $\rightarrow$ three rotations and three translations.
- $\{j_*\}$ can be taken to $\{j\}$ by

$$\mathrm{Rot}(\hat{Z}, \phi_{z_{j-1}})\mathrm{Trans}(\hat{Z}, \delta_{z_{j-1}})\mathrm{Rot}(\hat{Y}, \phi_{y_{j-1}})\mathrm{Trans}(\hat{Y}, \delta_{y_{j-1}})$$
$$\mathrm{Rot}(\hat{X}, \phi_{x_{j-1}})\mathrm{Trans}(\hat{X}, \delta_{x_{j-1}})$$

- Assuming *small elastic deformation*, sequence becomes (Book 1984)

$$^{j_*}_{j}[T_e] = \begin{pmatrix} 1 & -\phi_{z_{j-1}} & \phi_{y_{j-1}} & \delta_{x_{j-1}} \\ \phi_{z_{j-1}} & 1 & -\phi_{x_{j-1}} & \delta_{y_{j-1}} \\ -\phi_{y_{j-1}} & \phi_{x_{j-1}} & 1 & \delta_{z_{j-1}} \\ 0 & 0 & 0 & 1 \end{pmatrix}$$

Note: If link $j-1$ is rigid, $^{j_*}_{j}[T]$ is a 4×4 identity matrix.

- 4×4 homogeneous transformation matrix relating $\{j\}$ to $\{j-1\}$ is

$$^{j-1}_{j}[T] = {}^{j-1}_{j_*}[T_r]^{j_*}_{j}[T_e]$$

D-H Convention for Flexible Links (Contd.)

4×4 Transformation Matrix (Contd.)

- Any 3D spatial transformation $\rightarrow$ three rotations and three translations.
- $\{j_*\}$ can be taken to $\{j\}$ by

$$\mathrm{Rot}(\hat{Z}, \phi_{z_{j-1}})\mathrm{Trans}(\hat{Z}, \delta_{z_{j-1}})\mathrm{Rot}(\hat{Y}, \phi_{y_{j-1}})\mathrm{Trans}(\hat{Y}, \delta_{y_{j-1}})$$
$$\mathrm{Rot}(\hat{X}, \phi_{x_{j-1}})\mathrm{Trans}(\hat{X}, \delta_{x_{j-1}})$$

- Assuming *small elastic deformation*, sequence becomes (Book 1984)

$${}^{j_*}_{j}[T_e] = \begin{pmatrix} 1 & -\phi_{z_{j-1}} & \phi_{y_{j-1}} & \delta_{x_{j-1}} \\ \phi_{z_{j-1}} & 1 & -\phi_{x_{j-1}} & \delta_{y_{j-1}} \\ -\phi_{y_{j-1}} & \phi_{x_{j-1}} & 1 & \delta_{z_{j-1}} \\ 0 & 0 & 0 & 1 \end{pmatrix}$$

  Note: If link $j-1$ is rigid, ${}^{j_*}_{j}[T]$ is a 4×4 identity matrix.
- 4×4 homogeneous transformation matrix relating $\{j\}$ to $\{j-1\}$ is

$${}^{j-1}_{j}[T] = {}^{j-1}_{j_*}[T_r]{}^{j_*}_{j}[T_e]$$

D-H Convention for Flexible Links (Contd.)

Link Transformation Matrix

- ${}^{0}_{j}[T]$ can be obtained by usual matrix multiplication

$$ {}^{0}_{j}[T] = {}^{0}_{1_*}[T_r]^{1_*}_{1}[T_e]^{1}_{2_*}[T_r]^{2_*}_{2}[T_e] \cdots {}^{j-1}_{j_*}[T_r]^{j_*}_{j}[T_e] $$

- ${}^{0}_{j}[T]$, as in the rigid case, contains position vector ${}^{0}\mathbf{O}_j$ and the rotation matrix ${}^{0}_{j}[R]$.
- As in the rigid case, information is up to the *start* of the link.
- For a point on the link *after* the origin and *along the neutral axis*

$$ {}^{0}\mathbf{p}_j = {}^{0}\mathbf{O}_j + {}^{0}_{j}[R]\mathbf{r}_j $$

- Need to find vector $\mathbf{r}_j$!!

- ${}^{0}_{j}[T]$ can be obtained by usual matrix multiplication

$$ {}^{0}_{j}[T] = {}^{0}_{1_*}[T_r]^{1_*}_{1}[T_e]^{1}_{2_*}[T_r]^{2_*}_{2}[T_e] \cdots {}^{j-1}_{j_*}[T_r]^{j_*}_{j}[T_e] $$

- ${}^{0}_{j}[T]$, as in the rigid case, contains position vector ${}^{0}\mathbf{O}_j$ and the rotation matrix ${}^{0}_{j}[R]$.
- As in the rigid case, information is up to the *start* of the link.
- For a point on the link *after* the origin and *along the neutral axis*

$$ {}^{0}\mathbf{p}_j = {}^{0}\mathbf{O}_j + {}^{0}_{j}[R]\mathbf{r}_j $$

- Need to find vector $\mathbf{r}_j$!!

- ${}^{0}_{j}[T]$ can be obtained by usual matrix multiplication

$$ {}^{0}_{j}[T] = {}^{0}_{1_*}[T_r]^{1_*}_{1}[T_e]^{1}_{2_*}[T_r]^{2_*}_{2}[T_e] \cdots {}^{j-1}_{j_*}[T_r]^{j_*}_{j}[T_e] $$

- ${}^{0}_{j}[T]$, as in the rigid case, contains position vector ${}^{0}\mathbf{O}_j$ and the rotation matrix ${}^{0}_{j}[R]$.
- As in the rigid case, information is up to the *start* of the link.
- For a point on the link *after* the origin and *along the neutral axis*

$$ {}^{0}\mathbf{p}_j = {}^{0}\mathbf{O}_j + {}^{0}_{j}[R]\mathbf{r}_j $$

- Need to find vector $\mathbf{r}_j$!!

- ${}^{0}_{j}[T]$ can be obtained by usual matrix multiplication

$$ {}^{0}_{j}[T] = {}^{0}_{1_*}[T_r]^{1_*}_{1}[T_e]^{1}_{2_*}[T_r]^{2_*}_{2}[T_e] \cdots {}^{j-1}_{j_*}[T_r]^{j_*}_{j}[T_e] $$

- ${}^{0}_{j}[T]$, as in the rigid case, contains position vector ${}^{0}\mathbf{O}_j$ and the rotation matrix ${}^{0}_{j}[R]$.
- As in the rigid case, information is up to the *start* of the link.
- For a point on the link *after* the origin and *along the neutral axis*

$$ {}^{0}\mathbf{p}_j = {}^{0}\mathbf{O}_j + {}^{0}_{j}[R]\mathbf{r}_j $$

- Need to find vector $\mathbf{r}_j$!!

D-H Convention for Flexible Links (Contd.)

Link Transformation Matrix

- ${}^{0}_{j}[T]$ can be obtained by usual matrix multiplication

$$ {}^{0}_{j}[T] = {}^{0}_{1_*}[T_r]^{1_*}_{1}[T_e]^{1}_{2_*}[T_r]^{2_*}_{2}[T_e] \cdots {}^{j-1}_{j_*}[T_r]^{j_*}_{j}[T_e] $$

- ${}^{0}_{j}[T]$, as in the rigid case, contains position vector ${}^{0}\mathbf{O}_j$ and the rotation matrix ${}^{0}_{j}[R]$.
- As in the rigid case, information is up to the *start* of the link.
- For a point on the link *after* the origin and *along the neutral axis*

$$ {}^{0}\mathbf{p}_j = {}^{0}\mathbf{O}_j + {}^{0}_{j}[R]\mathbf{r}_j $$

- Need to find vector $\mathbf{r}_j$!!

- Link j can deflect in 3D space.
- Denote deformation along the X, Y and Z axes by $u_j(s,t)$, $v_j(s,t)$ and $w_j(s,t)$.
- Only *transverse* deformations $\rightarrow$ Only 2 out u, v and w are variable!
  - For a rotary joint $u_j(s,t) = s$ and $v_j(s,t)$, $w_j(s,t)$ represent the Y and Z transverse deformations.
  - For a prismatic joint, $w_j(s,t) = s$ and $u_j(s,t)$ and $v_j(s,t)$ represent the X and Y transverse deformations.
- Local position vector $\mathbf{r}_j$ is

$$\mathbf{r}_j = \begin{cases} \begin{pmatrix} s \\ 0 \\ 0 \end{pmatrix} + \begin{pmatrix} 0 \\ v_j(s,t) \\ w_j(s,t) \end{pmatrix} & \text{if joint } j \text{ is revolute} \\ \begin{pmatrix} 0 \\ 0 \\ s \end{pmatrix} + \begin{pmatrix} u_j(s,t) \\ v_j(s,t) \\ 0 \end{pmatrix} & \text{if joint } j \text{ is prismatic} \end{cases}$$

- Link j can deflect in 3D space.
- Denote deformation along the X, Y and Z axes by $u_j(s,t)$, $v_j(s,t)$ and $w_j(s,t)$.
- Only *transverse* deformations $\rightarrow$ Only 2 out u, v and w are variable!
  - For a rotary joint $u_j(s,t) = s$ and $v_j(s,t)$, $w_j(s,t)$ represent the Y and Z transverse deformations.
  - For a prismatic joint, $w_j(s,t) = s$ and $u_j(s,t)$ and $v_j(s,t)$ represent the X and Y transverse deformations.
- Local position vector $\mathbf{r}_j$ is

$$\mathbf{r}_j = \begin{cases} \begin{pmatrix} s \\ 0 \\ 0 \end{pmatrix} + \begin{pmatrix} 0 \\ v_j(s,t) \\ w_j(s,t) \end{pmatrix} & \text{if joint } j \text{ is revolute} \\ \begin{pmatrix} 0 \\ 0 \\ s \end{pmatrix} + \begin{pmatrix} u_j(s,t) \\ v_j(s,t) \\ 0 \end{pmatrix} & \text{if joint } j \text{ is prismatic} \end{cases}$$

D-H Convention for Flexible Links (Contd.)

Link Transformation Matrix

- Link j can deflect in 3D space.
- Denote deformation along the X, Y and Z axes by $u_j(s,t)$, $v_j(s,t)$ and $w_j(s,t)$.
- Only *transverse* deformations $\rightarrow$ Only 2 out u, v and w are variable!
  - For a rotary joint $u_j(s,t) = s$ and $v_j(s,t)$, $w_j(s,t)$ represent the Y and Z transverse deformations.
  - For a prismatic joint, $w_j(s,t) = s$ and $u_j(s,t)$ and $v_j(s,t)$ represent the X and Y transverse deformations.
- Local position vector $\mathbf{r}_j$ is

$$\mathbf{r}_j = \begin{cases} \begin{pmatrix} s \\ 0 \\ 0 \end{pmatrix} + \begin{pmatrix} 0 \\ v_j(s,t) \\ w_j(s,t) \end{pmatrix} & \text{if joint } j \text{ is revolute} \\ \begin{pmatrix} 0 \\ 0 \\ s \end{pmatrix} + \begin{pmatrix} u_j(s,t) \\ v_j(s,t) \\ 0 \end{pmatrix} & \text{if joint } j \text{ is prismatic} \end{cases}$$

D-H Convention for Flexible Links (Contd.)

Link Transformation Matrix

- Link j can deflect in 3D space.
- Denote deformation along the X, Y and Z axes by $u_j(s,t)$, $v_j(s,t)$ and $w_j(s,t)$.
- Only *transverse* deformations $\rightarrow$ Only 2 out u, v and w are variable!
  - For a rotary joint $u_j(s,t) = s$ and $v_j(s,t)$, $w_j(s,t)$ represent the Y and Z transverse deformations.
  - For a prismatic joint, $w_j(s,t) = s$ and $u_j(s,t)$ and $v_j(s,t)$ represent the X and Y transverse deformations.
- Local position vector $\mathbf{r}_j$ is

$$\mathbf{r}_j = \begin{cases} \begin{pmatrix} s \\ 0 \\ 0 \end{pmatrix} + \begin{pmatrix} 0 \\ v_j(s,t) \\ w_j(s,t) \end{pmatrix} & \text{if joint } j \text{ is revolute} \\ \begin{pmatrix} 0 \\ 0 \\ s \end{pmatrix} + \begin{pmatrix} u_j(s,t) \\ v_j(s,t) \\ 0 \end{pmatrix} & \text{if joint } j \text{ is prismatic} \end{cases}$$

Velocity of a Point on a Flexible Link

- The velocity of the material point ${}^0\mathbf{p}_j$ on link j in $\{0\}$

$$ {}^0\mathbf{V}_p \triangleq \frac{d}{dt}({}^0\mathbf{p}_j) = \frac{d}{dt}({}^0\mathbf{O}_j) + \frac{d}{dt}({}^0_j[R])\mathbf{r}_j + {}^0_j[R]\frac{d}{dt}(\mathbf{r}_j) $$

- $\frac{d}{dt}(\mathbf{r}_j)$ is given by

$$ \dot{\mathbf{r}}_j = \begin{cases} \begin{pmatrix} 0 \\ \dot{v}_j(s,t) \\ \dot{w}_j(s,t) \end{pmatrix} & \text{R joint} \\ \begin{pmatrix} 0 \\ 0 \\ U_j(t) \end{pmatrix} + \begin{pmatrix} \dot{u}_j(s,t) + \frac{\partial u_j(s,t)}{\partial s} U_j(t) \\ \dot{v}_j(s,t) + \frac{\partial v_j(s,t)}{\partial s} U_j(t) \\ 0 \end{pmatrix} & \text{P joint} \end{cases} $$

$U_j(t) \triangleq \dot{s}$ is the translational velocity of the prismatic jointed link j.

Velocity of a Point on a Flexible Link

- The velocity of the material point ${}^0\mathbf{p}_j$ on link j in $\{0\}$

$$
{}^0\mathbf{V}_p \triangleq \frac{d}{dt}({}^0\mathbf{p}_j) = \frac{d}{dt}({}^0\mathbf{O}_j) + \frac{d}{dt}({}^0_j[R])\mathbf{r}_j + {}^0_j[R]\frac{d}{dt}(\mathbf{r}_j)
$$

- $\frac{d}{dt}(\mathbf{r}_j)$ is given by

$$
\dot{\mathbf{r}}_j = \begin{cases} \begin{pmatrix} 0 \\ \dot{v}_j(s,t) \\ \dot{w}_j(s,t) \end{pmatrix} & \text{R joint} \\ \begin{pmatrix} 0 \\ 0 \\ U_j(t) \end{pmatrix} + \begin{pmatrix} \dot{u}_j(s,t) + \frac{\partial u_j(s,t)}{\partial s} U_j(t) \\ \dot{v}_j(s,t) + \frac{\partial v_j(s,t)}{\partial s} U_j(t) \\ 0 \end{pmatrix} & \text{P joint} \end{cases}
$$

$U_j(t) \triangleq \dot{s}$ is the translational velocity of the prismatic jointed link j.

Discretisation of PDE

- Elastic displacements $u_j(s,t)$, $v_j(s,t)$ and $w_j(s,t)$ are governed by PDE's and boundary conditions.
- PDE's are similar to the free transverse bending vibration equation discussed earlier.
- Infinite dimensional system – infinite number of natural frequencies and mode shapes.
- PDE's need to be discretised for analysis, simulation and development of controllers.
- Two approaches – Assumed Modes Method and Finite Element Method.
- After discretisation, expression for ${}^{j*}_{j}[T_e]$ can be obtained.

Discretisation of PDE

- Elastic displacements $u_j(s,t)$, $v_j(s,t)$ and $w_j(s,t)$ are governed by PDE's and boundary conditions.
- PDE's are similar to the free transverse bending vibration equation discussed earlier.
- Infinite dimensional system – infinite number of natural frequencies and mode shapes.
- PDE's need to be discretised for analysis, simulation and development of controllers.
- Two approaches – Assumed Modes Method and Finite Element Method.
- After discretisation, expression for ${}^{j*}_{j}[T_e]$ can be obtained.

Discretisation of PDE

- Elastic displacements $u_j(s,t)$, $v_j(s,t)$ and $w_j(s,t)$ are governed by PDE's and boundary conditions.
- PDE's are similar to the free transverse bending vibration equation discussed earlier.
- Infinite dimensional system – infinite number of natural frequencies and mode shapes.
- PDE's need to be discretised for analysis, simulation and development of controllers.
- Two approaches – Assumed Modes Method and Finite Element Method.
- After discretisation, expression for ${}^{j*}_{j}[T_e]$ can be obtained.

DISCRETISATION OF PDE

- Elastic displacements $u_j(s,t)$, $v_j(s,t)$ and $w_j(s,t)$ are governed by PDE's and boundary conditions.
- PDE's are similar to the free transverse bending vibration equation discussed earlier.
- Infinite dimensional system – infinite number of natural frequencies and mode shapes.
- PDE's need to be discretised for analysis, simulation and development of controllers.
- Two approaches – Assumed Modes Method and Finite Element Method.
- After discretisation, expression for ${}^{j}_{j*}[T_e]$ can be obtained.

Discretisation of PDE

- Elastic displacements $u_j(s,t)$, $v_j(s,t)$ and $w_j(s,t)$ are governed by PDE's and boundary conditions.
- PDE's are similar to the free transverse bending vibration equation discussed earlier.
- Infinite dimensional system – infinite number of natural frequencies and mode shapes.
- PDE's need to be discretised for analysis, simulation and development of controllers.
- Two approaches – Assumed Modes Method and Finite Element Method.
- After discretisation, expression for ${}^{j_*}_{j}[T_e]$ can be obtained.

Discretisation of PDE

- Elastic displacements $u_j(s,t)$, $v_j(s,t)$ and $w_j(s,t)$ are governed by PDE's and boundary conditions.
- PDE's are similar to the free transverse bending vibration equation discussed earlier.
- Infinite dimensional system – infinite number of natural frequencies and mode shapes.
- PDE's need to be discretised for analysis, simulation and development of controllers.
- Two approaches – Assumed Modes Method and Finite Element Method.
- After discretisation, expression for ${}^{j_*}_{j}[T_e]$ can be obtained.

- Elastic displacements, (u_j, v_j, and w_j) are written in terms of modal shape functions and time-dependent mode amplitudes.

$$X_j(\eta,t) = \sum_{i=1}^{N_j} \psi_i^{X_j}(\eta)\xi_i^{X_j}(t), \quad X \text{ is } u,\ v,\ \text{or } w$$

$\eta = s/l_j$ and N_j is the number of modes chosen.

- For a revolute joint, link length l_j is constant and for a prismatic joint, l_j and the mode shape functions are time dependent.
- The mode shape functions $\psi_i(\eta)$ are typically chosen as

$$\psi_i(\eta) = C_{1_i}\cos(\beta_i\eta) + C_{2_i}\sin(\beta_i\eta) + C_{3_i}\cosh(\beta_i\eta) + C_{4_i}\sinh(\beta_i\eta)$$

$\beta_i{}^4 \triangleq \frac{\rho_j A_j l_j^4}{E_j I_j}\omega_i{}^2$ and ω_i is the ith natural angular frequency of the eigenvalue problem for link j.

- Constants C_i, $i = 1,2,3,4$ are determined using boundary conditions.

- Elastic displacements, (u_j, v_j, and w_j) are written in terms of modal shape functions and time-dependent mode amplitudes.

$$X_j(\eta,t) = \sum_{i=1}^{N_j} \psi_i^{X_j}(\eta)\xi_i^{X_j}(t), \quad X \text{ is } u,\ v,\ \text{or } w$$

$\eta = s/l_j$ and N_j is the number of modes chosen.

- For a revolute joint, link length l_j is constant and for a prismatic joint, l_j and the mode shape functions are time dependent.
- The mode shape functions $\psi_i(\eta)$ are typically chosen as

$$\psi_i(\eta) = C_{1_i}\cos(\beta_i\eta) + C_{2_i}\sin(\beta_i\eta) + C_{3_i}\cosh(\beta_i\eta) + C_{4_i}\sinh(\beta_i\eta)$$

$\beta_i{}^4 \triangleq \frac{\rho_j A_j l_j^4}{E_j I_j}\omega_i{}^2$ and ω_i is the ith natural angular frequency of the eigenvalue problem for link j.

- Constants $C_i,\ i = 1,2,3,4$ are determined using boundary conditions.

Discretisation of PDE

Assumed Modes Method

- Elastic displacements, (u_j, v_j, and w_j) are written in terms of modal shape functions and time-dependent mode amplitudes.

$$X_j(\eta, t) = \sum_{i=1}^{N_j} \psi_i^{X_j}(\eta)\xi_i^{X_j}(t), \quad X \text{ is } u, \; v, \text{ or } w$$

  $\eta = s/l_j$ and N_j is the number of modes chosen.
- For a revolute joint, link length l_j is constant and for a prismatic joint, l_j and the mode shape functions are time dependent.
- The mode shape functions $\psi_i(\eta)$ are typically chosen as

$$\psi_i(\eta) = C_{1_i}\cos(\beta_i\eta) + C_{2_i}\sin(\beta_i\eta) + C_{3_i}\cosh(\beta_i\eta) + C_{4_i}\sinh(\beta_i\eta)$$

  $\beta_i{}^4 \triangleq \frac{\rho_j A_j l_j^4}{E_j I_j}\omega_i{}^2$ and ω_i is the ith natural angular frequency of the eigenvalue problem for link j.
- Constants C_i, $i = 1,2,3,4$ are determined using boundary conditions.

Discretisation of PDE

Assumed Modes Method

- Elastic displacements, (u_j, v_j, and w_j) are written in terms of modal shape functions and time-dependent mode amplitudes.

$$X_j(\eta,t) = \sum_{i=1}^{N_j} \psi_i^{X_j}(\eta)\xi_i^{X_j}(t), \quad X \text{ is } u,\ v,\ \text{or } w$$

  $\eta = s/l_j$ and N_j is the number of modes chosen.
- For a revolute joint, link length l_j is constant and for a prismatic joint, l_j and the mode shape functions are time dependent.
- The mode shape functions $\psi_i(\eta)$ are typically chosen as

$$\psi_i(\eta) = C_{1_i}\cos(\beta_i\eta) + C_{2_i}\sin(\beta_i\eta) + C_{3_i}\cosh(\beta_i\eta) + C_{4_i}\sinh(\beta_i\eta)$$

  $\beta_i{}^4 \triangleq \frac{\rho_j A_j l_j^4}{E_j I_j}\omega_i{}^2$ and ω_i is the ith natural angular frequency of the eigenvalue problem for link j.
- Constants $C_i,\ i = 1,2,3,4$ are determined using boundary conditions.

- For clamped conditions at $\eta = 0$ end:

$$[\psi_i(\eta)]_{\eta=0} = 0, \quad \left[\frac{d\psi_i(\eta)}{d\eta}\right]_{\eta=0} = 0$$

- For mass conditions at $\eta = 1$ end:

$$\left[\frac{d^2\psi_i(\eta)}{d\eta^2}\right]_{\eta=1} = \frac{J_{p_j}\beta_i^4}{\rho_j A_j l_j^3}\left[\frac{d\psi_i(\eta)}{d\eta}\right]_{\eta=1} + \frac{M_{Dp_j}\beta_i^4}{\rho_j A_j l_j^2}[\psi_i(\eta)]_{\eta=1}$$

$$\left[\frac{d^3\psi_i(\eta)}{d\eta^3}\right]_{\eta=1} = -\frac{M_{p_j}\beta_i^4}{\rho_j A_j l_j}[\psi_i(\eta)]_{\eta=1} - \frac{M_{Dp_j}\beta_i^4}{\rho_j A_j l_j^2}\left[\frac{d\psi_i(\eta)}{d\eta}\right]_{\eta=1}$$

  - ρ_j, A_j are density and cross-section area.
  - M_{p_j}, J_{p_j} reflects all masses and inertia beyond link j.
  - M_{Dp_j} accounts for the contributions of masses non-collocated at the end of link j.

DISCRETISATION OF PDE

ASSUMED MODES METHOD (CONTD.)

- For clamped conditions at $\eta = 0$ end:

$$[\psi_i(\eta)]_{\eta=0} = 0, \quad \left[\frac{d\psi_i(\eta)}{d\eta}\right]_{\eta=0} = 0$$

- For mass conditions at $\eta = 1$ end:

$$\begin{aligned}
\left[\frac{d^2\psi_i(\eta)}{d\eta^2}\right]_{\eta=1} &= \frac{J_{p_j}\beta_i^4}{\rho_j A_j l_j^3}\left[\frac{d\psi_i(\eta)}{d\eta}\right]_{\eta=1} + \frac{M_{Dp_j}\beta_i^4}{\rho_j A_j l_j^2}[\psi_i(\eta)]_{\eta=1} \\
\left[\frac{d^3\psi_i(\eta)}{d\eta^3}\right]_{\eta=1} &= -\frac{M_{p_j}\beta_i^4}{\rho_j A_j l_j}[\psi_i(\eta)]_{\eta=1} - \frac{M_{Dp_j}\beta_i^4}{\rho_j A_j l_j^2}\left[\frac{d\psi_i(\eta)}{d\eta}\right]_{\eta=1}
\end{aligned}$$

  - ρ_j, A_j are density and cross-section area.
  - M_{p_j}, J_{p_j} reflects all masses and inertia beyond link j.
  - M_{Dp_j} accounts for the contributions of masses non-collocated at the end of link j.

Discretisation of PDE

Assumed Modes Method (contd.)

- The clamped conditions at the link base yield $C_{3_i} = -C_{1_i}$ and $C_{4_i} = -C_{2_i}$
- The mass conditions at the $\eta = 1$ yield

$$[\mathbf{F}](\beta_i) \begin{pmatrix} C_{1_i} \\ C_{2_i} \end{pmatrix} = \mathbf{0}$$

- For non-trivial solution when $\det(\mathbf{F}) = 0 \rightarrow$ Simplify to

$$(1 + \cosh\beta_i \cos\beta_i) - M_j \beta_i (\cosh\beta_i \sin\beta_i - \sinh\beta_i \cos\beta_i)$$
$$-J_j {\beta_i}^3 (\cosh\beta_i \sin\beta_i + \sinh\beta_i \cos\beta_i) + M_j J_j {\beta_i}^4 (1 - \cosh\beta_i \cos\beta_i)$$
$$-D_j^2 {\beta_i}^4 (1 - \cosh\beta_i \cos\beta_i) - 2D_j {\beta_i}^2 \sinh\beta_i \sin\beta_i = 0$$

where $M_j = \dfrac{M_{p_j}}{\rho_j A_j l_j}$, $J_j = \dfrac{J_{p_j}}{\rho_j A_j {l_j}^3}$, and $D_j = \dfrac{M_{Dp_j}}{\rho_j A_j {l_j}^2}$.

- Infinite number of solutions $\rightarrow$ Truncated to N_j roots.
- Both C_{1_i} and C_{2_i} cannot be determined uniquely and hence mode shapes can be obtained upto a scale factor.

Assumed Modes Method (contd.)

- The clamped conditions at the link base yield $C_{3_i} = -C_{1_i}$ and $C_{4_i} = -C_{2_i}$
- The mass conditions at the $\eta = 1$ yield

$$[\mathbf{F}](\beta_i)\begin{pmatrix} C_{1_i} \\ C_{2_i} \end{pmatrix} = \mathbf{0}$$

- For non-trivial solution when $\det(\mathbf{F}) = 0 \rightarrow$ Simplify to

$$\begin{aligned}(1+\cosh\beta_i\cos\beta_i) - M_j\beta_i(\cosh\beta_i\sin\beta_i - \sinh\beta_i\cos\beta_i)\\ -J_j{\beta_i}^3(\cosh\beta_i\sin\beta_i + \sinh\beta_i\cos\beta_i) + M_jJ_j{\beta_i}^4(1-\cosh\beta_i\cos\beta_i)\\ -D_j^2{\beta_i}^4(1-\cosh\beta_i\cos\beta_i) - 2D_j{\beta_i}^2\sinh\beta_i\sin\beta_i = 0\end{aligned}$$

where $M_j = \dfrac{M_{p_j}}{\rho_j A_j l_j}$, $J_j = \dfrac{J_{p_j}}{\rho_j A_j {l_j}^3}$, and $D_j = \dfrac{M_{Dp_j}}{\rho_j A_j {l_j}^2}$.

- Infinite number of solutions $\rightarrow$ Truncated to N_j roots.
- Both C_{1_i} and C_{2_i} cannot be determined uniquely and hence mode shapes can be obtained upto a scale factor.

Discretisation of PDE

Assumed Modes Method (contd.)

- The clamped conditions at the link base yield $C_{3_i} = -C_{1_i}$ and $C_{4_i} = -C_{2_i}$
- The mass conditions at the $\eta = 1$ yield

$$[\mathbf{F}](\beta_i) \begin{pmatrix} C_{1_i} \\ C_{2_i} \end{pmatrix} = \mathbf{0}$$

- For non-trivial solution when $\det(\mathbf{F}) = 0 \rightarrow$ Simplify to

$$\begin{aligned}
&(1 + \cosh\beta_i \cos\beta_i) - M_j\beta_i(\cosh\beta_i \sin\beta_i - \sinh\beta_i \cos\beta_i) \\
&\quad - J_j{\beta_i}^3(\cosh\beta_i \sin\beta_i + \sinh\beta_i \cos\beta_i) + M_j J_j {\beta_i}^4(1 - \cosh\beta_i \cos\beta_i) \\
&\quad - D_j^2 {\beta_i}^4(1 - \cosh\beta_i \cos\beta_i) - 2D_j{\beta_i}^2 \sinh\beta_i \sin\beta_i = 0
\end{aligned}$$

where $M_j = \dfrac{M_{p_j}}{\rho_j A_j l_j}$, $J_j = \dfrac{J_{p_j}}{\rho_j A_j {l_j}^3}$, and $D_j = \dfrac{M_{Dp_j}}{\rho_j A_j {l_j}^2}$.

- Infinite number of solutions $\rightarrow$ Truncated to N_j roots.
- Both C_{1_i} and C_{2_i} cannot be determined uniquely and hence mode shapes can be obtained upto a scale factor.

Discretisation of PDE

Assumed Modes Method (contd.)

- The clamped conditions at the link base yield $C_{3_i} = -C_{1_i}$ and $C_{4_i} = -C_{2_i}$
- The mass conditions at the $\eta = 1$ yield

$$[\mathbf{F}](\beta_i)\begin{pmatrix} C_{1_i} \\ C_{2_i} \end{pmatrix} = \mathbf{0}$$

- For non-trivial solution when $\det(\mathbf{F}) = 0 \rightarrow$ Simplify to

$$\begin{aligned}(1+\cosh\beta_i \cos\beta_i) - M_j\beta_i(\cosh\beta_i \sin\beta_i - \sinh\beta_i \cos\beta_i) \\ -J_j{\beta_i}^3(\cosh\beta_i \sin\beta_i + \sinh\beta_i \cos\beta_i) + M_j J_j {\beta_i}^4(1-\cosh\beta_i \cos\beta_i) \\ -D_j^2{\beta_i}^4(1-\cosh\beta_i \cos\beta_i) - 2D_j{\beta_i}^2 \sinh\beta_i \sin\beta_i = 0\end{aligned}$$

where $M_j = \dfrac{M_{p_j}}{\rho_j A_j l_j}$, $J_j = \dfrac{J_{p_j}}{\rho_j A_j {l_j}^3}$, and $D_j = \dfrac{M_{Dp_j}}{\rho_j A_j {l_j}^2}$.

- Infinite number of solutions $\rightarrow$ Truncated to N_j roots.
- Both C_{1_i} and C_{2_i} cannot be determined uniquely and hence mode shapes can be obtained upto a scale factor.

Discretisation of PDE

Assumed Modes Method (Contd.)

- The clamped conditions at the link base yield $C_{3_i} = -C_{1_i}$ and $C_{4_i} = -C_{2_i}$
- The mass conditions at the $\eta = 1$ yield

$$[\mathbf{F}](\beta_i) \begin{pmatrix} C_{1_i} \\ C_{2_i} \end{pmatrix} = \mathbf{0}$$

- For non-trivial solution when $\det(\mathbf{F}) = 0 \rightarrow$ Simplify to

$$(1+\cosh\beta_i\cos\beta_i) - M_j\beta_i(\cosh\beta_i\sin\beta_i - \sinh\beta_i\cos\beta_i)$$
$$-J_j{\beta_i}^3(\cosh\beta_i\sin\beta_i + \sinh\beta_i\cos\beta_i) + M_jJ_j{\beta_i}^4(1-\cosh\beta_i\cos\beta_i)$$
$$-D_j^2{\beta_i}^4(1-\cosh\beta_i\cos\beta_i) - 2D_j{\beta_i}^2\sinh\beta_i\sin\beta_i = 0$$

where $M_j = \dfrac{M_{p_j}}{\rho_j A_j l_j}$, $J_j = \dfrac{J_{p_j}}{\rho_j A_j {l_j}^3}$, and $D_j = \dfrac{M_{Dp_j}}{\rho_j A_j {l_j}^2}$.

- Infinite number of solutions $\rightarrow$ Truncated to N_j roots.
- Both C_{1_i} and C_{2_i} cannot be determined uniquely and hence mode shapes can be obtained upto a scale factor.

- For clamped-mass boundary condition

$$\psi_i(\eta) = C_{2_i}\,[\,\cos(\beta_i\eta) - \cosh(\beta_i\eta) + \nu_i\,(\sin(\beta_i\eta) - \sinh(\beta_i\eta))\,]$$

where

$$\nu_i = \frac{\sin\beta_i - \sinh\beta_i + M_j\beta_i(\cos\beta_i - \cosh\beta_i) - D_j{\beta_i}^2(\sin\beta_i + \sinh\beta_i)}{\cos\beta_i + \cosh\beta_i - M_j\beta_i(\sin\beta_i - \sinh\beta_i) - D_j{\beta_i}^2(\cos\beta_i - \cosh\beta_i)}$$

- Above can be solved for *one link* with rotary joint!
- For a prismatic joint and a multi-link flexible manipulator, $M_{D_{p_j}}$ and J_{p_j} are functions of time t!
- Modes shapes and frequency are time dependent!!

Discretisation of PDE

Assumed Modes Method (Contd.)

- For clamped-mass boundary condition

$$\psi_i(\eta) = C_{2_i} [\, \cos(\beta_i \eta) - \cosh(\beta_i \eta) + \nu_i (\sin(\beta_i \eta) - \sinh(\beta_i \eta)) \,]$$

where

$$\nu_i = \frac{\sin\beta_i - \sinh\beta_i + M_j \beta_i (\cos\beta_i - \cosh\beta_i) - D_j {\beta_i}^2 (\sin\beta_i + \sinh\beta_i)}{\cos\beta_i + \cosh\beta_i - M_j \beta_i (\sin\beta_i - \sinh\beta_i) - D_j {\beta_i}^2 (\cos\beta_i - \cosh\beta_i)}$$

- Above can be solved for *one link* with rotary joint!
- For a prismatic joint and a multi-link flexible manipulator, $M_{D_{p_j}}$ and J_{p_j} are functions of time t!
- Modes shapes and frequency are time dependent!!

Discretisation of PDE

Assumed Modes Method (contd.)

- For clamped-mass boundary condition

$$\psi_i(\eta) = C_{2_i} [\ \cos(\beta_i \eta) - \cosh(\beta_i \eta) + \nu_i (\sin(\beta_i \eta) - \sinh(\beta_i \eta))\ ]$$

where

$$\nu_i = \frac{\sin \beta_i - \sinh \beta_i + M_j \beta_i (\cos \beta_i - \cosh \beta_i) - D_j {\beta_i}^2 (\sin \beta_i + \sinh \beta_i)}{\cos \beta_i + \cosh \beta_i - M_j \beta_i (\sin \beta_i - \sinh \beta_i) - D_j {\beta_i}^2 (\cos \beta_i - \cosh \beta_i)}$$

- Above can be solved for *one link* with rotary joint!
- For a prismatic joint and a multi-link flexible manipulator, $M_{D_{p_j}}$ and J_{p_j} are functions of time t!
- Modes shapes and frequency are time dependent!!

- For clamped-mass boundary condition

$$\psi_i(\eta) = C_{2_i}\,[\,\cos(\beta_i\eta) - \cosh(\beta_i\eta) + \nu_i\,(\sin(\beta_i\eta) - \sinh(\beta_i\eta))\,]$$

where

$$\nu_i = \frac{\sin\beta_i - \sinh\beta_i + M_j\beta_i(\cos\beta_i - \cosh\beta_i) - D_j{\beta_i}^2(\sin\beta_i + \sinh\beta_i)}{\cos\beta_i + \cosh\beta_i - M_j\beta_i(\sin\beta_i - \sinh\beta_i) - D_j{\beta_i}^2(\cos\beta_i - \cosh\beta_i)}$$

- Above can be solved for *one link* with rotary joint!
- For a prismatic joint and a multi-link flexible manipulator, $M_{D_{p_j}}$ and J_{p_j} are functions of time t!
- Modes shapes and frequency are time dependent!!

- Time dependent frequency equation

$$f(\beta_i, M_j, J_j, D_j) = (1 + \cosh\beta_i \cos\beta_i) - M_j\beta_i(\cosh\beta_i \sin\beta_i - \sinh\beta_i \cos\beta_i) \\ -J_j{\beta_i}^3(\cosh\beta_i \sin\beta_i + \sinh\beta_i \cos\beta_i) + M_j J_j{\beta_i}^4(1 - \cosh\beta_i \cos\beta_i) \\ -{D_j}^2{\beta_i}^4(1 - \cosh\beta_i \cos\beta_i) - 2D_j{\beta_i}^2 \sinh\beta_i \sin\beta_i = 0$$

- Above can be written as a ODE

$$\frac{d\beta_i}{dt} = \frac{-\left(\frac{\partial f}{\partial M_j}\frac{dM_j}{dt} + \frac{\partial f}{\partial J_j}\frac{dJ_j}{dt} + \frac{\partial f}{\partial D_j}\frac{dD_j}{dt}\right)}{\left(\frac{\partial f}{\partial \beta_i}\right)}$$

where the derivatives can be obtained from the frequency equation.

- Solve for β_i once at $t = 0$ and numerically integrate ODE with equations of motion $\rightarrow$ No need to update β_i with configuration.

- Time dependent frequency equation

$$
\begin{aligned}
f(\beta_i, M_j, J_j, D_j) = (1+\cosh\beta_i\cos\beta_i) - M_j\beta_i(\cosh\beta_i\sin\beta_i - \sinh\beta_i\cos\beta_i) \\
-J_j{\beta_i}^3(\cosh\beta_i\sin\beta_i + \sinh\beta_i\cos\beta_i) + M_jJ_j{\beta_i}^4(1-\cosh\beta_i\cos\beta_i) \\
-{D_j}^2{\beta_i}^4(1-\cosh\beta_i\cos\beta_i) - 2D_j{\beta_i}^2\sinh\beta_i\sin\beta_i = 0
\end{aligned}
$$

- Above can be written as a ODE

$$
\frac{d\beta_i}{dt} = \frac{-\left(\frac{\partial f}{\partial M_j}\frac{dM_j}{dt} + \frac{\partial f}{\partial J_j}\frac{dJ_j}{dt} + \frac{\partial f}{\partial D_j}\frac{dD_j}{dt}\right)}{\left(\frac{\partial f}{\partial \beta_i}\right)}
$$

where the derivatives can be obtained from the frequency equation.

- Solve for β_i once at $t=0$ and numerically integrate ODE with equations of motion $\rightarrow$ No need to update β_i with configuration.

Discretisation of PDE

Assumed Modes Method (Contd.)

- Time dependent frequency equation

$$\begin{aligned} f(\beta_i, M_j, J_j, D_j) = & (1+\cosh\beta_i\cos\beta_i) - M_j\beta_i(\cosh\beta_i\sin\beta_i - \sinh\beta_i\cos\beta_i) \\ & -J_j{\beta_i}^3(\cosh\beta_i\sin\beta_i + \sinh\beta_i\cos\beta_i) + M_jJ_j{\beta_i}^4(1-\cosh\beta_i\cos\beta_i) \\ & -{D_j}^2{\beta_i}^4(1-\cosh\beta_i\cos\beta_i) - 2D_j{\beta_i}^2\sinh\beta_i\sin\beta_i = 0 \end{aligned}$$

- Above can be written as a ODE

$$\frac{d\beta_i}{dt} = \frac{-\left(\frac{\partial f}{\partial M_j}\frac{dM_j}{dt} + \frac{\partial f}{\partial J_j}\frac{dJ_j}{dt} + \frac{\partial f}{\partial D_j}\frac{dD_j}{dt}\right)}{\left(\frac{\partial f}{\partial \beta_i}\right)}$$

where the derivatives can be obtained from the frequency equation.

- Solve for β_i once at $t=0$ and numerically integrate ODE with equations of motion $\rightarrow$ No need to update β_i with configuration.

Discretisation of PDE

Assumed Modes Method (contd.)

- After discretisation the 4×4 matrix ${}^{j_*}_{j}[T_e]$ can be obtained.
- If joint $j-1$ is revolute

$$
{}^{j_*}_{j}[T_e] = \sum_{i=1}^{N_{j-1}} \begin{pmatrix} 1 & -\frac{\partial \psi_i^v}{\partial \eta}(1)\xi_i^v(t) & \frac{\partial \psi_i^w}{\partial \eta}(1)\xi_i^w(t) & 0 \\ \frac{\partial \psi_i^v}{\partial \eta}(1)\xi_i^v(t) & 1 & 0 & \psi_i^v(1)\xi_i^v(t) \\ -\frac{\partial \psi_i^w}{\partial \eta}(1)\xi_i^w(t) & 0 & 1 & \psi_i^w(1)\xi_i^w(t) \\ 0 & 0 & 0 & 1 \end{pmatrix}
$$

- If joint $j-1$ is prismatic

$$
{}^{j_*}_{j}[T_e] = \sum_{i=1}^{N_{j-1}} \begin{pmatrix} 1 & 0 & \frac{\partial \psi_i^u}{\partial \eta}(1)\xi_i^u(t) & \psi_i^u(1)\xi_i^u(t) \\ 0 & 1 & -\frac{\partial \psi_i^v}{\partial \eta}(1)\xi_i^v(t) & \psi_i^v(1)\xi_i^v(t) \\ -\frac{\partial \psi_i^u}{\partial \eta}(1)\xi_i^u(t) & \frac{\partial \psi_i^v}{\partial \eta}(1)\xi_i^v(t) & 1 & 0 \\ 0 & 0 & 0 & 1 \end{pmatrix}
$$

Discretisation of PDE

Assumed Modes Method (contd.)

- After discretisation the 4×4 matrix ${}^{j_*}_{j}[T_e]$ can be obtained.
- If joint $j-1$ is revolute

$$
{}^{j_*}_{j}[T_e] = \sum_{i=1}^{N_{j-1}} \begin{pmatrix} 1 & -\frac{\partial \psi_i^v}{\partial \eta}(1)\xi_i^v(t) & \frac{\partial \psi_i^w}{\partial \eta}(1)\xi_i^w(t) & 0 \\ \frac{\partial \psi_i^v}{\partial \eta}(1)\xi_i^v(t) & 1 & 0 & \psi_i^v(1)\xi_i^v(t) \\ -\frac{\partial \psi_i^w}{\partial \eta}(1)\xi_i^w(t) & 0 & 1 & \psi_i^w(1)\xi_i^w(t) \\ 0 & 0 & 0 & 1 \end{pmatrix}
$$

- If joint $j-1$ is prismatic

$$
{}^{j_*}_{j}[T_e] = \sum_{i=1}^{N_{j-1}} \begin{pmatrix} 1 & 0 & \frac{\partial \psi_i^u}{\partial \eta}(1)\xi_i^u(t) & \psi_i^u(1)\xi_i^u(t) \\ 0 & 1 & -\frac{\partial \psi_i^v}{\partial \eta}(1)\xi_i^v(t) & \psi_i^v(1)\xi_i^v(t) \\ -\frac{\partial \psi_i^u}{\partial \eta}(1)\xi_i^u(t) & \frac{\partial \psi_i^v}{\partial \eta}(1)\xi_i^v(t) & 1 & 0 \\ 0 & 0 & 0 & 1 \end{pmatrix}
$$

Discretisation of PDE

Assumed Modes Method (contd.)

- After discretisation the 4×4 matrix ${}^{j_*}_{j}[T_e]$ can be obtained.
- If joint $j-1$ is revolute

$$
{}^{j_*}_{j}[T_e] = \sum_{i=1}^{N_{j-1}} \begin{pmatrix} 1 & -\frac{\partial \psi_i^v}{\partial \eta}(1)\xi_i^v(t) & \frac{\partial \psi_i^w}{\partial \eta}(1)\xi_i^w(t) & 0 \\ \frac{\partial \psi_i^v}{\partial \eta}(1)\xi_i^v(t) & 1 & 0 & \psi_i^v(1)\xi_i^v(t) \\ -\frac{\partial \psi_i^w}{\partial \eta}(1)\xi_i^w(t) & 0 & 1 & \psi_i^w(1)\xi_i^w(t) \\ 0 & 0 & 0 & 1 \end{pmatrix}
$$

- If joint $j-1$ is prismatic

$$
{}^{j_*}_{j}[T_e] = \sum_{i=1}^{N_{j-1}} \begin{pmatrix} 1 & 0 & \frac{\partial \psi_i^u}{\partial \eta}(1)\xi_i^u(t) & \psi_i^u(1)\xi_i^u(t) \\ 0 & 1 & -\frac{\partial \psi_i^v}{\partial \eta}(1)\xi_i^v(t) & \psi_i^v(1)\xi_i^v(t) \\ -\frac{\partial \psi_i^u}{\partial \eta}(1)\xi_i^u(t) & \frac{\partial \psi_i^v}{\partial \eta}(1)\xi_i^v(t) & 1 & 0 \\ 0 & 0 & 0 & 1 \end{pmatrix}
$$

- Derivative of $\mathbf{r}_j$ is given by

$$\dot{\mathbf{r}}_j = \begin{cases} \begin{pmatrix} 0 \\ \sum_{i=1}^{N_j} \psi_i^v(\eta) \frac{d\xi_i^v(t)}{dt} \\ \sum_{i=1}^{N_j} \psi_i^w(\eta) \frac{d\xi_i^w(t)}{dt} \end{pmatrix} & \text{if joint } j \text{ is revolute} \\ \begin{pmatrix} \sum_{i=1}^{N_j} \left[\psi_i^u(\eta) \frac{d\xi_i^u(t)}{dt} - \frac{\partial \psi_i^u(\eta)}{\partial \eta} \xi_i^u(t) \frac{\eta U_j(t)}{l_j(t)} \right] \\ \sum_{i=1}^{N_j} \left[\psi_i^v(\eta) \frac{d\xi_i^v(t)}{dt} - \frac{\partial \psi_i^v(\eta)}{\partial \eta} \xi_i^v(t) \frac{\eta U_j(t)}{l_j(t)} \right] \\ U_j(t) \end{pmatrix} & \text{if joint } j \text{ is prismatic} \end{cases}$$

- In ${}^0_j[T]$, there are j rigid-joint variables $\mathbf{q}_{r_j}$.
- Flexible variables $(\mathbf{q}_{f_1}, \mathbf{q}_{f_2}, \cdots, \mathbf{q}_{f_{j-1}})$, each $\mathbf{q}_{f_k}$ has $2 \times N_k$ variables.
- From $\mathbf{r}_j$, additional $2 \times N_j$ flexible variables.

- Derivative of $\mathbf{r}_j$ is given by

$$\dot{\mathbf{r}}_j = \begin{cases} \begin{pmatrix} 0 \\ \sum_{i=1}^{N_j} \psi_i^v(\eta) \dfrac{d\xi_i^v(t)}{dt} \\ \sum_{i=1}^{N_j} \psi_i^w(\eta) \dfrac{d\xi_i^w(t)}{dt} \end{pmatrix} & \text{if joint } j \text{ is revolute} \\ \begin{pmatrix} \sum_{i=1}^{N_j} \left[\psi_i^u(\eta) \dfrac{d\xi_i^u(t)}{dt} - \dfrac{\partial \psi_i^u(\eta)}{\partial \eta} \xi_i^u(t) \dfrac{\eta U_j(t)}{l_j(t)} \right] \\ \sum_{i=1}^{N_j} \left[\psi_i^v(\eta) \dfrac{d\xi_i^v(t)}{dt} - \dfrac{\partial \psi_i^v(\eta)}{\partial \eta} \xi_i^v(t) \dfrac{\eta U_j(t)}{l_j(t)} \right] \\ U_j(t) \end{pmatrix} & \text{if joint } j \text{ is prismatic} \end{cases}$$

- In ${}^0_j[T]$, there are j rigid-joint variables $\mathbf{q}_{r_j}$.
- Flexible variables $(\mathbf{q}_{f_1}, \mathbf{q}_{f_2}, \cdots, \mathbf{q}_{f_{j-1}})$, each $\mathbf{q}_{f_k}$ has $2 \times N_k$ variables.
- From $\mathbf{r}_j$, additional $2 \times N_j$ flexible variables.

Discretisation of PDE

Assumed Modes Method (Contd.)

- Derivative of $\mathbf{r}_j$ is given by

$$\dot{\mathbf{r}}_j = \begin{cases} \begin{pmatrix} 0 \\ \sum_{i=1}^{N_j} \psi_i^v(\eta) \frac{d\xi_i^v(t)}{dt} \\ \sum_{i=1}^{N_j} \psi_i^w(\eta) \frac{d\xi_i^w(t)}{dt} \end{pmatrix} & \text{if joint } j \text{ is revolute} \\ \begin{pmatrix} \sum_{i=1}^{N_j} \left[\psi_i^u(\eta) \frac{d\xi_i^u(t)}{dt} - \frac{\partial \psi_i^u(\eta)}{\partial \eta} \xi_i^u(t) \frac{\eta U_j(t)}{l_j(t)} \right] \\ \sum_{i=1}^{N_j} \left[\psi_i^v(\eta) \frac{d\xi_i^v(t)}{dt} - \frac{\partial \psi_i^v(\eta)}{\partial \eta} \xi_i^v(t) \frac{\eta U_j(t)}{l_j(t)} \right] \\ U_j(t) \end{pmatrix} & \text{if joint } j \text{ is prismatic} \end{cases}$$

- In ${}^0_j[T]$, there are j rigid-joint variables $\mathbf{q}_{r_j}$.
- Flexible variables $(\mathbf{q}_{f_1}, \mathbf{q}_{f_2}, \cdots, \mathbf{q}_{f_{j-1}})$, each $\mathbf{q}_{f_k}$ has $2 \times N_k$ variables.
- From $\mathbf{r}_j$, additional $2 \times N_j$ flexible variables.

Discretisation of PDE

Assumed Modes Method (contd.)

- Derivative of $\mathbf{r}_j$ is given by

$$\dot{\mathbf{r}}_j = \begin{cases} \begin{pmatrix} 0 \\ \sum_{i=1}^{N_j} \psi_i^v(\eta) \frac{d\xi_i^v(t)}{dt} \\ \sum_{i=1}^{N_j} \psi_i^w(\eta) \frac{d\xi_i^w(t)}{dt} \end{pmatrix} & \text{if joint } j \text{ is revolute} \\ \begin{pmatrix} \sum_{i=1}^{N_j} \left[\psi_i^u(\eta) \frac{d\xi_i^u(t)}{dt} - \frac{\partial \psi_i^u(\eta)}{\partial \eta} \xi_i^u(t) \frac{\eta U_j(t)}{l_j(t)} \right] \\ \sum_{i=1}^{N_j} \left[\psi_i^v(\eta) \frac{d\xi_i^v(t)}{dt} - \frac{\partial \psi_i^v(\eta)}{\partial \eta} \xi_i^v(t) \frac{\eta U_j(t)}{l_j(t)} \right] \\ U_j(t) \end{pmatrix} & \text{if joint } j \text{ is prismatic} \end{cases}$$

- In ${}^0_j[T]$, there are j rigid-joint variables $\mathbf{q}_{r_j}$.
- Flexible variables $(\mathbf{q}_{f_1}, \mathbf{q}_{f_2}, \cdots, \mathbf{q}_{f_{j-1}})$, each $\mathbf{q}_{f_k}$ has $2 \times N_k$ variables.
- From $\mathbf{r}_j$, additional $2 \times N_j$ flexible variables.

- Finite element method is popular in many applications involving deformation in solids and fluid flows.
- In flexible manipulators – each link is 'broken' into finite number of elements.
- Displacements are made *continuous* inside an element and *compatible* across elements.
- Internal force balance at points, called 'nodes', in an element.
- Displacement at any point inside an element is obtained from *nodal displacements* and by an *interpolation function*.

- Finite element method is popular in many applications involving deformation in solids and fluid flows.
- In flexible manipulators – each link is 'broken' into finite number of elements.
- Displacements are made *continuous* inside an element and *compatible* across elements.
- Internal force balance at points, called 'nodes', in an element.
- Displacement at any point inside an element is obtained from *nodal displacements* and by an *interpolation function*.

- Finite element method is popular in many applications involving deformation in solids and fluid flows.
- In flexible manipulators – each link is 'broken' into finite number of elements.
- Displacements are made *continuous* inside an element and *compatible* across elements.
- Internal force balance at points, called 'nodes', in an element.
- Displacement at any point inside an element is obtained from *nodal displacements* and by an *interpolation function*.

DISCRETISATION OF PDE

FINITE ELEMENT METHOD

- Finite element method is popular in many applications involving deformation in solids and fluid flows.
- In flexible manipulators – each link is 'broken' into finite number of elements.
- Displacements are made *continuous* inside an element and *compatible* across elements.
- Internal force balance at points, called 'nodes', in an element.
- Displacement at any point inside an element is obtained from *nodal displacements* and by an *interpolation function*.

- Finite element method is popular in many applications involving deformation in solids and fluid flows.
- In flexible manipulators – each link is 'broken' into finite number of elements.
- Displacements are made *continuous* inside an element and *compatible* across elements.
- Internal force balance at points, called 'nodes', in an element.
- Displacement at any point inside an element is obtained from *nodal displacements* and by an *interpolation function*.

Discretisation of PDE

Finite Element Method (contd.)

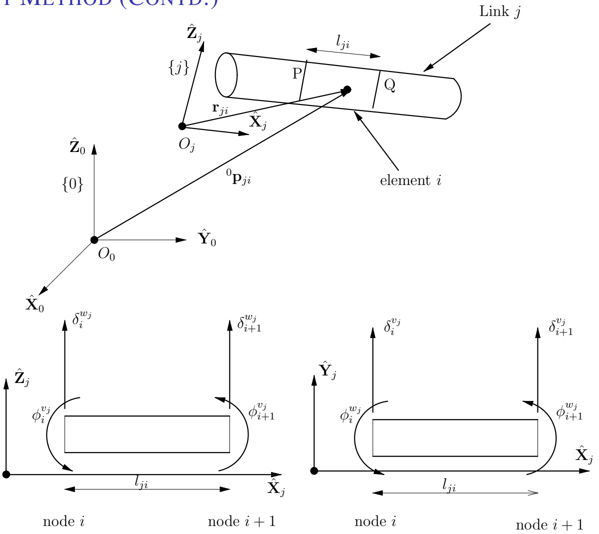

Figure 14: A finite element discretisation of a link j with beam element i and its nodal displacement variables.

Discretisation of PDE

Finite Element Method (Contd.)

- Figure 14 shows PQ, an element i on link j, with nodes i and $i+1$.
- Position vector $\mathbf{r}_{ji}$ of any point along the neutral axis of the ith element, expressed in the undeformed link coordinate system is given by

$$\mathbf{r}_{ji} = \begin{cases} \begin{pmatrix} (i-1)l_{ji}+s \\ 0 \\ 0 \end{pmatrix} + \begin{pmatrix} 0 \\ v_{ji}(s,t) \\ w_{ji}(s,t) \end{pmatrix} & \text{if joint } j \text{ is revolute} \\ \\ \begin{pmatrix} 0 \\ 0 \\ (i-1)l_{ji}+s \end{pmatrix} + \begin{pmatrix} u_{ji}(s,t) \\ v_{ji}(s,t) \\ 0 \end{pmatrix} & \text{if joint } j \text{ is prismatic} \end{cases}$$

  l_{ji} is the length of element i.
- l_{ji} is constant for revolute jointed link and variable for prismatic jointed link!

- Figure 14 shows PQ, an element i on link j, with nodes i and $i+1$.
- Position vector $\mathbf{r}_{ji}$ of any point along the neutral axis of the ith element, expressed in the undeformed link coordinate system is given by

$$\mathbf{r}_{ji} = \begin{cases} \begin{pmatrix} (i-1)l_{ji}+s \\ 0 \\ 0 \end{pmatrix} + \begin{pmatrix} 0 \\ v_{ji}(s,t) \\ w_{ji}(s,t) \end{pmatrix} & \text{if joint } j \text{ is revolute} \\ \begin{pmatrix} 0 \\ 0 \\ (i-1)l_{ji}+s \end{pmatrix} + \begin{pmatrix} u_{ji}(s,t) \\ v_{ji}(s,t) \\ 0 \end{pmatrix} & \text{if joint } j \text{ is prismatic} \end{cases}$$

l_{ji} is the length of element i.

- l_{ji} is constant for revolute jointed link and variable for prismatic jointed link!

Discretisation of PDE

Finite Element Method (Contd.)

- Figure 14 shows PQ, an element i on link j, with nodes i and $i+1$.
- Position vector $\mathbf{r}_{ji}$ of any point along the neutral axis of the ith element, expressed in the undeformed link coordinate system is given by

$$\mathbf{r}_{ji} = \begin{cases} \begin{pmatrix} (i-1)l_{ji}+s \\ 0 \\ 0 \end{pmatrix} + \begin{pmatrix} 0 \\ v_{ji}(s,t) \\ w_{ji}(s,t) \end{pmatrix} & \text{if joint } j \text{ is revolute} \\ \\ \begin{pmatrix} 0 \\ 0 \\ (i-1)l_{ji}+s \end{pmatrix} + \begin{pmatrix} u_{ji}(s,t) \\ v_{ji}(s,t) \\ 0 \end{pmatrix} & \text{if joint } j \text{ is prismatic} \end{cases}$$

  l_{ji} is the length of element i.
- l_{ji} is constant for revolute jointed link and variable for prismatic jointed link!

Discretisation of PDE

Finite Element Method (contd.)

- Elastic displacements if joint j is revolute,

$$v_{ji}(s,t) = \varphi_i^{v_j}(s)^T \mathbf{q}_{f_{ji}}^{v_j}(t), \quad w_{ji}(s,t) = \varphi_i^{w_j}(s)^T \mathbf{q}_{f_{ji}}^{w_j}(t)$$

with $\mathbf{q}_{f_{ji}}^{v_j}(t)$ denoting the vector $\left(\delta_i^{v_j}(t), \phi_i^{w_j}(t), \delta_{i+1}^{v_j}(t), \phi_{i+1}^{w_j}(t)\right)^T$ and $\mathbf{q}_{f_{ji}}^{w_j}(t)$ denoting the vector $\left(\delta_i^{w_j}(t), \phi_i^{v_j}(t), \delta_{i+1}^{w_j}(t), \phi_{i+1}^{v_j}(t)\right)^T$.

- Elastic displacements if joint j is prismatic

$$u_{ji}(s,t) = \varphi_i^{u_j}(s)^T \mathbf{q}_{f_{ji}}^{u_j}(t), \quad v_{ji}(s,t) = \varphi_i^{v_j}(s)^T \mathbf{q}_{f_{ji}}^{v_j}(t)$$

with $\mathbf{q}_{f_{ji}}^{u_j}(t)$ denoting the vector $\left(\delta_i^{u_j}(t), \phi_i^{v_j}(t), \delta_{i+1}^{u_j}(t), \phi_{i+1}^{v_j}(t)\right)^T$ and $\mathbf{q}_{f_{ji}}^{v_j}(t)$ denoting the vector $\left(\delta_i^{v_j}(t), \phi_i^{u_j}(t), \delta_{i+1}^{v_j}(t), \phi_{i+1}^{u_j}(t)\right)^T$.

- Elastic displacements if joint j is revolute,

$$v_{ji}(s,t) = \varphi_i^{v_j}(s)^T \mathbf{q}_{f_{ji}}^{v_j}(t), \quad w_{ji}(s,t) = \varphi_i^{w_j}(s)^T \mathbf{q}_{f_{ji}}^{w_j}(t)$$

  with $\mathbf{q}_{f_{ji}}^{v_j}(t)$ denoting the vector $\left(\delta_i^{v_j}(t), \phi_i^{w_j}(t), \delta_{i+1}^{v_j}(t), \phi_{i+1}^{w_j}(t)\right)^T$ and $\mathbf{q}_{f_{ji}}^{w_j}(t)$ denoting the vector $\left(\delta_i^{w_j}(t), \phi_i^{v_j}(t), \delta_{i+1}^{w_j}(t), \phi_{i+1}^{v_j}(t)\right)^T$.
- Elastic displacements if joint j is prismatic

$$u_{ji}(s,t) = \varphi_i^{u_j}(s)^T \mathbf{q}_{f_{ji}}^{u_j}(t), \quad v_{ji}(s,t) = \varphi_i^{v_j}(s)^T \mathbf{q}_{f_{ji}}^{v_j}(t)$$

  with $\mathbf{q}_{f_{ji}}^{u_j}(t)$ denoting the vector $\left(\delta_i^{u_j}(t), \phi_i^{v_j}(t), \delta_{i+1}^{u_j}(t), \phi_{i+1}^{v_j}(t)\right)^T$ and $\mathbf{q}_{f_{ji}}^{v_j}(t)$ denoting the vector $\left(\delta_i^{v_j}(t), \phi_i^{u_j}(t), \delta_{i+1}^{v_j}(t), \phi_{i+1}^{u_j}(t)\right)^T$.

- Interpolation functions are assumed same for u, v and w.
- Various choices possible → choose simple cubic polynomials

$$\varphi_i^{u_j}(s) = \varphi_i^{v_j}(s) = \varphi_i^{w_j}(s) = \begin{pmatrix} 1 - 3\left(\frac{s}{l_{ji}}\right)^2 + 2\left(\frac{s}{l_{ji}}\right)^3 \\ s\left(\frac{s}{l_{ji}} - 1\right)^2 \\ \left(\frac{s}{l_{ji}}\right)^2\left(3 - 2\frac{s}{l_{ji}}\right) \\ \frac{s^2}{l_{ji}}\left(\frac{s}{l_{ji}} - 1\right) \end{pmatrix}$$

- l_{ji} is constant for revolute jointed link and variable for prismatic jointed link → More difficult to model prismatic jointed link.

Discretisation of PDE

Finite Element Method (Contd.)

- Interpolation functions are assumed same for u, v and w.
- Various choices possible $\rightarrow$ choose simple cubic polynomials

$$\varphi_i^{u_j}(s) = \varphi_i^{v_j}(s) = \varphi_i^{w_j}(s) = \begin{pmatrix} 1 - 3\left(\frac{s}{l_{ji}}\right)^2 + 2\left(\frac{s}{l_{ji}}\right)^3 \\ s\left(\frac{s}{l_{ji}} - 1\right)^2 \\ \left(\frac{s}{l_{ji}}\right)^2\left(3 - 2\frac{s}{l_{ji}}\right) \\ \frac{s^2}{l_{ji}}\left(\frac{s}{l_{ji}} - 1\right) \end{pmatrix}$$

- l_{ji} is constant for revolute jointed link and variable for prismatic jointed link $\rightarrow$ More difficult to model prismatic jointed link.

- Interpolation functions are assumed same for u, v and w.
- Various choices possible → choose simple cubic polynomials

$$\varphi_i^{u_j}(s) = \varphi_i^{v_j}(s) = \varphi_i^{w_j}(s) = \begin{pmatrix} 1 - 3\left(\frac{s}{l_{ji}}\right)^2 + 2\left(\frac{s}{l_{ji}}\right)^3 \\ s\left(\frac{s}{l_{ji}} - 1\right)^2 \\ \left(\frac{s}{l_{ji}}\right)^2\left(3 - 2\frac{s}{l_{ji}}\right) \\ \frac{s^2}{l_{ji}}\left(\frac{s}{l_{ji}} - 1\right) \end{pmatrix}$$

- l_{ji} is constant for revolute jointed link and variable for prismatic jointed link → More difficult to model prismatic jointed link.

- 4×4 homogeneous transformation matrix ${}^{j_*}_{j}[T_e]$ in the finite element model reduces to

$$
{}^{j_*}_{j}[T_e] = \begin{pmatrix} 1 & -\phi^w_{N+1} & \phi^v_{N+1} & 0 \\ \phi^w_{N+1} & 1 & 0 & \delta^v_{N+1} \\ -\phi^v_{N+1} & 0 & 1 & \delta^w_{N+1} \\ 0 & 0 & 0 & 1 \end{pmatrix}, \quad \text{Joint } \; j-1 \text{ is revolute}
$$

$$
{}^{j_*}_{j}[T_e] = \begin{pmatrix} 1 & 0 & \phi^v_{N+1} & \delta^u_{N+1} \\ 0 & 1 & -\phi^u_{N+1} & \delta^v_{N+1} \\ -\phi^v_{N+1} & \phi^u_{N+1} & 1 & 0 \\ 0 & 0 & 0 & 1 \end{pmatrix}, \quad \text{Joint } \; j-1 \text{ is prismatic}
$$

- For clamped boundary conditions at element 1 $\rightarrow \delta_{j1} = \phi_{j1} = 0$.
- To enforce natural boundary conditions proper energy expressions for additional masses and inertia should be used.

- 4×4 homogeneous transformation matrix ${}^{j_*}_{j}[T_e]$ in the finite element model reduces to

$$
{}^{j_*}_{j}[T_e] = \begin{pmatrix} 1 & -\phi^w_{N+1} & \phi^v_{N+1} & 0 \\ \phi^w_{N+1} & 1 & 0 & \delta^v_{N+1} \\ -\phi^v_{N+1} & 0 & 1 & \delta^w_{N+1} \\ 0 & 0 & 0 & 1 \end{pmatrix}, \quad \text{Joint } \; j-1 \text{ is revolute}
$$

$$
{}^{j_*}_{j}[T_e] = \begin{pmatrix} 1 & 0 & \phi^v_{N+1} & \delta^u_{N+1} \\ 0 & 1 & -\phi^u_{N+1} & \delta^v_{N+1} \\ -\phi^v_{N+1} & \phi^u_{N+1} & 1 & 0 \\ 0 & 0 & 0 & 1 \end{pmatrix}, \quad \text{Joint } \; j-1 \text{ is prismatic}
$$

- For clamped boundary conditions at element 1 $\rightarrow \delta_{j1} = \phi_{j1} = 0$.
- To enforce natural boundary conditions proper energy expressions for additional masses and inertia should be used.

DISCRETISATION OF PDE

FINITE ELEMENT METHOD (CONTD.)

- 4×4 homogeneous transformation matrix ${}^{j_*}_{j}[T_e]$ in the finite element model reduces to

$$
{}^{j_*}_{j}[T_e] = \begin{pmatrix} 1 & -\phi^w_{N+1} & \phi^v_{N+1} & 0 \\ \phi^w_{N+1} & 1 & 0 & \delta^v_{N+1} \\ -\phi^v_{N+1} & 0 & 1 & \delta^w_{N+1} \\ 0 & 0 & 0 & 1 \end{pmatrix}, \quad \text{Joint } \; j-1 \text{ is revolute}
$$

$$
{}^{j_*}_{j}[T_e] = \begin{pmatrix} 1 & 0 & \phi^v_{N+1} & \delta^u_{N+1} \\ 0 & 1 & -\phi^u_{N+1} & \delta^v_{N+1} \\ -\phi^v_{N+1} & \phi^u_{N+1} & 1 & 0 \\ 0 & 0 & 0 & 1 \end{pmatrix}, \quad \text{Joint } \; j-1 \text{ is prismatic}
$$

- For clamped boundary conditions at element $1 \rightarrow \delta_{j1} = \phi_{j1} = 0$.
- To enforce natural boundary conditions proper energy expressions for additional masses and inertia should be used.

- Velocity of any point on the neutral axis of the ith element in the jth link in the local undeformed coordinate system

$$
\dot{\mathbf{r}}_{ji} = \begin{cases}
\begin{pmatrix}
0 \\
\sum_{k=1}^{4} \varphi_{ik}^{v}(s, l_{ji}) \frac{dq_{f_{jik}}^{v}(t)}{dt} \\
\sum_{k=1}^{4} \varphi_{ik}^{w}(s, l_{ji}) \frac{dq_{f_{jik}}^{w}(t)}{dt}
\end{pmatrix} & \text{joint } j \text{ is R} \\[2ex]
\begin{pmatrix}
\sum_{k=1}^{4} \left[\varphi_{ik}^{u}(s, l_{ji}) \frac{dq_{f_{jik}}^{u}(t)}{dt} + \frac{\partial \varphi_{ik}^{u}(s, l_{ji})}{\partial l_{ji}(t)} q_{f_{jik}}^{u}(t) \frac{U_j(t)}{N_j} \right] \\
\sum_{k=1}^{4} \left[\varphi_{ik}^{v}(s, l_{ji}) \frac{dq_{f_{jik}}^{v}(t)}{dt} + \frac{\partial \varphi_{ik}^{v}(s, l_{ji})}{\partial l_{ji}(t)} q_{f_{jik}}^{v}(t) \frac{U_j(t)}{N_j} \right] \\
\frac{i U_j(t)}{N_j}
\end{pmatrix} & \text{joint } j \text{ is P}
\end{cases}
$$

Comparison of AMM and FEM

- Number of modes Vs. Number of elements
  - AMM: k modes k natural frequencies, FEM: k elements $2k$ natural frequencies.

Mode No.	Number of Elements 1	2	3	Exact Values
1	$2.0963e+2$	$2.0873e+2$	$2.0864e+2$	$2.0864e+2$
2	$2.0654e+3$	$1.3186e+3$	$1.3118e+3$	$1.3075e+3$
3		$4.4597e+3$	$3.7067e+3$	$3.6611e+3$
4		$1.2944e+4$	$8.3473e+3$	$7.1742e+3$
5			$1.5709e+4$	$1.1860e+4$
6			$3.1318e+4$	$1.7716e+4$

Table 1: Natural frequencies(Hz) of a clamped-free beam, $m = 0.33kg$, $l = 1.0$m, Inertia of joint 3.2 $\mathrm{kg/m^2}$ and $EI = 1165.5\mathrm{N}/m^2$

- Only first k frequencies from FEM are close $\rightarrow$ k modes are equivalent to k elements.
- Typically 2 or three modes(elements) are enough to model dynamics.

Discretisation of PDE

Comparison of AMM and FEM

- Number of modes Vs. Number of elements
  - AMM: k modes k natural frequencies, FEM: k elements $2k$ natural frequencies.

Mode No.	Number of Elements 1	2	3	Exact Values
1	$2.0963e+2$	$2.0873e+2$	$2.0864e+2$	$2.0864e+2$
2	$2.0654e+3$	$1.3186e+3$	$1.3118e+3$	$1.3075e+3$
3		$4.4597e+3$	$3.7067e+3$	$3.6611e+3$
4		$1.2944e+4$	$8.3473e+3$	$7.1742e+3$
5			$1.5709e+4$	$1.1860e+4$
6			$3.1318e+4$	$1.7716e+4$

Table 1: Natural frequencies(Hz) of a clamped-free beam, $m = 0.33kg$, $l = 1.0$m, Inertia of joint 3.2 $\mathrm{kg/m^2}$ and $EI = 1165.5\mathrm{N}/m^2$

- Only first k frequencies from FEM are close $\rightarrow$ k modes are equivalent to k elements.
- Typically 2 or three modes(elements) are enough to model dynamics.

- Number of modes Vs. Number of elements
  - AMM: k modes k natural frequencies, FEM: k elements $2k$ natural frequencies.

Mode No.	Number of Elements 1	2	3	Exact Values
1	$2.0963e+2$	$2.0873e+2$	$2.0864e+2$	$2.0864e+2$
2	$2.0654e+3$	$1.3186e+3$	$1.3118e+3$	$1.3075e+3$
3		$4.4597e+3$	$3.7067e+3$	$3.6611e+3$
4		$1.2944e+4$	$8.3473e+3$	$7.1742e+3$
5			$1.5709e+4$	$1.1860e+4$
6			$3.1318e+4$	$1.7716e+4$

Table 1: Natural frequencies(Hz) of a clamped-free beam, $m = 0.33kg$, $l = 1.0$m, Inertia of joint 3.2 $\mathrm{kg/m}^2$ and $EI = 1165.5\mathrm{N}/m^2$

- Only first k frequencies from FEM are close $\rightarrow$ k modes are equivalent to k elements.
- Typically 2 or three modes(elements) are enough to model dynamics.

- AMM mode shapes are defined over *entire* beam with trigonometric functions $\rightarrow$ Diagonal mass and stiffness matrices.
- FEM interpolation function are *local* and are polynomials $\rightarrow$ Banded mass and stiffness matrices.
- FEM imposes more constraints (due to use of polynomials) $\rightarrow$ Overestimates natural frequencies more than AMM.
- Overestimation of natural frequencies leads to "locking" and difficulties in using model-based control.
- Local interpolations functions – easier to use for complex geometries.
- 3D and other kinds of elements available in large body of research on FEM can be used.

- AMM mode shapes are defined over *entire* beam with trigonometric functions $\rightarrow$ Diagonal mass and stiffness matrices.
- FEM interpolation function are *local* and are polynomials $\rightarrow$ Banded mass and stiffness matrices.
- FEM imposes more constraints (due to use of polynomials) $\rightarrow$ Overestimates natural frequencies more than AMM.
- Overestimation of natural frequencies leads to "locking" and difficulties in using model-based control.
- Local interpolations functions – easier to use for complex geometries.
- 3D and other kinds of elements available in large body of research on FEM can be used.

- AMM mode shapes are defined over *entire* beam with trigonometric functions $\rightarrow$ Diagonal mass and stiffness matrices.
- FEM interpolation function are *local* and are polynomials $\rightarrow$ Banded mass and stiffness matrices.
- FEM imposes more constraints (due to use of polynomials) $\rightarrow$ Overestimates natural frequencies more than AMM.
- Overestimation of natural frequencies leads to "locking" and difficulties in using model-based control.
- Local interpolations functions – easier to use for complex geometries.
- 3D and other kinds of elements available in large body of research on FEM can be used.

- AMM mode shapes are defined over *entire* beam with trigonometric functions $\rightarrow$ Diagonal mass and stiffness matrices.
- FEM interpolation function are *local* and are polynomials $\rightarrow$ Banded mass and stiffness matrices.
- FEM imposes more constraints (due to use of polynomials) $\rightarrow$ Overestimates natural frequencies more than AMM.
- Overestimation of natural frequencies leads to "locking" and difficulties in using model-based control.
- Local interpolations functions – easier to use for complex geometries.
- 3D and other kinds of elements available in large body of research on FEM can be used.

- AMM mode shapes are defined over *entire* beam with trigonometric functions $\rightarrow$ Diagonal mass and stiffness matrices.
- FEM interpolation function are *local* and are polynomials $\rightarrow$ Banded mass and stiffness matrices.
- FEM imposes more constraints (due to use of polynomials) $\rightarrow$ Overestimates natural frequencies more than AMM.
- Overestimation of natural frequencies leads to "locking" and difficulties in using model-based control.
- Local interpolations functions – easier to use for complex geometries.
- 3D and other kinds of elements available in large body of research on FEM can be used.

- AMM mode shapes are defined over *entire* beam with trigonometric functions $\rightarrow$ Diagonal mass and stiffness matrices.
- FEM interpolation function are *local* and are polynomials $\rightarrow$ Banded mass and stiffness matrices.
- FEM imposes more constraints (due to use of polynomials) $\rightarrow$ Overestimates natural frequencies more than AMM.
- Overestimation of natural frequencies leads to "locking" and difficulties in using model-based control.
- Local interpolations functions – easier to use for complex geometries.
- 3D and other kinds of elements available in large body of research on FEM can be used.

SUMMARY

- Extension of Denavit-Hartenberg convention to flexible links.
  - Rigid 4×4 transformation matrix ${}^{j-1}_{j*}[T_r]$
  - Small deformation and linear elasticity $\rightarrow$ Elastic 4×4 transformation matrix ${}^{j*}_{j}[T_e]$.
  - Complete 4×4 transformation matrix ${}^{j-1}_{j}[T] = {}^{j-1}_{j*}[T_r]{}^{j*}_{j}[T_e]$.
- Position vector and velocity of a point on the flexible link for rotary jointed and prismatic jointed link.
- Assumed modes method to discretise PDE.
- Frequency equation as an ODE.
- FEM approach to discretise PDE.
- Comparison of AMM and FEM approaches.

SUMMARY

- Extension of Denavit-Hartenberg convention to flexible links.
  - Rigid 4×4 transformation matrix ${}^{j-1}_{j_*}[T_r]$
  - Small deformation and linear elasticity $\rightarrow$ Elastic 4×4 transformation matrix ${}^{j_*}_{j}[T_e]$.
  - Complete 4×4 transformation matrix ${}^{j-1}_{j}[T] = {}^{j-1}_{j_*}[T_r]{}^{j_*}_{j}[T_e]$.
- Position vector and velocity of a point on the flexible link for rotary jointed and prismatic jointed link.
- Assumed modes method to discretise PDE.
- Frequency equation as an ODE.
- FEM approach to discretise PDE.
- Comparison of AMM and FEM approaches.

SUMMARY

- Extension of Denavit-Hartenberg convention to flexible links.
  - Rigid 4×4 transformation matrix ${}^{j-1}_{j_*}[T_r]$
  - Small deformation and linear elasticity $\rightarrow$ Elastic 4×4 transformation matrix ${}^{j_*}_{j}[T_e]$.
  - Complete 4×4 transformation matrix ${}^{j-1}_{j}[T] = {}^{j-1}_{j_*}[T_r]{}^{j_*}_{j}[T_e]$.
- Position vector and velocity of a point on the flexible link for rotary jointed and prismatic jointed link.
- Assumed modes method to discretise PDE.
- Frequency equation as an ODE.
- FEM approach to discretise PDE.
- Comparison of AMM and FEM approaches.

Summary

- Extension of Denavit-Hartenberg convention to flexible links.
  - Rigid 4×4 transformation matrix ${}_{j_*}^{j-1}[T_r]$
  - Small deformation and linear elasticity $\rightarrow$ Elastic 4×4 transformation matrix ${}_{j}^{j_*}[T_e]$.
  - Complete 4×4 transformation matrix ${}_{j}^{j-1}[T] = {}_{j_*}^{j-1}[T_r]{}_{j}^{j_*}[T_e]$.
- Position vector and velocity of a point on the flexible link for rotary jointed and prismatic jointed link.
- Assumed modes method to discretise PDE.
- Frequency equation as an ODE.
- FEM approach to discretise PDE.
- Comparison of AMM and FEM approaches.

Summary

- Extension of Denavit-Hartenberg convention to flexible links.
  - Rigid 4×4 transformation matrix ${}^{j-1}_{j*}[T_r]$
  - Small deformation and linear elasticity $\rightarrow$ Elastic 4×4 transformation matrix ${}^{j*}_{j}[T_e]$.
  - Complete 4×4 transformation matrix ${}^{j-1}_{j}[T] = {}^{j-1}_{j*}[T_r]{}^{j*}_{j}[T_e]$.
- Position vector and velocity of a point on the flexible link for rotary jointed and prismatic jointed link.
- Assumed modes method to discretise PDE.
- Frequency equation as an ODE.
- FEM approach to discretise PDE.
- Comparison of AMM and FEM approaches.

Summary

- Extension of Denavit-Hartenberg convention to flexible links.
  - Rigid 4×4 transformation matrix ${}^{j-1}_{j*}[T_r]$
  - Small deformation and linear elasticity $\rightarrow$ Elastic 4×4 transformation matrix ${}^{j*}_{j}[T_e]$.
  - Complete 4×4 transformation matrix ${}^{j-1}_{j}[T] = {}^{j-1}_{j*}[T_r]^{j*}_{j}[T_e]$.
- Position vector and velocity of a point on the flexible link for rotary jointed and prismatic jointed link.
- Assumed modes method to discretise PDE.
- Frequency equation as an ODE.
- FEM approach to discretise PDE.
- Comparison of AMM and FEM approaches.

Outline

1. Contents
2. Lecture 1
   - Flexible Manipulators
3. Lecture 2*
   - Kinematic Modeling of Flexible Link Manipulators
4. Lecture 3*
   - Dynamic Modeling of Flexible Link Manipulators
   - Control of Flexible Link Manipulators
5. Lecture 4
   - Experiments with a Planar Two Link Flexible System
6. Module 8 – Additional Material
   - Problems, References and Suggested Reading

- Dynamic equations of motion for flexible link manipulators.
- Controllability of flexible-link manipulators.
- Control of joint motion & tip vibration in flexible link manipulator.
- Robustness issues in model-based control schemes.
- Numerical simulation of a multi-link flexible manipulator.

- Dynamic equations of motion for flexible link manipulators.
- Controllability of flexible-link manipulators.
- Control of joint motion & tip vibration in flexible link manipulator.
- Robustness issues in model-based control schemes.
- Numerical simulation of a multi-link flexible manipulator.

INTRODUCTION

OVERVIEW

- Dynamic equations of motion for flexible link manipulators.
- Controllability of flexible-link manipulators.
- Control of joint motion & tip vibration in flexible link manipulator.
- Robustness issues in model-based control schemes.
- Numerical simulation of a multi-link flexible manipulator.

- Dynamic equations of motion for flexible link manipulators.
- Controllability of flexible-link manipulators.
- Control of joint motion & tip vibration in flexible link manipulator.
- Robustness issues in model-based control schemes.
- Numerical simulation of a multi-link flexible manipulator.

- Dynamic equations of motion for flexible link manipulators.
- Controllability of flexible-link manipulators.
- Control of joint motion & tip vibration in flexible link manipulator.
- Robustness issues in model-based control schemes.
- Numerical simulation of a multi-link flexible manipulator.

Equations of motion of multi-link flexible manipulators

- Symbolic equations of motion using MAPLE or Mathematica.
- Lagrangian formulation (see Module 6, Lecture 1).
- Lagrangian equations of motion
  - For joint variable q_{r_j}:

$$\frac{d}{dt}\left(\frac{\partial KE}{\partial \dot{q}_{r_j}}\right) - \frac{\partial KE}{\partial q_{r_j}} + \frac{\partial PE}{\partial q_{r_j}} = \tau_j$$

  - For flexible variable $q_{f_{ji}}$:

$$\frac{d}{dt}\left(\frac{\partial KE}{\partial \dot{q}_{f_{ji}}}\right) - \frac{\partial KE}{\partial q_{f_{ji}}} + \frac{\partial PE}{\partial q_{f_{ji}}} = 0$$

- *KE* is total kinetic energy & *PE* is total potential energy due to *elastic deformation* and *gravity*.

Equations of motion of multi-link flexible manipulators

- Symbolic equations of motion using MAPLE or Mathematica.
- Lagrangian formulation (see Module 6, Lecture 1).
- Lagrangian equations of motion
  - For joint variable q_{r_j}:

$$\frac{d}{dt}\left(\frac{\partial KE}{\partial \dot{q}_{r_j}}\right) - \frac{\partial KE}{\partial q_{r_j}} + \frac{\partial PE}{\partial q_{r_j}} = \tau_j$$

  - For flexible variable $q_{f_{ji}}$:

$$\frac{d}{dt}\left(\frac{\partial KE}{\partial \dot{q}_{f_{ji}}}\right) - \frac{\partial KE}{\partial q_{f_{ji}}} + \frac{\partial PE}{\partial q_{f_{ji}}} = 0$$

- *KE* is total kinetic energy & *PE* is total potential energy due to *elastic deformation* and *gravity*.

Equations of motion of multi-link flexible manipulators

- Symbolic equations of motion using MAPLE or Mathematica.
- Lagrangian formulation (see Module 6, Lecture 1).
- Lagrangian equations of motion
  - For joint variable q_{r_j}:

$$\frac{d}{dt}\left(\frac{\partial KE}{\partial \dot{q}_{r_j}}\right) - \frac{\partial KE}{\partial q_{r_j}} + \frac{\partial PE}{\partial q_{r_j}} = \tau_j$$

  - For flexible variable $q_{f_{ji}}$:

$$\frac{d}{dt}\left(\frac{\partial KE}{\partial \dot{q}_{f_{ji}}}\right) - \frac{\partial KE}{\partial q_{f_{ji}}} + \frac{\partial PE}{\partial q_{f_{ji}}} = 0$$

- *KE* is total kinetic energy & *PE* is total potential energy due to *elastic deformation* and *gravity*.

Equations of motion of multi-link flexible manipulators

- Symbolic equations of motion using MAPLE or Mathematica.
- Lagrangian formulation (see Module 6, Lecture 1).
- Lagrangian equations of motion
  - For joint variable q_{r_j}:

$$\frac{d}{dt}\left(\frac{\partial KE}{\partial \dot{q}_{r_j}}\right) - \frac{\partial KE}{\partial q_{r_j}} + \frac{\partial PE}{\partial q_{r_j}} = \tau_j$$

  - For flexible variable $q_{f_{ji}}$:

$$\frac{d}{dt}\left(\frac{\partial KE}{\partial \dot{q}_{f_{ji}}}\right) - \frac{\partial KE}{\partial q_{f_{ji}}} + \frac{\partial PE}{\partial q_{f_{ji}}} = 0$$

- KE is total kinetic energy & PE is total potential energy due to *elastic deformation* and *gravity*.

EQUATIONS OF MOTION OF MULTI-LINK FLEXIBLE MANIPULATORS

KINETIC ENERGY

- Total kinetic energy: $KE = \sum_{j=1}^{n}(KE_{joint_j} + KE_{link_j}) + KE_{payload}$
- Kinetic energy of joint in terms of mass, inertia and derivative of position vector

$$KE_{joint_j} = \frac{1}{2}{}^0\Omega_j^{\,T}\ {}^0[I_{joint}]_j\ {}^0\Omega_j + \frac{1}{2}m_{joint_j}\left(\frac{d\,{}^0\mathbf{O}_j}{dt}\right)^T\left(\frac{d\,{}^0\mathbf{O}_j}{dt}\right)$$

- Kinetic energy of flexible link j in terms of density, cross-sectional area and number of elements

$$KE_{link_j} = \begin{cases} \frac{1}{2}\int_0^{l_j}\rho_j A_j\left(\frac{d\,{}^0\mathbf{p}_j}{dt}\right)^T\left(\frac{d\,{}^0\mathbf{p}_j}{dt}\right)ds, & \text{for AMM} \\ \frac{1}{2}\sum_{i=1}^{N_j}\int_0^{l_{ji}}\rho_j A_j\left(\frac{d\,{}^0\mathbf{p}_{ji}}{dt}\right)^T\left(\frac{d\,{}^0\mathbf{p}_{ji}}{dt}\right)ds, & \text{for FEM} \end{cases}$$

Equations of motion of multi-link flexible manipulators

Kinetic Energy

- Total kinetic energy: $KE = \sum_{j=1}^{n}(KE_{joint_j} + KE_{link_j}) + KE_{payload}$
- Kinetic energy of joint in terms of mass, inertia and derivative of position vector

$$KE_{joint_j} = \frac{1}{2}{}^0\Omega_j{}^T\ {}^0[I_{joint}]_j\ {}^0\Omega_j + \frac{1}{2}m_{joint_j}\left(\frac{d\,{}^0\mathbf{O}_j}{dt}\right)^T\left(\frac{d\,{}^0\mathbf{O}_j}{dt}\right)$$

- Kinetic energy of flexible link j in terms of density, cross-sectional area and number of elements

$$KE_{link_j} = \begin{cases} \frac{1}{2}\int_0^{l_j}\rho_j A_j\left(\frac{d\,{}^0\mathbf{p}_j}{dt}\right)^T\left(\frac{d\,{}^0\mathbf{p}_j}{dt}\right)ds, & \text{for AMM} \\ \frac{1}{2}\sum_{i=1}^{N_j}\int_0^{l_{ji}}\rho_j A_j\left(\frac{d\,{}^0\mathbf{p}_{ji}}{dt}\right)^T\left(\frac{d\,{}^0\mathbf{p}_{ji}}{dt}\right)ds, & \text{for FEM} \end{cases}$$

EQUATIONS OF MOTION OF MULTI-LINK FLEXIBLE MANIPULATORS

KINETIC ENERGY

- Total kinetic energy: $KE = \sum_{j=1}^{n}(KE_{joint_j} + KE_{link_j}) + KE_{payload}$
- Kinetic energy of joint in terms of mass, inertia and derivative of position vector

$$KE_{joint_j} = \frac{1}{2} {}^0\Omega_j^{\,T}\; {}^0[I_{joint}]_j\; {}^0\Omega_j + \frac{1}{2} m_{joint_j} \left(\frac{d\,{}^0\mathbf{O}_j}{dt}\right)^T \left(\frac{d\,{}^0\mathbf{O}_j}{dt}\right)$$

- Kinetic energy of flexible link j in terms of density, cross-sectional area and number of elements

$$KE_{link_j} = \begin{cases} \frac{1}{2}\int_0^{l_j} \rho_j A_j \left(\frac{d\,{}^0\mathbf{p}_j}{dt}\right)^T \left(\frac{d\,{}^0\mathbf{p}_j}{dt}\right) ds, & \text{for AMM} \\ \frac{1}{2}\sum_{i=1}^{N_j}\int_0^{l_{ji}} \rho_j A_j \left(\frac{d\,{}^0\mathbf{p}_{ji}}{dt}\right)^T \left(\frac{d\,{}^0\mathbf{p}_{ji}}{dt}\right) ds, & \text{for FEM} \end{cases}$$

Equations of motion of multi-link flexible manipulators

Kinetic Energy (Contd.)

- If link j is rigid, kinetic energy, in terms of position of centre of mass

$$KE_{link_j} = \frac{1}{2} m_j \left(\frac{d\,^0\mathbf{p}_{c_j}}{dt} \right)^T \left(\frac{d\,^0\mathbf{p}_{c_j}}{dt} \right)$$

- Kinetic energy of payload

$$KE_{payload} = \frac{1}{2} m_p \left(\frac{d\,^0\mathbf{p}_{Tool}}{dt} \right)^T \left(\frac{d\,^0\mathbf{p}_{Tool}}{dt} \right) + \frac{1}{2}\,{}^0\Omega_{Tool}{}^T\;{}^0[J_p]\,{}^0\Omega_{Tool}$$

  ${}^0\mathbf{p}_{Tool}$ is the position vector of the centre of mass of the payload, m_p is mass of the payload, ${}^0[J_p]$ and ${}^{0\cdot}{}_{Tool}$ are the moment of inertia matrix of the payload and the angular velocity vector of the payload, respectively.

- If link j is rigid, kinetic energy, in terms of position of centre of mass

$$KE_{link_j} = \frac{1}{2} m_j \left(\frac{d\,{}^0\mathbf{p}_{c_j}}{dt} \right)^T \left(\frac{d\,{}^0\mathbf{p}_{c_j}}{dt} \right)$$

- Kinetic energy of payload

$$KE_{payload} = \frac{1}{2} m_p \left(\frac{d\,{}^0\mathbf{p}_{Tool}}{dt} \right)^T \left(\frac{d\,{}^0\mathbf{p}_{Tool}}{dt} \right) + \frac{1}{2} {}^0\Omega_{Tool}{}^T\ {}^0[J_p]\,{}^0\Omega_{Tool}$$

${}^0\mathbf{p}_{Tool}$ is the position vector of the centre of mass of the payload, m_p is mass of the payload, ${}^0[J_p]$ and ${}^{0\bullet}{}_{Tool}$ are the moment of inertia matrix of the payload and the angular velocity vector of the payload, respectively.

Potential Energy

- Total potential energy: $PE = \sum_{i=1}^{n} (PE_{f_j} + PE_{g_j}) + PE_{g_{payload}}$
- Payload: $PE_{g_{payload}} = m_p \mathbf{g}^{T\,0}\mathbf{p}_{Tool}$
- Gravity: $PE_{g_j} = m_{joint_j}\mathbf{g}^{T\,0}\mathbf{O}_j + \int_0^{l_j} \rho_j A_j \mathbf{g}^{T\,0}\mathbf{p}_j ds$
- Strain energy, assuming linear elasticity and neglecting axial and torsional deformation
- For assumed modes model:

$$PE_{f_j} = \int_0^1 \left(\frac{E_j I_{jy}}{2l_j^3} \left[\sum_{i=1}^{N_j} \frac{\partial^2 \psi_i^{v_j}(\eta)}{\partial \eta^2} \xi_i^{v_j}(t) \right]^2 + \frac{E_j I_{jz}}{2l_j^3} \left[\sum_{i=1}^{N_j} \frac{\partial^2 \psi_i^{w_j}(\eta)}{\partial \eta^2} \xi_i^{w_j}(t) \right]^2 \right) d\eta$$

- For finite element model:

$$PE_{f_j} = \sum_{i=1}^{N_j} \int_0^{l_{ji}} \left(\frac{E_j I_{jy}}{2} \left[\sum_{k=1}^{4} \frac{\partial^2 \varphi_{ik}^{v_j}(s)}{\partial s^2} q_{f_{jik}}^{v_j}(t) \right]^2 + \frac{E_j I_{jz}}{2} \left[\sum_{k=1}^{4} \frac{\partial^2 \varphi_{ik}^{w_j}(s)}{\partial s^2} q_{f_{jik}}^{w_j}(t) \right]^2 \right) ds$$

Equations of motion of multi-link flexible manipulators

Potential Energy

- Total potential energy: $PE = \sum_{i=1}^{n}(PE_{f_j} + PE_{g_j}) + PE_{g_{payload}}$
- Payload: $PE_{g_{payload}} = m_p \mathbf{g}^{T\,0}\mathbf{p}_{Tool}$
- Gravity: $PE_{g_j} = m_{joint_j}\mathbf{g}^{T\,0}\mathbf{O}_j + \int_0^{l_j} \rho_j A_j \mathbf{g}^{T\,0}\mathbf{p}_j ds$
- Strain energy, assuming linear elasticity and neglecting axial and torsional deformation
- For assumed modes model:

$$PE_{f_j} = \int_0^1 \left(\frac{E_j I_{jy}}{2 l_j^3} \left[\sum_{i=1}^{N_j} \frac{\partial^2 \psi_i^{v_j}(\eta)}{\partial \eta^2} \xi_i^{v_j}(t) \right]^2 + \frac{E_j I_{jz}}{2 l_j^3} \left[\sum_{i=1}^{N_j} \frac{\partial^2 \psi_i^{w_j}(\eta)}{\partial \eta^2} \xi_i^{w_j}(t) \right]^2 \right) d\eta$$

- For finite element model:

$$PE_{f_j} = \sum_{i=1}^{N_j} \int_0^{l_{ji}} \left(\frac{E_j I_{jy}}{2} \left[\sum_{k=1}^{4} \frac{\partial^2 \varphi_{ik}^{v_j}(s)}{\partial s^2} q_{f_{jik}}^{v_j}(t) \right]^2 + \frac{E_j I_{jz}}{2} \left[\sum_{k=1}^{4} \frac{\partial^2 \varphi_{ik}^{w_j}(s)}{\partial s^2} q_{f_{jik}}^{w_j}(t) \right]^2 \right) ds$$

Equations of motion of multi-link flexible manipulators

Potential Energy

- Total potential energy: $PE = \sum_{i=1}^{n}(PE_{f_j} + PE_{g_j}) + PE_{g_{payload}}$
- Payload: $PE_{g_{payload}} = m_p \mathbf{g}^{T\,0}\mathbf{p}_{Tool}$
- Gravity: $PE_{g_j} = m_{joint_j}\mathbf{g}^{T\,0}\mathbf{O}_j + \int_0^{l_j} \rho_j A_j \mathbf{g}^{T\,0}\mathbf{p}_j ds$
- Strain energy, assuming linear elasticity and neglecting axial and torsional deformation
- For assumed modes model:

$$PE_{f_j} = \int_0^1 \left(\frac{E_j I_{jy}}{2 l_j^3} \left[\sum_{i=1}^{N_j} \frac{\partial^2 \psi_i^{v_j}(\eta)}{\partial \eta^2} \xi_i^{v_j}(t) \right]^2 + \frac{E_j I_{jz}}{2 l_j^3} \left[\sum_{i=1}^{N_j} \frac{\partial^2 \psi_i^{w_j}(\eta)}{\partial \eta^2} \xi_i^{w_j}(t) \right]^2 \right) d\eta$$

- For finite element model:

$$PE_{f_j} = \sum_{i=1}^{N_j} \int_0^{l_{ji}} \left(\frac{E_j I_{jy}}{2} \left[\sum_{k=1}^{4} \frac{\partial^2 \varphi_{ik}^{v_j}(s)}{\partial s^2} q_{f_{jik}}^{v_j}(t) \right]^2 + \frac{E_j I_{jz}}{2} \left[\sum_{k=1}^{4} \frac{\partial^2 \varphi_{ik}^{w_j}(s)}{\partial s^2} q_{f_{jik}}^{w_j}(t) \right]^2 \right) ds$$

Equations of motion of multi-link flexible manipulators

Potential Energy

- Total potential energy: $PE = \sum_{i=1}^{n}(PE_{f_j} + PE_{g_j}) + PE_{g_{payload}}$
- Payload: $PE_{g_{payload}} = m_p \mathbf{g}^{T\,0}\mathbf{p}_{Tool}$
- Gravity: $PE_{g_j} = m_{joint_j}\mathbf{g}^{T\,0}\mathbf{O}_j + \int_0^{l_j} \rho_j A_j \mathbf{g}^{T\,0}\mathbf{p}_j ds$
- Strain energy, assuming linear elasticity and neglecting axial and torsional deformation
- For assumed modes model:

$$PE_{f_j} = \int_0^1 \left(\frac{E_j I_{jy}}{2 l_j^3} \left[\sum_{i=1}^{N_j} \frac{\partial^2 \psi_i^{v_j}(\eta)}{\partial \eta^2} \xi_i^{v_j}(t) \right]^2 + \frac{E_j I_{jz}}{2 l_j^3} \left[\sum_{i=1}^{N_j} \frac{\partial^2 \psi_i^{w_j}(\eta)}{\partial \eta^2} \xi_i^{w_j}(t) \right]^2 \right) d\eta$$

- For finite element model:

$$PE_{f_j} = \sum_{i=1}^{N_j} \int_0^{l_{ji}} \left(\frac{E_j I_{jy}}{2} \left[\sum_{k=1}^{4} \frac{\partial^2 \varphi_{ik}^{v_j}(s)}{\partial s^2} q_{f_{jik}}^{v_j}(t) \right]^2 + \frac{E_j I_{jz}}{2} \left[\sum_{k=1}^{4} \frac{\partial^2 \varphi_{ik}^{w_j}(s)}{\partial s^2} q_{f_{jik}}^{w_j}(t) \right]^2 \right) ds$$

Equations of motion of multi-link flexible manipulators

Potential Energy

- Total potential energy: $PE = \sum_{i=1}^{n} (PE_{f_i} + PE_{g_i}) + PE_{g_{payload}}$
- Payload: $PE_{g_{payload}} = m_p \mathbf{g}^{T\,0}\mathbf{p}_{Tool}$
- Gravity: $PE_{g_j} = m_{joint_j} \mathbf{g}^{T\,0}\mathbf{O}_j + \int_0^{l_j} \rho_j A_j \mathbf{g}^{T\,0}\mathbf{p}_j ds$
- Strain energy, assuming linear elasticity and neglecting axial and torsional deformation
- For assumed modes model:

$$PE_{f_j} = \int_0^1 \left(\frac{E_j I_{jy}}{2 l_j^3} \left[\sum_{i=1}^{N_j} \frac{\partial^2 \psi_i^{v_j}(\eta)}{\partial \eta^2} \xi_i^{v_j}(t) \right]^2 + \frac{E_j I_{jz}}{2 l_j^3} \left[\sum_{i=1}^{N_j} \frac{\partial^2 \psi_i^{w_j}(\eta)}{\partial \eta^2} \xi_i^{w_j}(t) \right]^2 \right) d\eta$$

- For finite element model:

$$PE_{f_j} = \sum_{i=1}^{N_j} \int_0^{l_{ji}} \left(\frac{E_j I_{jy}}{2} \left[\sum_{k=1}^{4} \frac{\partial^2 \varphi_{ik}^{v_j}(s)}{\partial s^2} q_{f_{jik}}^{v_j}(t) \right]^2 + \frac{E_j I_{jz}}{2} \left[\sum_{k=1}^{4} \frac{\partial^2 \varphi_{ik}^{w_j}(s)}{\partial s^2} q_{f_{jik}}^{w_j}(t) \right]^2 \right) ds$$

Equations of motion of multi-link flexible manipulators

Potential Energy

- Total potential energy: $PE = \sum_{i=1}^{n} (PE_{f_j} + PE_{g_j}) + PE_{g_{payload}}$
- Payload: $PE_{g_{payload}} = m_p \mathbf{g}^{T\,0}\mathbf{p}_{Tool}$
- Gravity: $PE_{g_j} = m_{joint_j} \mathbf{g}^{T\,0}\mathbf{O}_j + \int_0^{l_j} \rho_j A_j \mathbf{g}^{T\,0}\mathbf{p}_j ds$
- Strain energy, assuming linear elasticity and neglecting axial and torsional deformation
- For assumed modes model:

$$PE_{f_j} = \int_0^1 \left(\frac{E_j I_{jy}}{2 l_j^3} \left[\sum_{i=1}^{N_j} \frac{\partial^2 \psi_i^{v_j}(\eta)}{\partial \eta^2} \xi_i^{v_j}(t) \right]^2 + \frac{E_j I_{jz}}{2 l_j^3} \left[\sum_{i=1}^{N_j} \frac{\partial^2 \psi_i^{w_j}(\eta)}{\partial \eta^2} \xi_i^{w_j}(t) \right]^2 \right) d\eta$$

- For finite element model:

$$PE_{f_j} = \sum_{i=1}^{N_j} \int_0^{l_{ji}} \left(\frac{E_j I_{jy}}{2} \left[\sum_{k=1}^{4} \frac{\partial^2 \varphi_{ik}^{v_j}(s)}{\partial s^2} q_{f_{jik}}^{v_j}(t) \right]^2 + \frac{E_j I_{jz}}{2} \left[\sum_{k=1}^{4} \frac{\partial^2 \varphi_{ik}^{w_j}(s)}{\partial s^2} q_{f_{jik}}^{w_j}(t) \right]^2 \right) ds$$

Equations of motion of multi-link flexible manipulators

- Kinetic and potential energy $\rightarrow$ Lagrangian formulation $\rightarrow$ equations of motion.
- Equations of motion in a compact form

$$\begin{pmatrix} [\mathbf{M}_{rr}] & [\mathbf{M}_{rf}]^T \\ [\mathbf{M}_{rf}] & [\mathbf{M}_{ff}] \end{pmatrix} \begin{pmatrix} \ddot{\mathbf{q}}_r \\ \ddot{\mathbf{q}}_f \end{pmatrix} + \begin{pmatrix} \mathbf{C}_r(\mathbf{q}, \dot{\mathbf{q}}) \\ \mathbf{C}_f(\mathbf{q}, \dot{\mathbf{q}}) \end{pmatrix} + \begin{pmatrix} \mathbf{G}_r(\mathbf{q}) \\ \mathbf{G}_f(\mathbf{q}) \end{pmatrix}$$
$$+ \begin{pmatrix} \mathbf{0} & \mathbf{0} \\ \mathbf{0} & [\mathbf{K}] \end{pmatrix} \begin{pmatrix} \mathbf{q}_r \\ \mathbf{q}_f \end{pmatrix} = \begin{pmatrix} \tau \\ \mathbf{0} \end{pmatrix}$$

- Variables $\mathbf{q}$: joint variables $\mathbf{q}_r \in \Re^n$ and flexible variables $\mathbf{q}_f \in \Re^N$.
- For AMM with $n_f \leq n$ flexible links and N_j modes for each flexible link, $N = 2\sum_{j=1}^{n_f} N_j$ in 3D and $N = \sum_{j=1}^{n_f} N_j$ for plane.
- For FEM with N_j elements for each flexible link, $N = 4\sum_{j=1}^{n_f} N_j$ in 3D and $N = 2\sum_{j=1}^{n_f} N_j$ for plane.
- In FEM, in the *first* element in each link, $\delta_{j1} = \phi_{j1} = 0$ to represent clamped boundary conditions.

Equations of motion of multi-link flexible manipulators

- Kinetic and potential energy → Lagrangian formulation → equations of motion.
- Equations of motion in a compact form

$$\begin{pmatrix} [\mathbf{M}_{rr}] & [\mathbf{M}_{rf}]^T \\ [\mathbf{M}_{rf}] & [\mathbf{M}_{ff}] \end{pmatrix} \begin{pmatrix} \ddot{\mathbf{q}}_r \\ \ddot{\mathbf{q}}_f \end{pmatrix} + \begin{pmatrix} \mathbf{C}_r(\mathbf{q}, \dot{\mathbf{q}}) \\ \mathbf{C}_f(\mathbf{q}, \dot{\mathbf{q}}) \end{pmatrix} + \begin{pmatrix} \mathbf{G}_r(\mathbf{q}) \\ \mathbf{G}_f(\mathbf{q}) \end{pmatrix}$$
$$+ \begin{pmatrix} 0 & 0 \\ 0 & [\mathbf{K}] \end{pmatrix} \begin{pmatrix} \mathbf{q}_r \\ \mathbf{q}_f \end{pmatrix} = \begin{pmatrix} \tau \\ 0 \end{pmatrix}$$

- Variables $\mathbf{q}$: joint variables $\mathbf{q}_r \in \Re^n$ and flexible variables $\mathbf{q}_f \in \Re^N$.
- For AMM with $n_f \leq n$ flexible links and N_j modes for each flexible link, $N = 2\sum_{j=1}^{n_f} N_j$ in 3D and $N = \sum_{j=1}^{n_f} N_j$ for plane.
- For FEM with N_j elements for each flexible link, $N = 4\sum_{j=1}^{n_f} N_j$ in 3D and $N = 2\sum_{j=1}^{n_f} N_j$ for plane.
- In FEM, in the *first* element in each link, $\delta_{j1} = \phi_{j1} = 0$ to represent clamped boundary conditions.

Equations of motion of multi-link flexible manipulators

- Kinetic and potential energy → Lagrangian formulation → equations of motion.
- Equations of motion in a compact form

$$\begin{pmatrix} [\mathbf{M}_{rr}] & [\mathbf{M}_{rf}]^T \\ [\mathbf{M}_{rf}] & [\mathbf{M}_{ff}] \end{pmatrix} \begin{pmatrix} \ddot{\mathbf{q}}_r \\ \ddot{\mathbf{q}}_f \end{pmatrix} + \begin{pmatrix} \mathbf{C}_r(\mathbf{q}, \dot{\mathbf{q}}) \\ \mathbf{C}_f(\mathbf{q}, \dot{\mathbf{q}}) \end{pmatrix} + \begin{pmatrix} \mathbf{G}_r(\mathbf{q}) \\ \mathbf{G}_f(\mathbf{q}) \end{pmatrix} + \begin{pmatrix} 0 & 0 \\ 0 & [\mathbf{K}] \end{pmatrix} \begin{pmatrix} \mathbf{q}_r \\ \mathbf{q}_f \end{pmatrix} = \begin{pmatrix} \tau \\ 0 \end{pmatrix}$$

- Variables $\mathbf{q}$: joint variables $\mathbf{q}_r \in \Re^n$ and flexible variables $\mathbf{q}_f \in \Re^N$.
- For AMM with $n_f \leq n$ flexible links and N_j modes for each flexible link, $N = 2\sum_{j=1}^{n_f} N_j$ in 3D and $N = \sum_{j=1}^{n_f} N_j$ for plane.
- For FEM with N_j elements for each flexible link, $N = 4\sum_{j=1}^{n_f} N_j$ in 3D and $N = 2\sum_{j=1}^{n_f} N_j$ for plane.
- In FEM, in the *first* element in each link, $\delta_{j1} = \phi_{j1} = 0$ to represent clamped boundary conditions.

Equations of motion of multi-link flexible manipulators

- Kinetic and potential energy $\rightarrow$ Lagrangian formulation $\rightarrow$ equations of motion.
- Equations of motion in a compact form

$$\begin{pmatrix} [\mathbf{M}_{rr}] & [\mathbf{M}_{rf}]^T \\ [\mathbf{M}_{rf}] & [\mathbf{M}_{ff}] \end{pmatrix} \begin{pmatrix} \ddot{\mathbf{q}}_r \\ \ddot{\mathbf{q}}_f \end{pmatrix} + \begin{pmatrix} \mathbf{C}_r(\mathbf{q}, \dot{\mathbf{q}}) \\ \mathbf{C}_f(\mathbf{q}, \dot{\mathbf{q}}) \end{pmatrix} + \begin{pmatrix} \mathbf{G}_r(\mathbf{q}) \\ \mathbf{G}_f(\mathbf{q}) \end{pmatrix}$$
$$+ \begin{pmatrix} \mathbf{0} & \mathbf{0} \\ \mathbf{0} & [\mathbf{K}] \end{pmatrix} \begin{pmatrix} \mathbf{q}_r \\ \mathbf{q}_f \end{pmatrix} = \begin{pmatrix} \tau \\ \mathbf{0} \end{pmatrix}$$

- Variables $\mathbf{q}$: joint variables $\mathbf{q}_r \in \Re^n$ and flexible variables $\mathbf{q}_f \in \Re^N$.
- For AMM with $n_f \leq n$ flexible links and N_j modes for each flexible link, $N = 2\sum_{j=1}^{n_f} N_j$ in 3D and $N = \sum_{j=1}^{n_f} N_j$ for plane.
- For FEM with N_j elements for each flexible link, $N = 4\sum_{j=1}^{n_f} N_j$ in 3D and $N = 2\sum_{j=1}^{n_f} N_j$ for plane.
- In FEM, in the *first* element in each link, $\delta_{j1} = \phi_{j1} = 0$ to represent clamped boundary conditions.

Equations of motion of multi-link flexible manipulators

- Kinetic and potential energy $\rightarrow$ Lagrangian formulation $\rightarrow$ equations of motion.
- Equations of motion in a compact form

$$\begin{pmatrix} [\mathbf{M}_{rr}] & [\mathbf{M}_{rf}]^T \\ [\mathbf{M}_{rf}] & [\mathbf{M}_{ff}] \end{pmatrix} \begin{pmatrix} \ddot{\mathbf{q}}_r \\ \ddot{\mathbf{q}}_f \end{pmatrix} + \begin{pmatrix} \mathbf{C}_r(\mathbf{q}, \dot{\mathbf{q}}) \\ \mathbf{C}_f(\mathbf{q}, \dot{\mathbf{q}}) \end{pmatrix} + \begin{pmatrix} \mathbf{G}_r(\mathbf{q}) \\ \mathbf{G}_f(\mathbf{q}) \end{pmatrix}$$
$$+ \begin{pmatrix} \mathbf{0} & \mathbf{0} \\ \mathbf{0} & [\mathbf{K}] \end{pmatrix} \begin{pmatrix} \mathbf{q}_r \\ \mathbf{q}_f \end{pmatrix} = \begin{pmatrix} \tau \\ \mathbf{0} \end{pmatrix}$$

- Variables $\mathbf{q}$: joint variables $\mathbf{q}_r \in \Re^n$ and flexible variables $\mathbf{q}_f \in \Re^N$.
- For AMM with $n_f \leq n$ flexible links and N_j modes for each flexible link, $N = 2\sum_{j=1}^{n_f} N_j$ in 3D and $N = \sum_{j=1}^{n_f} N_j$ for plane.
- For FEM with N_j elements for each flexible link, $N = 4\sum_{j=1}^{n_f} N_j$ in 3D and $N = 2\sum_{j=1}^{n_f} N_j$ for plane.
- In FEM, in the *first* element in each link, $\delta_{j1} = \phi_{j1} = 0$ to represent clamped boundary conditions.

Equations of motion of multi-link flexible manipulators

- Kinetic and potential energy → Lagrangian formulation → equations of motion.
- Equations of motion in a compact form

$$\begin{pmatrix} [\mathbf{M}_{rr}] & [\mathbf{M}_{rf}]^T \\ [\mathbf{M}_{rf}] & [\mathbf{M}_{ff}] \end{pmatrix} \begin{pmatrix} \ddot{\mathbf{q}}_r \\ \ddot{\mathbf{q}}_f \end{pmatrix} + \begin{pmatrix} \mathbf{C}_r(\mathbf{q}, \dot{\mathbf{q}}) \\ \mathbf{C}_f(\mathbf{q}, \dot{\mathbf{q}}) \end{pmatrix} + \begin{pmatrix} \mathbf{G}_r(\mathbf{q}) \\ \mathbf{G}_f(\mathbf{q}) \end{pmatrix}$$
$$+ \begin{pmatrix} \mathbf{0} & \mathbf{0} \\ \mathbf{0} & [\mathbf{K}] \end{pmatrix} \begin{pmatrix} \mathbf{q}_r \\ \mathbf{q}_f \end{pmatrix} = \begin{pmatrix} \tau \\ \mathbf{0} \end{pmatrix}$$

- Variables $\mathbf{q}$: joint variables $\mathbf{q}_r \in \Re^n$ and flexible variables $\mathbf{q}_f \in \Re^N$.
- For AMM with $n_f \leq n$ flexible links and N_j modes for each flexible link, $N = 2\sum_{j=1}^{n_f} N_j$ in 3D and $N = \sum_{j=1}^{n_f} N_j$ for plane.
- For FEM with N_j elements for each flexible link, $N = 4\sum_{j=1}^{n_f} N_j$ in 3D and $N = 2\sum_{j=1}^{n_f} N_j$ for plane.
- In FEM, in the *first* element in each link, $\delta_{j1} = \phi_{j1} = 0$ to represent clamped boundary conditions.

Equations of motion of multi-link flexible manipulators

Properties of terms in equations of motion

- Generalised mass matrix $[\mathbf{M}(\mathbf{q})]$ contain
  - $n \times n$ symmetric, positive definite sub-matrix $[\mathbf{M}_{rr}]$ related to the rigid joint variables.
  - $N \times N$ symmetric, positive definite sub-matrix $[\mathbf{M}_{ff}]$ related to the flexible variables.
  - $N \times n$ sub-matrix $[\mathbf{M}_{rf}]$ representing coupling between the rigid joint and the elastic displacement variables.
- The Coriolis/centripetal terms and the gravity terms can also be partitioned.
- $N \times N$ symmetric, positive definite matrix $[\mathbf{K}]$ is called the flexural stiffness matrix and arises from the strain energy of the flexible links – $[\mathbf{M}_{ff}]$ and $[\mathbf{K}]$ are used in FEM to compute natural frequencies.
- Only joint torques are acting $\rightarrow$ τ is an $n \times 1$ vector.

Equations of motion of multi-link flexible manipulators

Properties of terms in equations of motion

- Generalised mass matrix $[\mathbf{M}(\mathbf{q})]$ contain
  - $n \times n$ symmetric, positive definite sub-matrix $[\mathbf{M}_{rr}]$ related to the rigid joint variables.
  - $N \times N$ symmetric, positive definite sub-matrix $[\mathbf{M}_{ff}]$ related to the flexible variables.
  - $N \times n$ sub-matrix $[\mathbf{M}_{rf}]$ representing coupling between the rigid joint and the elastic displacement variables.
- The Coriolis/centripetal terms and the gravity terms can also be partitioned.
- $N \times N$ symmetric, positive definite matrix $[\mathbf{K}]$ is called the flexural stiffness matrix and arises from the strain energy of the flexible links – $[\mathbf{M}_{ff}]$ and $[\mathbf{K}]$ are used in FEM to compute natural frequencies.
- Only joint torques are acting $\rightarrow$ τ is an $n \times 1$ vector.

- Generalised mass matrix $[\mathbf{M}(\mathbf{q})]$ contain
  - $n \times n$ symmetric, positive definite sub-matrix $[\mathbf{M}_{rr}]$ related to the rigid joint variables.
  - $N \times N$ symmetric, positive definite sub-matrix $[\mathbf{M}_{ff}]$ related to the flexible variables.
  - $N \times n$ sub-matrix $[\mathbf{M}_{rf}]$ representing coupling between the rigid joint and the elastic displacement variables.
- The Coriolis/centripetal terms and the gravity terms can also be partitioned.
- $N \times N$ symmetric, positive definite matrix $[\mathbf{K}]$ is called the flexural stiffness matrix and arises from the strain energy of the flexible links – $[\mathbf{M}_{ff}]$ and $[\mathbf{K}]$ are used in FEM to compute natural frequencies.
- Only joint torques are acting $\rightarrow$ τ is an $n \times 1$ vector.

- Generalised mass matrix $[\mathbf{M}(\mathbf{q})]$ contain
  - $n \times n$ symmetric, positive definite sub-matrix $[\mathbf{M}_{rr}]$ related to the rigid joint variables.
  - $N \times N$ symmetric, positive definite sub-matrix $[\mathbf{M}_{ff}]$ related to the flexible variables.
  - $N \times n$ sub-matrix $[\mathbf{M}_{rf}]$ representing coupling between the rigid joint and the elastic displacement variables.
- The Coriolis/centripetal terms and the gravity terms can also be partitioned.
- $N \times N$ symmetric, positive definite matrix $[\mathbf{K}]$ is called the flexural stiffness matrix and arises from the strain energy of the flexible links – $[\mathbf{M}_{ff}]$ and $[\mathbf{K}]$ are used in FEM to compute natural frequencies.
- Only joint torques are acting $\rightarrow$ τ is an $n \times 1$ vector.

Outline

- Control of a single link flexible manipulator – controllability.
- Two control tasks: trajectory following & tip vibration control.
- Active control using joint actuator[2] *only*.
- Two stage control strategy – Model-based control strategy for trajectory following and end-position vibration control at the end of trajectory following.
- Stability and robustness analysis.
- Numerical simulation results.

[2] One can use passive vibration damping and, more recently, active vibration control using piezo-actuators have been used.

- Control of a single link flexible manipulator – controllability.
- Two control tasks: trajectory following & tip vibration control.
- Active control using joint actuator[2] *only*.
- Two stage control strategy – Model-based control strategy for trajectory following and end-position vibration control at the end of trajectory following.
- Stability and robustness analysis.
- Numerical simulation results.

[2] One can use passive vibration damping and, more recently, active vibration control using piezo-actuators have been used.

- Control of a single link flexible manipulator – controllability.
- Two control tasks: trajectory following & tip vibration control.
- Active control using joint actuator[2] *only*.
- Two stage control strategy – Model-based control strategy for trajectory following and end-position vibration control at the end of trajectory following.
- Stability and robustness analysis.
- Numerical simulation results.

[2] One can use passive vibration damping and, more recently, active vibration control using piezo-actuators have been used.

- Control of a single link flexible manipulator – controllability.
- Two control tasks: trajectory following & tip vibration control.
- Active control using joint actuator[2] *only*.
- Two stage control strategy – Model-based control strategy for trajectory following and end-position vibration control at the end of trajectory following.
- Stability and robustness analysis.
- Numerical simulation results.

[2] One can use passive vibration damping and, more recently, active vibration control using piezo-actuators have been used.

- Control of a single link flexible manipulator – controllability.
- Two control tasks: trajectory following & tip vibration control.
- Active control using joint actuator[2] *only*.
- Two stage control strategy – Model-based control strategy for trajectory following and end-position vibration control at the end of trajectory following.
- Stability and robustness analysis.
- Numerical simulation results.

[2]One can use passive vibration damping and, more recently, active vibration control using piezo-actuators have been used.

- Control of a single link flexible manipulator – controllability.
- Two control tasks: trajectory following & tip vibration control.
- Active control using joint actuator[2] *only*.
- Two stage control strategy – Model-based control strategy for trajectory following and end-position vibration control at the end of trajectory following.
- Stability and robustness analysis.
- Numerical simulation results.

[2] One can use passive vibration damping and, more recently, active vibration control using piezo-actuators have been used.

Block Diagram of a Single Link Flexible Manipulator

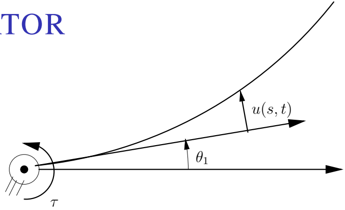

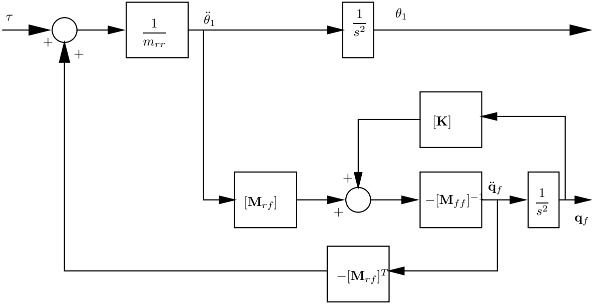

Figure 15: Block diagram of a single flexible-link manipulator

- Recall: Rigid manipulator τ directly influenced θ_m and in flexible joint manipulator τ related to θ_m and θ_l.
- Flexible manipulator: τ directly influence θ_1 and indirectly $\mathbf{q}_f$!
- Not clear if tip vibration ($\mathbf{q}_f$) can be controlled by τ!
- Coupling between rigid and flexible variables!!
  - $\ddot{\theta}_1$ can excite flexible dynamics through $[\mathbf{M}_{rf}]$
  - Resulting $\ddot{\mathbf{q}}_f$ can in turn influence rigid dynamics through $[\mathbf{M}_{rf}]^T$.
- In a multi-link flexible manipulator, there will be additional coupling due to the centripetal/Coriolis terms.

Block Diagram (Contd.)

- Recall: Rigid manipulator τ directly influenced θ_m and in flexible joint manipulator τ related to θ_m and θ_l.
- Flexible manipulator: τ directly influence θ_1 and indirectly $\mathbf{q}_f$!
- Not clear if tip vibration ($\mathbf{q}_f$) can be controlled by τ!
- Coupling between rigid and flexible variables!!
  - $\ddot{\theta}_1$ can excite flexible dynamics through $[\mathbf{M}_{rf}]$
  - Resulting $\ddot{\mathbf{q}}_f$ can in turn influence rigid dynamics through $[\mathbf{M}_{rf}]^T$.
- In a multi-link flexible manipulator, there will be additional coupling due to the centripetal/Coriolis terms.

Block Diagram (contd.)

- Recall: Rigid manipulator τ directly influenced θ_m and in flexible joint manipulator τ related to θ_m and θ_l.
- Flexible manipulator: τ directly influence θ_1 and indirectly $\mathbf{q}_f$!
- Not clear if tip vibration ($\mathbf{q}_f$) can be controlled by τ!
- Coupling between rigid and flexible variables!!
  - $\ddot{\theta}_1$ can excite flexible dynamics through $[\mathbf{M}_{rf}]$
  - Resulting $\ddot{\mathbf{q}}_f$ can in turn influence rigid dynamics through $[\mathbf{M}_{rf}]^T$.
- In a multi-link flexible manipulator, there will be additional coupling due to the centripetal/Coriolis terms.

Block Diagram (Contd.)

- Recall: Rigid manipulator τ directly influenced θ_m and in flexible joint manipulator τ related to θ_m and θ_l.
- Flexible manipulator: τ directly influence θ_1 and indirectly $\mathbf{q}_f$!
- Not clear if tip vibration ($\mathbf{q}_f$) can be controlled by τ!
- Coupling between rigid and flexible variables!!
  - $\ddot{\theta}_1$ can excite flexible dynamics through $[\mathbf{M}_{rf}]$
  - Resulting $\ddot{\mathbf{q}}_f$ can in turn influence rigid dynamics through $[\mathbf{M}_{rf}]^T$.
- In a multi-link flexible manipulator, there will be additional coupling due to the centripetal/Coriolis terms.

Block Diagram (Contd.)

- Recall: Rigid manipulator τ directly influenced θ_m and in flexible joint manipulator τ related to θ_m and θ_l.
- Flexible manipulator: τ directly influence θ_1 and indirectly $\mathbf{q}_f$!
- Not clear if tip vibration ($\mathbf{q}_f$) can be controlled by τ!
- Coupling between rigid and flexible variables!!
  - $\ddot{\theta}_1$ can excite flexible dynamics through $[\mathbf{M}_{rf}]$
  - Resulting $\ddot{\mathbf{q}}_f$ can in turn influence rigid dynamics through $[\mathbf{M}_{rf}]^T$.
- In a multi-link flexible manipulator, there will be additional coupling due to the centripetal/Coriolis terms.

- Rewrite equations of motion as

$$\begin{aligned}\ddot{\mathbf{q}}_r &= [\mathbf{H}_{rr}]\tau - [\mathbf{H}_{rr}](\mathbf{C}_r + \mathbf{G}_r) - [\mathbf{H}_{rf}]^T(\mathbf{C}_f + \mathbf{G}_f + [\mathbf{K}]\mathbf{q}_f) \\ \ddot{\mathbf{q}}_f &= [\mathbf{H}_{rf}]\tau - [\mathbf{H}_{rf}](\mathbf{C}_r + \mathbf{G}_r) - [\mathbf{H}_{ff}](\mathbf{C}_f + \mathbf{G}_f + [\mathbf{K}]\mathbf{q}_f)\end{aligned}$$

where

$$\begin{aligned}[\mathbf{H}_{rr}] &= ([\mathbf{M}_{rr}] - [\mathbf{M}_{rf}]^T[\mathbf{M}_{ff}]^{-1}[\mathbf{M}_{rf}])^{-1} \\ [\mathbf{H}_{rf}]^T &= -[\mathbf{H}_{rr}][\mathbf{M}_{rf}]^T[\mathbf{M}_{ff}]^{-1} \\ [\mathbf{H}_{ff}] &= ([\mathbf{M}_{ff}] - [\mathbf{M}_{rf}][\mathbf{M}_{rr}]^{-1}[\mathbf{M}_{rf}]^T)^{-1}\end{aligned}$$

- If a row of $[\mathbf{H}_{rf}]$ is $\mathbf{0}$ $\rightarrow$ corresponding $\ddot{q}_f$ *cannot* be *directly* controlled by τ – *inaccessibility condition*.
- q_{f_i} induces a moment about the joint axis $\rightarrow$ *controllable*.
- Joint axis lies in plane of deflection components $\rightarrow$ *cannot be controlled*.
- q_{f_i} influenced *indirectly* by *non-zero* $[\mathbf{H}_{ff}](\mathbf{C}_f + \mathbf{G}_f + [\mathbf{K}]\mathbf{q}_f)$ $\rightarrow$ Can be *controlled* even if the row of $[\mathbf{H}_{rf}]$ is $\mathbf{0}$!

Controllability of Flexible-link Manipulators

- Rewrite equations of motion as

$$\begin{aligned}\ddot{\mathbf{q}}_r &= [\mathbf{H}_{rr}]\tau - [\mathbf{H}_{rr}](\mathbf{C}_r + \mathbf{G}_r) - [\mathbf{H}_{rf}]^T(\mathbf{C}_f + \mathbf{G}_f + [\mathbf{K}]\mathbf{q}_f) \\ \ddot{\mathbf{q}}_f &= [\mathbf{H}_{rf}]\tau - [\mathbf{H}_{rf}](\mathbf{C}_r + \mathbf{G}_r) - [\mathbf{H}_{ff}](\mathbf{C}_f + \mathbf{G}_f + [\mathbf{K}]\mathbf{q}_f)\end{aligned}$$

where

$$\begin{aligned}[\mathbf{H}_{rr}] &= ([\mathbf{M}_{rr}] - [\mathbf{M}_{rf}]^T[\mathbf{M}_{ff}]^{-1}[\mathbf{M}_{rf}])^{-1} \\ [\mathbf{H}_{rf}]^T &= -[\mathbf{H}_{rr}][\mathbf{M}_{rf}]^T[\mathbf{M}_{ff}]^{-1} \\ [\mathbf{H}_{ff}] &= ([\mathbf{M}_{ff}] - [\mathbf{M}_{rf}][\mathbf{M}_{rr}]^{-1}[\mathbf{M}_{rf}]^T)^{-1}\end{aligned}$$

- If a row of $[\mathbf{H}_{rf}]$ is $\mathbf{0}$ $\rightarrow$ corresponding $\ddot{q}_f$ *cannot* be *directly* controlled by τ – *inaccessibility condition*.
- q_{f_i} induces a moment about the joint axis $\rightarrow$ *controllable*.
- Joint axis lies in plane of deflection components $\rightarrow$ *cannot be controlled*.
- q_{f_i} influenced *indirectly* by *non-zero* $[\mathbf{H}_{ff}](\mathbf{C}_f + \mathbf{G}_f + [\mathbf{K}]\mathbf{q}_f)$ $\rightarrow$ Can be *controlled* even if the row of $[\mathbf{H}_{rf}]$ is $\mathbf{0}$!

- Rewrite equations of motion as

$$\begin{aligned}\ddot{\mathbf{q}}_r &= [\mathbf{H}_{rr}]\tau - [\mathbf{H}_{rr}](\mathbf{C}_r + \mathbf{G}_r) - [\mathbf{H}_{rf}]^T(\mathbf{C}_f + \mathbf{G}_f + [\mathbf{K}]\mathbf{q}_f) \\ \ddot{\mathbf{q}}_f &= [\mathbf{H}_{rf}]\tau - [\mathbf{H}_{rf}](\mathbf{C}_r + \mathbf{G}_r) - [\mathbf{H}_{ff}](\mathbf{C}_f + \mathbf{G}_f + [\mathbf{K}]\mathbf{q}_f)\end{aligned}$$

where

$$\begin{aligned}[\mathbf{H}_{rr}] &= ([\mathbf{M}_{rr}] - [\mathbf{M}_{rf}]^T[\mathbf{M}_{ff}]^{-1}[\mathbf{M}_{rf}])^{-1} \\ [\mathbf{H}_{rf}]^T &= -[\mathbf{H}_{rr}][\mathbf{M}_{rf}]^T[\mathbf{M}_{ff}]^{-1} \\ [\mathbf{H}_{ff}] &= ([\mathbf{M}_{ff}] - [\mathbf{M}_{rf}][\mathbf{M}_{rr}]^{-1}[\mathbf{M}_{rf}]^T)^{-1}\end{aligned}$$

- If a row of $[\mathbf{H}_{rf}]$ is $\mathbf{0}$ → corresponding $\ddot{q}_f$ *cannot* be *directly* controlled by τ – *inaccessibility condition*.
- q_{f_i} induces a moment about the joint axis → *controllable*.
- Joint axis lies in plane of deflection components → *cannot be controlled*.
- q_{f_i} influenced *indirectly* by *non-zero* $[\mathbf{H}_{ff}](\mathbf{C}_f + \mathbf{G}_f + [\mathbf{K}]\mathbf{q}_f)$ → Can be *controlled* even if the row of $[\mathbf{H}_{rf}]$ is $\mathbf{0}$!

- Rewrite equations of motion as

$$\begin{aligned}
\ddot{\mathbf{q}}_r &= [\mathbf{H}_{rr}]\tau - [\mathbf{H}_{rr}](\mathbf{C}_r + \mathbf{G}_r) - [\mathbf{H}_{rf}]^T(\mathbf{C}_f + \mathbf{G}_f + [\mathbf{K}]\mathbf{q}_f) \\
\ddot{\mathbf{q}}_f &= [\mathbf{H}_{rf}]\tau - [\mathbf{H}_{rf}](\mathbf{C}_r + \mathbf{G}_r) - [\mathbf{H}_{ff}](\mathbf{C}_f + \mathbf{G}_f + [\mathbf{K}]\mathbf{q}_f)
\end{aligned}$$

  where

$$\begin{aligned}
[\mathbf{H}_{rr}] &= ([\mathbf{M}_{rr}] - [\mathbf{M}_{rf}]^T[\mathbf{M}_{ff}]^{-1}[\mathbf{M}_{rf}])^{-1} \\
[\mathbf{H}_{rf}]^T &= -[\mathbf{H}_{rr}][\mathbf{M}_{rf}]^T[\mathbf{M}_{ff}]^{-1} \\
[\mathbf{H}_{ff}] &= ([\mathbf{M}_{ff}] - [\mathbf{M}_{rf}][\mathbf{M}_{rr}]^{-1}[\mathbf{M}_{rf}]^T)^{-1}
\end{aligned}$$

- If a row of $[\mathbf{H}_{rf}]$ is $\mathbf{0}$ $\rightarrow$ corresponding $\ddot{q}_f$ *cannot* be *directly* controlled by τ – *inaccessibility condition*.
- q_{f_i} induces a moment about the joint axis $\rightarrow$ *controllable*.
- Joint axis lies in plane of deflection components $\rightarrow$ *cannot be controlled*.
- q_{f_i} influenced *indirectly* by *non-zero* $[\mathbf{H}_{ff}](\mathbf{C}_f + \mathbf{G}_f + [\mathbf{K}]\mathbf{q}_f)$ $\rightarrow$ Can be *controlled* even if the row of $[\mathbf{H}_{rf}]$ is $\mathbf{0}$!

Controllability of Flexible-link Manipulato

- Rewrite equations of motion as

$$
\begin{aligned}
\ddot{\mathbf{q}}_r &= [\mathbf{H}_{rr}]\tau - [\mathbf{H}_{rr}](\mathbf{C}_r + \mathbf{G}_r) - [\mathbf{H}_{rf}]^T(\mathbf{C}_f + \mathbf{G}_f + [\mathbf{K}]\mathbf{q}_f) \\
\ddot{\mathbf{q}}_f &= [\mathbf{H}_{rf}]\tau - [\mathbf{H}_{rf}](\mathbf{C}_r + \mathbf{G}_r) - [\mathbf{H}_{ff}](\mathbf{C}_f + \mathbf{G}_f + [\mathbf{K}]\mathbf{q}_f)
\end{aligned}
$$

where

$$
\begin{aligned}
[\mathbf{H}_{rr}] &= ([\mathbf{M}_{rr}] - [\mathbf{M}_{rf}]^T[\mathbf{M}_{ff}]^{-1}[\mathbf{M}_{rf}])^{-1} \\
[\mathbf{H}_{rf}]^T &= -[\mathbf{H}_{rr}][\mathbf{M}_{rf}]^T[\mathbf{M}_{ff}]^{-1} \\
[\mathbf{H}_{ff}] &= ([\mathbf{M}_{ff}] - [\mathbf{M}_{rf}][\mathbf{M}_{rr}]^{-1}[\mathbf{M}_{rf}]^T)^{-1}
\end{aligned}
$$

- If a row of $[\mathbf{H}_{rf}]$ is $\mathbf{0}$ $\rightarrow$ corresponding $\ddot{q}_f$ *cannot* be *directly* controlled by τ – *inaccessibility condition*.
- q_{f_i} induces a moment about the joint axis $\rightarrow$ *controllable*.
- Joint axis lies in plane of deflection components $\rightarrow$ *cannot be controlled*.
- q_{f_i} influenced *indirectly* by *non-zero* $[\mathbf{H}_{ff}](\mathbf{C}_f + \mathbf{G}_f + [\mathbf{K}]\mathbf{q}_f)$ $\rightarrow$ Can be *controlled* even if the row of $[\mathbf{H}_{rf}]$ is $\mathbf{0}$!

Model-based Control for Trajectory Following

- Rewrite equations of motion as

$$
\begin{aligned}
[\mathbf{M}_{rr}]\ddot{\mathbf{q}}_r + [\mathbf{M}_{rf}]^T\ddot{\mathbf{q}}_f + \mathbf{C}_r(\mathbf{q},\dot{\mathbf{q}}) + \mathbf{G}_r(\mathbf{q}) &= \tau \\
[\mathbf{M}_{rf}]\ddot{\mathbf{q}}_r + [\mathbf{M}_{ff}]\ddot{\mathbf{q}}_f + \mathbf{C}_f(\mathbf{q},\dot{\mathbf{q}}) + \mathbf{G}_f(\mathbf{q}) + [\mathbf{K}]\mathbf{q}_f &= 0
\end{aligned}
$$

- Solve for $\ddot{\mathbf{q}}_f$ as

$$\ddot{\mathbf{q}}_f = -[\mathbf{M}_{ff}]^{-1}([\mathbf{M}_{rf}]\ddot{\mathbf{q}}_r + \mathbf{C}_f + \mathbf{G}_f + [\mathbf{K}]\mathbf{q}_f)$$

  and substitute in first equation to get

$$
\begin{aligned}
&([\mathbf{M}_{rr}] - [\mathbf{M}_{rf}]^T[\mathbf{M}_{ff}]^{-1}[\mathbf{M}_{rf}])\ddot{\mathbf{q}}_r + \\
&\quad (\mathbf{C}_r + \mathbf{G}_r - [\mathbf{M}_{rf}]^T[\mathbf{M}_{ff}]^{-1}(\mathbf{C}_f + \mathbf{G}_f + [\mathbf{K}]\mathbf{q}_f)) = \tau
\end{aligned}
$$

- Similar to rigid manipulators, choose $\tau_{\mathbf{q}_r} = [\alpha]\tau'_{\mathbf{q}_r} + \beta$ where

$$
\begin{aligned}
[\alpha] &= [\mathbf{M}_{rr}] - [\mathbf{M}_{rf}]^T[\mathbf{M}_{ff}]^{-1}[\mathbf{M}_{rf}] \\
\beta &= \mathbf{C}_r + \mathbf{G}_r - [\mathbf{M}_{rf}]^T [\mathbf{M}_{ff}]^{-1}(\mathbf{C}_f + \mathbf{G}_f + [\mathbf{K}]\mathbf{q}_f)
\end{aligned}
$$

Model-based Control for Trajectory Following

- Rewrite equations of motion as

$$\begin{aligned}[M_{rr}]\ddot{\mathbf{q}}_r + [M_{rf}]^T\ddot{\mathbf{q}}_f + \mathbf{C}_r(\mathbf{q},\dot{\mathbf{q}}) + \mathbf{G}_r(\mathbf{q}) &= \tau \\ [M_{rf}]\ddot{\mathbf{q}}_r + [M_{ff}]\ddot{\mathbf{q}}_f + \mathbf{C}_f(\mathbf{q},\dot{\mathbf{q}}) + \mathbf{G}_f(\mathbf{q}) + [K]\mathbf{q}_f &= \mathbf{0}\end{aligned}$$

- Solve for $\ddot{\mathbf{q}}_f$ as

$$\ddot{\mathbf{q}}_f = -[M_{ff}]^{-1}([M_{rf}]\ddot{\mathbf{q}}_r + \mathbf{C}_f + \mathbf{G}_f + [K]\mathbf{q}_f)$$

and substitute in first equation to get

$$\begin{aligned}&([M_{rr}] - [M_{rf}]^T[M_{ff}]^{-1}[M_{rf}])\ddot{\mathbf{q}}_r + \\ &(\mathbf{C}_r + \mathbf{G}_r - [M_{rf}]^T[M_{ff}]^{-1}(\mathbf{C}_f + \mathbf{G}_f + [K]\mathbf{q}_f)) = \tau\end{aligned}$$

- Similar to rigid manipulators, choose $\tau_{\mathbf{q}_r} = [\alpha]\tau'_{\mathbf{q}_r} + \beta$ where

$$\begin{aligned}[\alpha] &= [M_{rr}] - [M_{rf}]^T[M_{ff}]^{-1}[M_{rf}] \\ \beta &= \mathbf{C}_r + \mathbf{G}_r - [M_{rf}]^T\,[M_{ff}]^{-1}(\mathbf{C}_f + \mathbf{G}_f + [K]\mathbf{q}_f)\end{aligned}$$

Model-based Control for Trajectory Following

- Rewrite equations of motion as

$$\begin{aligned}[\mathbf{M}_{rr}]\ddot{\mathbf{q}}_r + [\mathbf{M}_{rf}]^T\ddot{\mathbf{q}}_f + \mathbf{C}_r(\mathbf{q},\dot{\mathbf{q}}) + \mathbf{G}_r(\mathbf{q}) &= \tau \\ [\mathbf{M}_{rf}]\ddot{\mathbf{q}}_r + [\mathbf{M}_{ff}]\ddot{\mathbf{q}}_f + \mathbf{C}_f(\mathbf{q},\dot{\mathbf{q}}) + \mathbf{G}_f(\mathbf{q}) + [\mathbf{K}]\mathbf{q}_f &= \mathbf{0}\end{aligned}$$

- Solve for $\ddot{\mathbf{q}}_f$ as

$$\ddot{\mathbf{q}}_f = -[\mathbf{M}_{ff}]^{-1}([\mathbf{M}_{rf}]\ddot{\mathbf{q}}_r + \mathbf{C}_f + \mathbf{G}_f + [\mathbf{K}]\mathbf{q}_f)$$

  and substitute in first equation to get

$$\begin{aligned}&([\mathbf{M}_{rr}] - [\mathbf{M}_{rf}]^T[\mathbf{M}_{ff}]^{-1}[\mathbf{M}_{rf}])\ddot{\mathbf{q}}_r + \\ &(\mathbf{C}_r + \mathbf{G}_r - [\mathbf{M}_{rf}]^T[\mathbf{M}_{ff}]^{-1}(\mathbf{C}_f + \mathbf{G}_f + [\mathbf{K}]\mathbf{q}_f)) = \tau\end{aligned}$$

- Similar to rigid manipulators, choose $\tau_{\mathbf{q}_r} = [\alpha]\tau'_{\mathbf{q}_r} + \beta$ where

$$\begin{aligned}[\alpha] &= [\mathbf{M}_{rr}] - [\mathbf{M}_{rf}]^T[\mathbf{M}_{ff}]^{-1}[\mathbf{M}_{rf}] \\ \beta &= \mathbf{C}_r + \mathbf{G}_r - [\mathbf{M}_{rf}]^T\,[\mathbf{M}_{ff}]^{-1}(\mathbf{C}_f + \mathbf{G}_f + [\mathbf{K}]\mathbf{q}_f)\end{aligned}$$

Model-based Control for Trajectory Following

- Similar to rigid manipulators, substitute $[\alpha]$ and β to get an *unit inertia* plant with new input $\tau'_{\mathbf{q}_r}$

$$\tau'_{\mathbf{q}_r} = \ddot{\mathbf{q}}_r$$

- Choose $\tau'_{\mathbf{q}_r}$ as

$$\tau'_{\mathbf{q}_r} = \ddot{\mathbf{q}}_{r_d}(t) + [K_p]_{\mathbf{q}_r}\mathbf{e}(t) + [K_v]_{\mathbf{q}_r}\dot{\mathbf{e}}(t)$$

- For $\mathbf{e}(t) = \mathbf{q}_{r_d} - \mathbf{q}_r$ and $\mathbf{q}_{r_d}(t)$ as the desired joint trajectory, the error equation becomes

$$\ddot{\mathbf{e}}_r(t) + [K_p]_{\mathbf{q}_r}\mathbf{e}_r(t) + [K_v]_{\mathbf{q}_r}\dot{\mathbf{e}}_r(t) = \mathbf{0}$$

- For appropriate controller gains $[K_p]_{\mathbf{q}_r}$ and $[K_v]_{\mathbf{q}_r}$, $\mathbf{e}_r(t)$, $\dot{\mathbf{e}}_r(t) \rightarrow 0$ asymptotically and desired trajectory can be followed.

Model-based Control for Trajectory Following

- Similar to rigid manipulators, substitute $[\alpha]$ and β to get an *unit inertia* plant with new input $\tau'_{\mathbf{q}_r}$

$$\tau'_{\mathbf{q}_r} = \ddot{\mathbf{q}}_r$$

- Choose $\tau'_{\mathbf{q}_r}$ as

$$\tau'_{\mathbf{q}_r} = \ddot{\mathbf{q}}_{r_d}(t) + [K_p]_{\mathbf{q}_r}\mathbf{e}(t) + [K_v]_{\mathbf{q}_r}\dot{\mathbf{e}}(t)$$

- For $\mathbf{e}(t) = \mathbf{q}_{r_d} - \mathbf{q}_r$ and $\mathbf{q}_{r_d}(t)$ as the desired joint trajectory, the error equation becomes

$$\ddot{\mathbf{e}}_r(t) + [K_p]_{\mathbf{q}_r}\mathbf{e}_r(t) + [K_v]_{\mathbf{q}_r}\dot{\mathbf{e}}_r(t) = \mathbf{0}$$

- For appropriate controller gains $[K_p]_{\mathbf{q}_r}$ and $[K_v]_{\mathbf{q}_r}$, $\mathbf{e}_r(t)$, $\dot{\mathbf{e}}_r(t) \to 0$ asymptotically and desired trajectory can be followed.

Model-based Control for Trajectory Following

- Similar to rigid manipulators, substitute $[\alpha]$ and β to get an *unit inertia* plant with new input $\tau'_{\mathbf{q}_r}$

$$\tau'_{\mathbf{q}_r} = \ddot{\mathbf{q}}_r$$

- Choose $\tau'_{\mathbf{q}_r}$ as

$$\tau'_{\mathbf{q}_r} = \ddot{\mathbf{q}}_{r_d}(t) + [K_p]_{\mathbf{q}_r}\mathbf{e}(t) + [K_v]_{\mathbf{q}_r}\dot{\mathbf{e}}(t)$$

- For $\mathbf{e}(t) = \mathbf{q}_{r_d} - \mathbf{q}_r$ and $\mathbf{q}_{r_d}(t)$ as the desired joint trajectory, the error equation becomes

$$\ddot{\mathbf{e}}_r(t) + [K_p]_{\mathbf{q}_r}\mathbf{e}_r(t) + [K_v]_{\mathbf{q}_r}\dot{\mathbf{e}}_r(t) = \mathbf{0}$$

- For appropriate controller gains $[K_p]_{\mathbf{q}_r}$ and $[K_v]_{\mathbf{q}_r}$, $\mathbf{e}_r(t)$, $\dot{\mathbf{e}}_r(t) \to 0$ asymptotically and desired trajectory can be followed.

Model-based Control for Trajectory Following

- Similar to rigid manipulators, substitute $[\alpha]$ and β to get an *unit inertia* plant with new input $\tau'_{\mathbf{q}_r}$

$$\tau'_{\mathbf{q}_r} = \ddot{\mathbf{q}}_r$$

- Choose $\tau'_{\mathbf{q}_r}$ as

$$\tau'_{\mathbf{q}_r} = \ddot{\mathbf{q}}_{r_d}(t) + [K_p]_{\mathbf{q}_r}\mathbf{e}(t) + [K_v]_{\mathbf{q}_r}\dot{\mathbf{e}}(t)$$

- For $\mathbf{e}(t) = \mathbf{q}_{r_d} - \mathbf{q}_r$ and $\mathbf{q}_{r_d}(t)$ as the desired joint trajectory, the error equation becomes

$$\ddot{\mathbf{e}}_r(t) + [K_p]_{\mathbf{q}_r}\mathbf{e}_r(t) + [K_v]_{\mathbf{q}_r}\dot{\mathbf{e}}_r(t) = \mathbf{0}$$

- For appropriate controller gains $[K_p]_{\mathbf{q}_r}$ and $[K_v]_{\mathbf{q}_r}$, $\mathbf{e}_r(t)$, $\dot{\mathbf{e}}_r(t) \rightarrow 0$ asymptotically and desired trajectory can be followed.

- The *closed-loop system equations* for the model-based controller are

$$\ddot{\mathbf{q}}_r(t) = \tau'_{\mathbf{q}_r}$$
$$[\mathbf{M}_{ff}]\ddot{\mathbf{q}}_f + \mathbf{C}_f(\mathbf{q}, \dot{\mathbf{q}}) + \mathbf{G}_f(\mathbf{q}) \ + \ [\mathbf{K}]\mathbf{q}_f = -[\mathbf{M}_{rf}]\tau'_{\mathbf{q}_r}$$

- Smooth tracking of $\mathbf{q}_{r_d}(t)$ as long as flexible variables $\mathbf{q}_f$ are stable.
- The flexible variables $\mathbf{q}_f$ are coupled to control input $\tau'_{\mathbf{q}_r}$ through the matrix $[\mathbf{M}_{rf}]$.
- The stability of $\mathbf{q}_f$ are determined by the zero dynamics[3].

$$\ddot{\mathbf{q}}_f = -[\mathbf{M}_{ff}]^{-1}(\mathbf{C}_f + \mathbf{G}_f + [\mathbf{K}]\mathbf{q}_f)$$

where all terms are evaluated for a constant $\mathbf{q}_r^*$ and $\dot{\mathbf{q}}_r = \mathbf{0}$.

[3] The zero dynamics of a non-linear system describe the dynamic behaviour of the system when inputs are chosen to constrain the outputs of the system to be zero or constant (Isidori 1989).

- The *closed-loop system equations* for the model-based controller are

$$\ddot{\mathbf{q}}_r(t) = {\tau'}_{\mathbf{q}_r}$$
$$[\mathbf{M}_{ff}]\ddot{\mathbf{q}}_f + \mathbf{C}_f(\mathbf{q}, \dot{\mathbf{q}}) + \mathbf{G}_f(\mathbf{q}) \ + \ [\mathbf{K}]\mathbf{q}_f = -[\mathbf{M}_{rf}]{\tau'}_{\mathbf{q}_r}$$

- Smooth tracking of $\mathbf{q}_{r_d}(t)$ as long as flexible variables $\mathbf{q}_f$ are stable.
- The flexible variables $\mathbf{q}_f$ are coupled to control input ${\tau'}_{\mathbf{q}_r}$ through the matrix $[\mathbf{M}_{rf}]$.
- The stability of $\mathbf{q}_f$ are determined by the zero dynamics[3].

$$\ddot{\mathbf{q}}_f = -[\mathbf{M}_{ff}]^{-1}(\mathbf{C}_f + \mathbf{G}_f + [\mathbf{K}]\mathbf{q}_f)$$

where all terms are evaluated for a constant $\mathbf{q}_r^*$ and $\dot{\mathbf{q}}_r \ = \ \mathbf{0}$.

[3] The zero dynamics of a non-linear system describe the dynamic behaviour of the system when inputs are chosen to constrain the outputs of the system to be zero or constant (Isidori 1989).

- The *closed-loop system equations* for the model-based controller are

$$\ddot{\mathbf{q}}_r(t) = \tau'_{\mathbf{q}_r}$$
$$[\mathbf{M}_{ff}]\ddot{\mathbf{q}}_f + \mathbf{C}_f(\mathbf{q},\dot{\mathbf{q}}) + \mathbf{G}_f(\mathbf{q}) \; + \; [\mathbf{K}]\mathbf{q}_f = -[\mathbf{M}_{rf}]\tau'_{\mathbf{q}_r}$$

- Smooth tracking of $\mathbf{q}_{r_d}(t)$ as long as flexible variables $\mathbf{q}_f$ are stable.
- The flexible variables $\mathbf{q}_f$ are coupled to control input $\tau'_{\mathbf{q}_r}$ through the matrix $[\mathbf{M}_{rf}]$.
- The stability of $\mathbf{q}_f$ are determined by the zero dynamics[3].

$$\ddot{\mathbf{q}}_f = -[\mathbf{M}_{ff}]^{-1}(\mathbf{C}_f + \mathbf{G}_f + [\mathbf{K}]\mathbf{q}_f)$$

where all terms are evaluated for a constant $\mathbf{q}_r^*$ and $\dot{\mathbf{q}}_r = \mathbf{0}$.

[3] The zero dynamics of a non-linear system describe the dynamic behaviour of the system when inputs are chosen to constrain the outputs of the system to be zero or constant (Isidori 1989).

- The *closed-loop system equations* for the model-based controller are

$$\ddot{\mathbf{q}}_r(t) = {\tau'}_{\mathbf{q}_r}$$
$$[\mathbf{M}_{ff}]\ddot{\mathbf{q}}_f + \mathbf{C}_f(\mathbf{q},\dot{\mathbf{q}}) + \mathbf{G}_f(\mathbf{q}) \ + \ [\mathbf{K}]\mathbf{q}_f = -[\mathbf{M}_{rf}]{\tau'}_{\mathbf{q}_r}$$

- Smooth tracking of $\mathbf{q}_{r_d}(t)$ as long as flexible variables $\mathbf{q}_f$ are stable.
- The flexible variables $\mathbf{q}_f$ are coupled to control input ${\tau'}_{\mathbf{q}_r}$ through the matrix $[\mathbf{M}_{rf}]$.
- The stability of $\mathbf{q}_f$ are determined by the zero dynamics[3].

$$\ddot{\mathbf{q}}_f = -[\mathbf{M}_{ff}]^{-1}(\mathbf{C}_f + \mathbf{G}_f + [\mathbf{K}]\mathbf{q}_f)$$

where all terms are evaluated for a constant $\mathbf{q}_r^*$ and $\dot{\mathbf{q}}_r \ = \ \mathbf{0}$.

[3]The zero dynamics of a non-linear system describe the dynamic behaviour of the system when inputs are chosen to constrain the outputs of the system to be zero or constant (Isidori 1989).

Model-based Control for Trajectory Following

Stability Analysis (contd.)

- Equilibrium points: $\dot{\mathbf{q}}_f = \mathbf{0}$ and a static deflection $\mathbf{q}_f^*$ which satisfies

$$[\mathbf{K}]\mathbf{q}_f^* + \mathbf{G}_f(\mathbf{q}_r^*, \mathbf{q}_f^*) = \mathbf{0}$$

- Candidate Lyapunov function

$$\begin{aligned} V(\mathbf{q}_f, \dot{\mathbf{q}}_f) &= \frac{1}{2}\dot{\mathbf{q}}_f^T[\mathbf{M}_{ff}]\dot{\mathbf{q}}_f + \frac{1}{2}(\mathbf{q}_f^* - \mathbf{q}_f)^T[\mathbf{K}](\mathbf{q}_f^* - \mathbf{q}_f) \\ &\quad + (V_G(\mathbf{q}_r^*, \mathbf{q}_f) - V_G(\mathbf{q}_r^*, \mathbf{q}_f^*)) + (\mathbf{q}_f^* - \mathbf{q}_f)^T\mathbf{G}_f(\mathbf{q}_r^*, \mathbf{q}_f^*) \end{aligned}$$

  V_G denotes the gravitational potential energy yielding $\mathbf{G}_f$.

- The time derivative, after simplification and using skew-symmetric nature of $\left[[\dot{\mathbf{M}}_{ff}] - 2[\mathbf{C}_{ff}]\right]$, is

$$\dot{V} = \frac{1}{2}\dot{\mathbf{q}}_f^T\left([\dot{\mathbf{M}}_{ff}] - 2[\mathbf{C}_{ff}]\right)\dot{\mathbf{q}}_f - \dot{\mathbf{q}}_f^T\left([\mathbf{K}]\mathbf{q}_f^* + \mathbf{G}_f(\mathbf{q}_r^*, \mathbf{q}_f^*)\right) = 0$$

- *Critically stable* $\rightarrow$ With damping *asymptotically* stable.

Stability Analysis (contd.)

- Equilibrium points: $\dot{\mathbf{q}}_f = \mathbf{0}$ and a static deflection $\mathbf{q}_f^*$ which satisfies

$$[\mathbf{K}]\mathbf{q}_f^* + \mathbf{G}_f(\mathbf{q}_r^*, \mathbf{q}_f^*) = \mathbf{0}$$

- Candidate Lyapunov function

$$\begin{aligned} V(\mathbf{q}_f, \dot{\mathbf{q}}_f) &= \frac{1}{2}\dot{\mathbf{q}}_f^T[\mathbf{M}_{ff}]\dot{\mathbf{q}}_f + \frac{1}{2}(\mathbf{q}_f^* - \mathbf{q}_f)^T[\mathbf{K}](\mathbf{q}_f^* - \mathbf{q}_f) \\ &\quad + (V_G(\mathbf{q}_r^*, \mathbf{q}_f) - V_G(\mathbf{q}_r^*, \mathbf{q}_f^*)) + (\mathbf{q}_f^* - \mathbf{q}_f)^T \mathbf{G}_f(\mathbf{q}_r^*, \mathbf{q}_f^*) \end{aligned}$$

V_G denotes the gravitational potential energy yielding $\mathbf{G}_f$.

- The time derivative, after simplification and using skew-symmetric nature of $\left[[\dot{\mathbf{M}}_{ff}] - 2[\mathbf{C}_{ff}]\right]$, is

$$\dot{V} = \frac{1}{2}\dot{\mathbf{q}}_f^T\left([\dot{\mathbf{M}}_{ff}] - 2[\mathbf{C}_{ff}]\right)\dot{\mathbf{q}}_f - \dot{\mathbf{q}}_f^T\left([\mathbf{K}]\mathbf{q}_f^* + \mathbf{G}_f(\mathbf{q}_r^*, \mathbf{q}_f^*)\right) = 0$$

- *Critically stable* → With damping *asymptotically* stable.

Model-based Control for Trajectory Following

Stability Analysis (contd.)

- Equilibrium points: $\dot{\mathbf{q}}_f = \mathbf{0}$ and a static deflection $\mathbf{q}_f^*$ which satisfies

$$[\mathbf{K}]\mathbf{q}_f^* + \mathbf{G}_f(\mathbf{q}_r^*, \mathbf{q}_f^*) = \mathbf{0}$$

- Candidate Lyapunov function

$$\begin{aligned} V(\mathbf{q}_f, \dot{\mathbf{q}}_f) &= \frac{1}{2}\dot{\mathbf{q}}_f^T[\mathbf{M}_{ff}]\dot{\mathbf{q}}_f + \frac{1}{2}(\mathbf{q}_f^* - \mathbf{q}_f)^T[\mathbf{K}](\mathbf{q}_f^* - \mathbf{q}_f) \\ &\quad + (V_G(\mathbf{q}_r^*, \mathbf{q}_f) - V_G(\mathbf{q}_r^*, \mathbf{q}_f^*)) + (\mathbf{q}_f^* - \mathbf{q}_f)^T\mathbf{G}_f(\mathbf{q}_r^*, \mathbf{q}_f^*) \end{aligned}$$

  V_G denotes the gravitational potential energy yielding $\mathbf{G}_f$.
- The time derivative, after simplification and using skew-symmetric nature of $\left[[\dot{\mathbf{M}}_{ff}] - 2[\mathbf{C}_{ff}]\right]$, is

$$\dot{V} = \frac{1}{2}\dot{\mathbf{q}}_f^T\left([\dot{\mathbf{M}}_{ff}] - 2[\mathbf{C}_{ff}]\right)\dot{\mathbf{q}}_f - \dot{\mathbf{q}}_f^T\left([\mathbf{K}]\mathbf{q}_f^* + \mathbf{G}_f(\mathbf{q}_r^*, \mathbf{q}_f^*)\right) = 0$$

- *Critically stable* → With damping *asymptotically* stable.

Stability Analysis (Contd.)

- Equilibrium points: $\dot{\mathbf{q}}_f = \mathbf{0}$ and a static deflection $\mathbf{q}_f^*$ which satisfies

$$[\mathbf{K}]\mathbf{q}_f^* + \mathbf{G}_f(\mathbf{q}_r^*, \mathbf{q}_f^*) = \mathbf{0}$$

- Candidate Lyapunov function

$$\begin{aligned} V(\mathbf{q}_f, \dot{\mathbf{q}}_f) \quad = \quad & \frac{1}{2}\dot{\mathbf{q}}_f^T[\mathbf{M}_{ff}]\dot{\mathbf{q}}_f + \frac{1}{2}(\mathbf{q}_f^* - \mathbf{q}_f)^T[\mathbf{K}](\mathbf{q}_f^* - \mathbf{q}_f) \\ & + (V_G(\mathbf{q}_r^*, \mathbf{q}_f) - V_G(\mathbf{q}_r^*, \mathbf{q}_f^*)) + (\mathbf{q}_f^* - \mathbf{q}_f)^T\mathbf{G}_f(\mathbf{q}_r^*, \mathbf{q}_f^*) \end{aligned}$$

  V_G denotes the gravitational potential energy yielding $\mathbf{G}_f$.
- The time derivative, after simplification and using skew-symmetric nature of $\left[[\dot{\mathbf{M}}_{ff}] - 2[\mathbf{C}_{ff}]\right]$, is

$$\dot{V} = \frac{1}{2}\dot{\mathbf{q}}_f^T\left([\dot{\mathbf{M}}_{ff}] - 2[\mathbf{C}_{ff}]\right)\dot{\mathbf{q}}_f - \dot{\mathbf{q}}_f^T([\mathbf{K}]\mathbf{q}_f^* + \mathbf{G}_f(\mathbf{q}_r^*, \mathbf{q}_f^*)) = 0$$

- *Critically stable* $\rightarrow$ With damping *asymptotically* stable.

- Joint motion excites vibration in link $\rightarrow$ Need to be suppressed for task.
- Tip vibration to be controlled by joint rotation alone!
- Relationship between tip motion and joint motion – Jacobian matrix (similar to rigid case).
- Full Jacobian contain *joint rotation* variables $\mathbf{q}_r$ and *flexible* variable $\mathbf{q}_f$ – Difficult to measure *all* components of $\mathbf{q}_f$.
- Control law using Jacobian derived from *desired* rigid variables – same as the rigid Jacobian matrix – *always exist*.

$$[{J^r}_{\mathbf{q}_r}(\mathbf{q}_{r_d})] = \left(\frac{\partial \mathbf{f}}{\partial \mathbf{q}_r}\right)_{\mathbf{q}_r=\mathbf{q}_{r_d},\mathbf{q}_f=\mathbf{0}}$$

$\mathscr{X} = \mathbf{f}(\mathbf{q}_r, \mathbf{q}_f)$ represents the kinematic equations of the flexible manipulator.

End Position Vibration Control

- Joint motion excites vibration in link $\rightarrow$ Need to be suppressed for task.
- Tip vibration to be controlled by joint rotation alone!
- Relationship between tip motion and joint motion – Jacobian matrix (similar to rigid case).
- Full Jacobian contain *joint rotation* variables $\mathbf{q}_r$ and *flexible* variable $\mathbf{q}_f$ – Difficult to measure *all* components of $\mathbf{q}_f$.
- Control law using Jacobian derived from *desired* rigid variables – same as the rigid Jacobian matrix – *always exist*.

$$[J^r{}_{\mathbf{q}_r}(\mathbf{q}_{r_d})] = \left(\frac{\partial \mathbf{f}}{\partial \mathbf{q}_r}\right)_{\mathbf{q}_r=\mathbf{q}_{r_d},\mathbf{q}_f=\mathbf{0}}$$

$\mathscr{X} = \mathbf{f}(\mathbf{q}_r, \mathbf{q}_f)$ represents the kinematic equations of the flexible manipulator.

End Position Vibration Control

- Joint motion excites vibration in link $\rightarrow$ Need to be suppressed for task.
- Tip vibration to be controlled by joint rotation alone!
- Relationship between tip motion and joint motion – Jacobian matrix (similar to rigid case).
- Full Jacobian contain *joint rotation* variables $\mathbf{q}_r$ and *flexible* variable $\mathbf{q}_f$ – Difficult to measure *all* components of $\mathbf{q}_f$.
- Control law using Jacobian derived from *desired* rigid variables – same as the rigid Jacobian matrix – *always exist*.

$$[J^r{}_{\mathbf{q}_r}(\mathbf{q}_{r_d})] = \left(\frac{\partial \mathbf{f}}{\partial \mathbf{q}_r} \right)_{\mathbf{q}_r = \mathbf{q}_{r_d}, \mathbf{q}_f = \mathbf{0}}$$

$\mathscr{X} = \mathbf{f}(\mathbf{q}_r, \mathbf{q}_f)$ represents the kinematic equations of the flexible manipulator.

End Position Vibration Control

- Joint motion excites vibration in link $\rightarrow$ Need to be suppressed for task.
- Tip vibration to be controlled by joint rotation alone!
- Relationship between tip motion and joint motion – Jacobian matrix (similar to rigid case).
- Full Jacobian contain *joint rotation* variables $\mathbf{q}_r$ and *flexible* variable $\mathbf{q}_f$ – Difficult to measure *all* components of $\mathbf{q}_f$.
- Control law using Jacobian derived from *desired* rigid variables – same as the rigid Jacobian matrix – *always exist*.

$$[{J^r}_{\mathbf{q}_r}(\mathbf{q}_{r_d})] = \left(\frac{\partial \mathbf{f}}{\partial \mathbf{q}_r}\right)_{\mathbf{q}_r=\mathbf{q}_{r_d},\mathbf{q}_f=\mathbf{0}}$$

$\mathscr{X} = \mathbf{f}(\mathbf{q}_r, \mathbf{q}_f)$ represents the kinematic equations of the flexible manipulator.

End Position Vibration Control

- Joint motion excites vibration in link $\rightarrow$ Need to be suppressed for task.
- Tip vibration to be controlled by joint rotation alone!
- Relationship between tip motion and joint motion – Jacobian matrix (similar to rigid case).
- Full Jacobian contain *joint rotation* variables $\mathbf{q}_r$ and *flexible* variable $\mathbf{q}_f$ – Difficult to measure *all* components of $\mathbf{q}_f$.
- Control law using Jacobian derived from *desired* rigid variables – same as the rigid Jacobian matrix – *always exist*.

$$[{J^r}_{\mathbf{q}_r}(\mathbf{q}_{r_d})] = \left(\frac{\partial \mathbf{f}}{\partial \mathbf{q}_r}\right)_{\mathbf{q}_r=\mathbf{q}_{r_d},\mathbf{q}_f=\mathbf{0}}$$

$\mathscr{X} = \mathbf{f}(\mathbf{q}_r, \mathbf{q}_f)$ represents the kinematic equations of the flexible manipulator.

End Position Vibration Control

- A controller using the rigid Jacobian

$$\tau_{\mathscr{X}} = [J^r_{\mathbf{q}_r}]^T \left(-[K_p]_{\mathscr{X}} \delta \mathscr{X} - [K_v]_{\mathscr{X}} \dot{\mathscr{X}} \right) + \mathbf{G}_r(\mathbf{q}_{r_d}, \mathbf{q}_{f_d})$$

  - $\mathscr{X}$ represents position and orientation of the end-effector & $\delta \mathscr{X} = \mathscr{X} - \mathscr{X}_d$[4].
  - Gain matrices $[K_p]_{\mathscr{X}}$ and $[K_v]_{\mathscr{X}}$ are constant diagonal matrices.
  - $\mathbf{q}_{r_d}$ is the final point of the desired joint trajectory and $\mathbf{q}_{f_d}$ is obtained from the static deflection under gravity

$$\mathbf{q}_{f_d} = -[\mathbf{K}]^{-1} \mathbf{G}_f(\mathbf{q}_{r_d}, \mathbf{q}_{f_d})$$

  - $\mathscr{X} - \mathscr{X}_d$ is due to *flexible* vibrations and is expected to be small.
  - Control torque $\tau_{\mathscr{X}}$ at joint although $\mathscr{X} - \mathscr{X}_d$ is a Cartesian error vector – Similar to Cartesian control of rigid robots, Jacobian $[J^r_{\mathbf{q}_r}]^T$ relates Cartesian force/moments to joint torques (see Module 7, Lecture 4).

[4] Error defined *opposite* to definition $(\cdot)_d - (\cdot)$ till now and hence the $-$ sign in control law. This is required for consistency in definition of rigid Jacobian using Taylor series expansion.

- Equilibrium points under end-position control: $\mathbf{q} = \mathbf{q}_d$ and $\dot{\mathbf{q}} = \mathbf{0}$.
- Equilibrium points are unique (see Ghosal 2006) if for a positive constant c

$$\lambda_{min}([\mathbf{K}]) > c, \quad \lambda_{min}\left([J^r_{\mathbf{q}_r}]^T [K_p]_{\mathscr{X}}\right) > c$$

- Physically: The manipulator can be placed at an *arbitrary* $\mathbf{q} = \mathbf{q}_d$ and $\dot{\mathbf{q}} = \mathbf{0}$, if the minimum stiffness and minimum controller gains are large enough to overcome static deflection due to gravity!
- Candidate Lyapunov function

$$\begin{aligned} V &= \frac{1}{2}\dot{\mathbf{q}}^T[\mathbf{M}(\mathbf{q})]\dot{\mathbf{q}} + \frac{1}{2}(\mathbf{q}_{f_d} - \mathbf{q}_f)^T[\mathbf{K}](\mathbf{q}_{f_d} - \mathbf{q}_f) \\ &+ (V_G(\mathbf{q}) - V_G(\mathbf{q}_d)) + (\mathbf{q}_d - \mathbf{q})^T\mathbf{G}(\mathbf{q}_d) + \frac{1}{2}\delta\mathscr{X}^T[K_p]_{\mathscr{X}}\delta\mathscr{X} \end{aligned}$$

V_G denotes the gravitational potential energy giving rise to $\mathbf{G}(\mathbf{q})$.

- Equilibrium points under end-position control: $\mathbf{q} = \mathbf{q}_d$ and $\dot{\mathbf{q}} = \mathbf{0}$.
- Equilibrium points are unique (see Ghosal 2006) if for a positive constant c

$$\lambda_{min}([\mathbf{K}]) > c, \quad \lambda_{min}\left([J^r_{\mathbf{q}_r}]^T [K_p]_{\mathscr{X}}\right) > c$$

- Physically: The manipulator can be placed at an *arbitrary* $\mathbf{q} = \mathbf{q}_d$ and $\dot{\mathbf{q}} = \mathbf{0}$, if the minimum stiffness and minimum controller gains are large enough to overcome static deflection due to gravity!
- Candidate Lyapunov function

$$\begin{aligned} V &= \frac{1}{2}\dot{\mathbf{q}}^T[\mathbf{M}(\mathbf{q})]\dot{\mathbf{q}} + \frac{1}{2}(\mathbf{q}_{f_d} - \mathbf{q}_f)^T[\mathbf{K}](\mathbf{q}_{f_d} - \mathbf{q}_f) \\ &\quad + (V_G(\mathbf{q}) - V_G(\mathbf{q}_d)) + (\mathbf{q}_d - \mathbf{q})^T\mathbf{G}(\mathbf{q}_d) + \frac{1}{2}\delta\mathscr{X}^T[K_p]_{\mathscr{X}}\delta\mathscr{X} \end{aligned}$$

V_G denotes the gravitational potential energy giving rise to $\mathbf{G}(\mathbf{q})$.

- Equilibrium points under end-position control: $\mathbf{q} = \mathbf{q}_d$ and $\dot{\mathbf{q}} = \mathbf{0}$.
- Equilibrium points are unique (see Ghosal 2006) if for a positive constant c

$$\lambda_{min}([\mathbf{K}]) > c, \quad \lambda_{min}\left([J^r_{\mathbf{q}_r}]^T [K_p]_{\mathscr{X}}\right) > c$$

- Physically: The manipulator can be placed at an *arbitrary* $\mathbf{q} = \mathbf{q}_d$ and $\dot{\mathbf{q}} = \mathbf{0}$, if the minimum stiffness and minimum controller gains are large enough to overcome static deflection due to gravity!
- Candidate Lyapunov function

$$\begin{aligned} V = & \frac{1}{2}\dot{\mathbf{q}}^T[\mathbf{M}(\mathbf{q})]\dot{\mathbf{q}} + \frac{1}{2}(\mathbf{q}_{f_d} - \mathbf{q}_f)^T[\mathbf{K}](\mathbf{q}_{f_d} - \mathbf{q}_f) \\ & + (V_G(\mathbf{q}) - V_G(\mathbf{q}_d)) + (\mathbf{q}_d - \mathbf{q})^T\mathbf{G}(\mathbf{q}_d) + \frac{1}{2}\delta\mathscr{X}^T[K_p]_{\mathscr{X}}\delta\mathscr{X} \end{aligned}$$

V_G denotes the gravitational potential energy giving rise to $\mathbf{G}(\mathbf{q})$.

- Equilibrium points under end-position control: $\mathbf{q} = \mathbf{q}_d$ and $\dot{\mathbf{q}} = \mathbf{0}$.
- Equilibrium points are unique (see Ghosal 2006) if for a positive constant c

$$\lambda_{min}([\mathbf{K}]) > c, \quad \lambda_{min}\left([J^r_{\mathbf{q}_r}]^T[K_p]_{\mathscr{X}}\right) > c$$

- Physically: The manipulator can be placed at an *arbitrary* $\mathbf{q} = \mathbf{q}_d$ and $\dot{\mathbf{q}} = \mathbf{0}$, if the minimum stiffness and minimum controller gains are large enough to overcome static deflection due to gravity!
- Candidate Lyapunov function

$$\begin{aligned} V &= \frac{1}{2}\dot{\mathbf{q}}^T[\mathbf{M}(\mathbf{q})]\dot{\mathbf{q}} + \frac{1}{2}(\mathbf{q}_{f_d} - \mathbf{q}_f)^T[\mathbf{K}](\mathbf{q}_{f_d} - \mathbf{q}_f) \\ &\quad + (V_G(\mathbf{q}) - V_G(\mathbf{q}_d)) + (\mathbf{q}_d - \mathbf{q})^T\mathbf{G}(\mathbf{q}_d) + \frac{1}{2}\delta\mathscr{X}^T[K_p]_{\mathscr{X}}\delta\mathscr{X} \end{aligned}$$

V_G denotes the gravitational potential energy giving rise to $\mathbf{G}(\mathbf{q})$.

END POSITION VIBRATION CONTROL

STABILITY ANALYSIS (CONTD.)

- Time derivative of V, after simplification using equations of motion, the skew-symmetry property and the control law based on rigid Jacobian

$$\dot{V} = -\dot{\mathscr{X}}^T [K_v]_{\mathscr{X}} \dot{\mathscr{X}} + \left(\dot{\mathscr{X}} - [J^r_{\mathbf{q}_r}]\dot{\mathbf{q}}_r\right)^T \left([K_p]_{\mathscr{X}} \delta\mathscr{X} + [K_v]_{\mathscr{X}} \dot{\mathscr{X}}\right)$$

- $\dot{V}$ is *strictly* negative if

$$\left|\left(\dot{\mathscr{X}} - [J^r_{\mathbf{q}_r}]\dot{\mathbf{q}}_r\right)^T \left([K_p]_{\mathscr{X}} \delta\mathscr{X} + [K_v]_{\mathscr{X}} \dot{\mathscr{X}}\right)\right| \quad < \quad \left|\dot{\mathscr{X}}^T [K_v]_{\mathscr{X}} \dot{\mathscr{X}}\right|$$

- $[K_v]_{\mathscr{X}}$ satisfies inequality if *minimum* eigenvalue of $[K_v]_{\mathscr{X}}$, λ_v, satisfy

$$\lambda_v \quad > \quad \frac{\gamma\, \lambda_p\, \alpha}{\beta(\beta - \gamma)}$$

  where $\| (\dot{\mathscr{X}} - [J^r_{\mathbf{q}_r}]\dot{\mathbf{q}}_r) \| = \gamma$, $\| \delta\mathscr{X} \| = \alpha$, $\| \dot{\mathscr{X}} \| = \beta$, $\lambda_{min}([K_p]_{\mathscr{X}}) = \lambda_p$, at the end of the trajectory following phase.

- Note: Link vibration are not zero at the end of the trajectory following phase $\Rightarrow \beta \neq 0$.

- Time derivative of V, after simplification using equations of motion, the skew-symmetry property and the control law based on rigid Jacobian

$$\dot{V} = -\dot{\mathscr{X}}^T [K_v]_{\mathscr{X}} \dot{\mathscr{X}} + \left(\dot{\mathscr{X}} - [J^r_{\mathbf{q}_r}]\dot{\mathbf{q}}_r\right)^T \left([K_p]_{\mathscr{X}} \delta\mathscr{X} + [K_v]_{\mathscr{X}} \dot{\mathscr{X}}\right)$$

- $\dot{V}$ is *strictly* negative if

$$\mid \left(\dot{\mathscr{X}} - [J^r_{\mathbf{q}_r}]\dot{\mathbf{q}}_r\right)^T \left([K_p]_{\mathscr{X}} \delta\mathscr{X} + [K_v]_{\mathscr{X}} \dot{\mathscr{X}}\right) \mid \quad < \quad \mid \dot{\mathscr{X}}^T [K_v]_{\mathscr{X}} \dot{\mathscr{X}} \mid$$

- $[K_v]_{\mathscr{X}}$ satisfies inequality if *minimum* eigenvalue of $[K_v]_{\mathscr{X}}$, λ_v, satisfy

$$\lambda_v \quad > \quad \frac{\gamma\, \lambda_p\, \alpha}{\beta(\beta - \gamma)}$$

where $\| \, (\dot{\mathscr{X}} - [J^r_{\mathbf{q}_r}]\dot{\mathbf{q}}_r) \, \| = \gamma$, $\| \, \delta\mathscr{X} \, \| = \alpha$, $\| \, \dot{\mathscr{X}} \, \| = \beta$, $\lambda_{min}([K_p]_{\mathscr{X}}) = \lambda_p$, at the end of the trajectory following phase.

- Note: Link vibration are not zero at the end of the trajectory following phase $\Rightarrow \beta \neq 0$.

- Time derivative of V, after simplification using equations of motion, the skew-symmetry property and the control law based on rigid Jacobian

$$\dot{V} = -\dot{\mathscr{X}}^T [K_v]_{\mathscr{X}} \dot{\mathscr{X}} + \left(\dot{\mathscr{X}} - [J^r_{\mathbf{q}_r}] \dot{\mathbf{q}}_r \right)^T \left([K_p]_{\mathscr{X}} \delta \mathscr{X} + [K_v]_{\mathscr{X}} \dot{\mathscr{X}} \right)$$

- $\dot{V}$ is *strictly* negative if

$$\left| \left(\dot{\mathscr{X}} - [J^r_{\mathbf{q}_r}] \dot{\mathbf{q}}_r \right)^T \left([K_p]_{\mathscr{X}} \delta \mathscr{X} + [K_v]_{\mathscr{X}} \dot{\mathscr{X}} \right) \right| \quad < \quad \left| \dot{\mathscr{X}}^T [K_v]_{\mathscr{X}} \dot{\mathscr{X}} \right|$$

- $[K_v]_{\mathscr{X}}$ satisfies inequality if *minimum* eigenvalue of $[K_v]_{\mathscr{X}}$, λ_v, satisfy

$$\lambda_v \quad > \quad \frac{\gamma \, \lambda_p \, \alpha}{\beta(\beta - \gamma)}$$

where $\| \, (\dot{\mathscr{X}} - [J^r_{\mathbf{q}_r}] \dot{\mathbf{q}}_r) \, \| = \gamma$, $\| \, \delta \mathscr{X} \, \| = \alpha$, $\| \, \dot{\mathscr{X}} \, \| = \beta$, $\lambda_{min}([K_p]_{\mathscr{X}}) = \lambda_p$, at the end of the trajectory following phase.

- Note: Link vibration are not zero at the end of the trajectory following phase $\Rightarrow \beta \neq 0$.

- Time derivative of V, after simplification using equations of motion, the skew-symmetry property and the control law based on rigid Jacobian

$$\dot{V} = -\dot{\mathscr{X}}^T [K_v]_{\mathscr{X}} \dot{\mathscr{X}} + \left(\dot{\mathscr{X}} - [J^r_{\mathbf{q}_r}]\dot{\mathbf{q}}_r\right)^T \left([K_p]_{\mathscr{X}} \delta \mathscr{X} + [K_v]_{\mathscr{X}} \dot{\mathscr{X}}\right)$$

- $\dot{V}$ is *strictly* negative if

$$\left| \left(\dot{\mathscr{X}} - [J^r_{\mathbf{q}_r}]\dot{\mathbf{q}}_r\right)^T \left([K_p]_{\mathscr{X}} \delta \mathscr{X} + [K_v]_{\mathscr{X}} \dot{\mathscr{X}}\right) \right| \quad < \quad \left| \dot{\mathscr{X}}^T [K_v]_{\mathscr{X}} \dot{\mathscr{X}} \right|$$

- $[K_v]_{\mathscr{X}}$ satisfies inequality if *minimum* eigenvalue of $[K_v]_{\mathscr{X}}$, λ_v, satisfy

$$\lambda_v \quad > \quad \frac{\gamma \, \lambda_p \, \alpha}{\beta(\beta - \gamma)}$$

where $\| \, (\dot{\mathscr{X}} - [J^r_{\mathbf{q}_r}]\dot{\mathbf{q}}_r) \, \| = \gamma$, $\| \, \delta \mathscr{X} \, \| = \alpha$, $\| \, \dot{\mathscr{X}} \, \| = \beta$, $\lambda_{min}([K_p]_{\mathscr{X}}) = \lambda_p$, at the end of the trajectory following phase.

- Note: Link vibration are not zero at the end of the trajectory following phase $\Rightarrow \beta \neq 0$.

Two-stage Control Algorithm

- Model based control law

$$\tau_{\mathbf{q}_r} = [\alpha]\tau'_{\mathbf{q}_r} + \beta$$

with

$$\begin{aligned} [\alpha] &= [\mathbf{M}_{rr}] - [\mathbf{M}_{rf}]^T [\mathbf{M}_{ff}]^{-1} [\mathbf{M}_{rf}] \\ \beta &= \mathbf{C}_r + \mathbf{G}_r - [\mathbf{M}_{rf}]^T \; [\mathbf{M}_{ff}]^{-1} (\mathbf{C}_f + \mathbf{G}_f + [\mathbf{K}]\mathbf{q}_f) \\ \tau'_{\mathbf{q}_r} &= \ddot{\mathbf{q}}_{r_d}(t) + [K_p]_{\mathbf{q}_r}\mathbf{e}(t) + [K_v]_{\mathbf{q}_r}\dot{\mathbf{e}}(t) \end{aligned}$$

provide *asymptotic* trajectory following for $\mathbf{q}_r$.

- End-effector vibrations *induced* can be damped out by

$$\tau_{\mathscr{X}} = [J^r_{\mathbf{q}_r}]^T \left(-[K_p]_{\mathscr{X}} \delta \mathscr{X} - [K_v]_{\mathscr{X}} \dot{\mathscr{X}} \right) + \mathbf{G}_r(\mathbf{q}_{r_d}, \mathbf{q}_{f_d})$$

- Two-stage controller

$$\tau = ([U] - [\mathbf{S}])\tau_{\mathbf{q}_r} + [\mathbf{S}]\tau_{\mathscr{X}}$$

$$[\mathbf{S}] = \begin{cases} [0] & \text{null matrix during joint trajectory tracking stage} \\ [U] & \text{identity matrix during end position vibration control} \end{cases}$$

Two-stage Control Algorithm

- Model based control law

$$\tau_{\mathbf{q}_r} = [\alpha]\tau'_{\mathbf{q}_r} + \beta$$

with

$$\begin{aligned} [\alpha] &= [\mathbf{M}_{rr}] - [\mathbf{M}_{rf}]^T [\mathbf{M}_{ff}]^{-1} [\mathbf{M}_{rf}] \\ \beta &= \mathbf{C}_r + \mathbf{G}_r - [\mathbf{M}_{rf}]^T \ [\mathbf{M}_{ff}]^{-1} (\mathbf{C}_f + \mathbf{G}_f + [\mathbf{K}]\mathbf{q}_f) \\ \tau'_{\mathbf{q}_r} &= \ddot{\mathbf{q}}_{r_d}(t) + [K_p]_{\mathbf{q}_r}\mathbf{e}(t) + [K_v]_{\mathbf{q}_r}\dot{\mathbf{e}}(t) \end{aligned}$$

provide *asymptotic* trajectory following for $\mathbf{q}_r$.

- End-effector vibrations *induced* can be damped out by

$$\tau_{\mathscr{X}} = [J^r_{\mathbf{q}_r}]^T \left(-[K_p]_{\mathscr{X}} \delta \mathscr{X} - [K_v]_{\mathscr{X}} \dot{\mathscr{X}} \right) + \mathbf{G}_r(\mathbf{q}_{r_d}, \mathbf{q}_{f_d})$$

- Two-stage controller

$$\tau = ([U] - [\mathbf{S}])\tau_{\mathbf{q}_r} + [\mathbf{S}]\tau_{\mathscr{X}}$$

$$[\mathbf{S}] = \begin{cases} [0] & \text{null matrix during joint trajectory tracking stage} \\ [U] & \text{identity matrix during end position vibration control} \end{cases}$$

Two-stage Control Algorithm

- Model based control law

$$\tau_{\mathbf{q}_r} = [\alpha]\tau'_{\mathbf{q}_r} + \beta$$

with

$$\begin{aligned}
[\alpha] &= [\mathbf{M}_{rr}] - [\mathbf{M}_{rf}]^T [\mathbf{M}_{ff}]^{-1} [\mathbf{M}_{rf}] \\
\beta &= \mathbf{C}_r + \mathbf{G}_r - [\mathbf{M}_{rf}]^T \ [\mathbf{M}_{ff}]^{-1} (\mathbf{C}_f + \mathbf{G}_f + [\mathbf{K}]\mathbf{q}_f) \\
\tau'_{\mathbf{q}_r} &= \ddot{\mathbf{q}}_{r_d}(t) + [K_p]_{\mathbf{q}_r} \mathbf{e}(t) + [K_v]_{\mathbf{q}_r} \dot{\mathbf{e}}(t)
\end{aligned}$$

provide *asymptotic* trajectory following for $\mathbf{q}_r$.

- End-effector vibrations *induced* can be damped out by

$$\tau_{\mathscr{X}} = [J^r_{\mathbf{q}_r}]^T \left(-[K_p]_{\mathscr{X}} \delta \mathscr{X} - [K_v]_{\mathscr{X}} \dot{\mathscr{X}} \right) + \mathbf{G}_r(\mathbf{q}_{r_d}, \mathbf{q}_{f_d})$$

- Two-stage controller

$$\tau = ([U] - [\mathbf{S}])\tau_{\mathbf{q}_r} + [\mathbf{S}]\tau_{\mathscr{X}}$$

$$[\mathbf{S}] = \begin{cases} [0] & \text{null matrix during joint trajectory tracking stage} \\ [U] & \text{identity matrix during end position vibration control} \end{cases}$$

TWO-STAGE CONTROL ALGORITHM

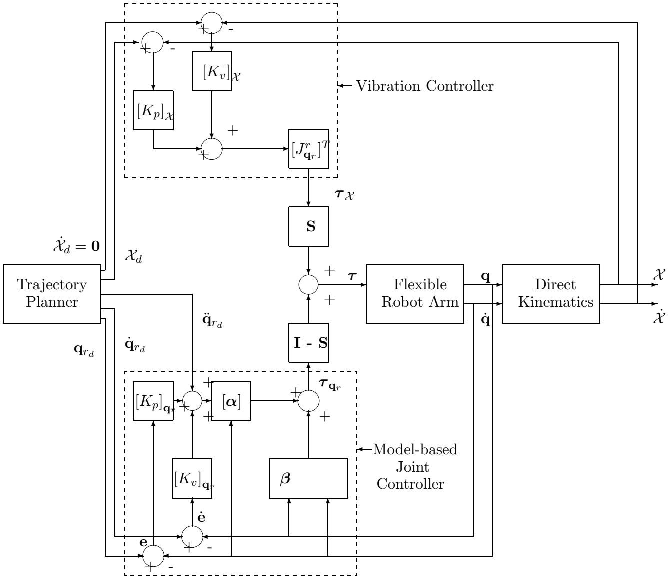

Figure 16: Two-stage controller for flexible link manipulators – $[\alpha]$, β are model-based terms

Robustness of Trajectory Following Controller

- Uncertainty in stiffness matrix [**K**] & in mass matrix [**M**(**q**)].
- Considered together as uncertainty in structural *natural* frequencies

$$\omega_i^2 = \lambda_i([\Omega]) = \lambda_i([\mathbf{M}_{ff}]^{-1}[\mathbf{K}]), \qquad i = 1, 2, \ldots, N$$

  $\lambda_i(\cdot)$ denotes the ith eigenvalue.
- AMM and FEM (or any discretisation method) *always overestimates* stiffness matrix.
- Due to mechanical joints and play, estimated stiffness is *more* than actual stiffness!
- Model (estimated) natural frequencies *larger* than actual natural frequencies.

Robustness of Trajectory Following Controller

- Uncertainty in stiffness matrix $[\mathbf{K}]$ & in mass matrix $[\mathbf{M}(\mathbf{q})]$.
- Considered together as uncertainty in structural *natural* frequencies

$$\omega_i^2 = \lambda_i([\Omega]) = \lambda_i([\mathbf{M}_{ff}]^{-1}[\mathbf{K}]), \qquad i = 1, 2, \ldots, N$$

$\lambda_i(\cdot)$ denotes the ith eigenvalue.

- AMM and FEM (or any discretisation method) *always overestimates* stiffness matrix.
- Due to mechanical joints and play, estimated stiffness is *more* than actual stiffness!
- Model (estimated) natural frequencies *larger* than actual natural frequencies.

Robustness of Trajectory Following Controller

- Uncertainty in stiffness matrix $[\mathbf{K}]$ & in mass matrix $[\mathbf{M}(\mathbf{q})]$.
- Considered together as uncertainty in structural *natural* frequencies

$$\omega_i^2 = \lambda_i([\Omega]) = \lambda_i([\mathbf{M}_{ff}]^{-1}[\mathbf{K}]), \qquad i = 1, 2, \ldots, N$$

  $\lambda_i(\cdot)$ denotes the ith eigenvalue.
- AMM and FEM (or any discretisation method) *always overestimates* stiffness matrix.
- Due to mechanical joints and play, estimated stiffness is *more* than actual stiffness!
- Model (estimated) natural frequencies *larger* than actual natural frequencies.

Robustness of Trajectory Following Controller

- Uncertainty in stiffness matrix $[\mathbf{K}]$ & in mass matrix $[\mathbf{M}(\mathbf{q})]$.
- Considered together as uncertainty in structural *natural* frequencies

$$\omega_i^2 = \lambda_i([\Omega]) = \lambda_i([\mathbf{M}_{ff}]^{-1}[\mathbf{K}]), \qquad i = 1, 2, \ldots, N$$

  $\lambda_i(\cdot)$ denotes the ith eigenvalue.
- AMM and FEM (or any discretisation method) *always overestimates* stiffness matrix.
- Due to mechanical joints and play, estimated stiffness is *more* than actual stiffness!
- Model (estimated) natural frequencies *larger* than actual natural frequencies.

Robustness of Trajectory Following Controller

- Uncertainty in stiffness matrix $[\mathbf{K}]$ & in mass matrix $[\mathbf{M}(\mathbf{q})]$.
- Considered together as uncertainty in structural *natural* frequencies

$$\omega_i^2 = \lambda_i([\Omega]) = \lambda_i([\mathbf{M}_{ff}]^{-1}[\mathbf{K}]), \qquad i = 1, 2, \ldots, N$$

  $\lambda_i(\cdot)$ denotes the ith eigenvalue.
- AMM and FEM (or any discretisation method) *always overestimates* stiffness matrix.
- Due to mechanical joints and play, estimated stiffness is *more* than actual stiffness!
- Model (estimated) natural frequencies *larger* than actual natural frequencies.

Robustness of Trajectory Following Controller

Effect of overestimation of natural frequency

- Rewrite trajectory following control law as

$$
\begin{aligned}
\tau_{\mathbf{q}_r} \;&=\; ([\mathbf{M}_{rr}] - [\mathbf{M}_{rf}]^T[\mathbf{M}_{ff}]^{-1}[\mathbf{M}_{rf}])\tau'_{\mathbf{q}_r} \\
&\quad + (\mathbf{C}_r + \mathbf{G}_r - [\mathbf{M}_{rf}]^T([\mathbf{M}_{ff}]^{-1}(\mathbf{C}_f + \mathbf{G}_f) + [\widehat{\Omega}]\mathbf{q}_f))
\end{aligned}
$$

  Symbol $[\widehat{\Omega}]$ denotes estimated (computed) $[\mathbf{M}_{ff}]^{-1}[\mathbf{K}]$.

- The closed-loop error equation becomes

$$
\ddot{\mathrm{e}}(t) + [K_v]_{\mathbf{q}_r}\dot{\mathrm{e}}(t) + [K_p]_{\mathbf{q}_r}\mathrm{e}(t) = -([\mathbf{M}_{rr}] - [\mathbf{M}_{rf}]^T[\mathbf{M}_{ff}]^{-1}[\mathbf{M}_{rf}])^{-1}[\mathbf{M}_{rf}]^T
$$

  Flexible variables $\mathbf{q}_f$ are governed by

$$
\ddot{\mathbf{q}}_f + [\mathbf{M}_{ff}]^{-1}(\mathbf{C}_f + \mathbf{G}_f) + ([\Omega] - [\mathscr{M}][\Delta\,\Omega])\mathbf{q}_f = -[\mathbf{M}_{ff}]^{-1}[\mathbf{M}_{rf}]\tau'_{\mathbf{q}_r}
$$

  where $[\mathscr{M}] = [\mathbf{M}_{ff}]^{-1}[\mathbf{M}_{rf}](\,[\mathbf{M}_{rr}] - [\mathbf{M}_{rf}]^T[\mathbf{M}_{ff}]^{-1}[\mathbf{M}_{rf}]\,)^{-1}[\mathbf{M}_{rf}]^T$
  and $[\Delta\Omega] = [\widehat{\Omega}] - [\Omega]$.

ROBUSTNESS OF TRAJECTORY FOLLOWING CONTROLLER

EFFECT OF OVERESTIMATION OF NATURAL FREQUENCY

- Rewrite trajectory following control law as

$$\begin{aligned}\tau_{\mathbf{q}_r} &= ([\mathbf{M}_{rr}] - [\mathbf{M}_{rf}]^T [\mathbf{M}_{ff}]^{-1} [\mathbf{M}_{rf}])\tau'_{\mathbf{q}_r} \\ &\quad + (\mathbf{C}_r + \mathbf{G}_r - [\mathbf{M}_{rf}]^T ([\mathbf{M}_{ff}]^{-1} (\mathbf{C}_f + \mathbf{G}_f) + \widehat{[\Omega]}\mathbf{q}_f))\end{aligned}$$

  Symbol $\widehat{[\Omega]}$ denotes estimated (computed) $[\mathbf{M}_{ff}]^{-1}[\mathbf{K}]$.

- The closed-loop error equation becomes

$$\ddot{\mathbf{e}}(t) + [K_v]_{\mathbf{q}_r}\dot{\mathbf{e}}(t) + [K_p]_{\mathbf{q}_r}\mathbf{e}(t) = -([\mathbf{M}_{rr}] - [\mathbf{M}_{rf}]^T [\mathbf{M}_{ff}]^{-1} [\mathbf{M}_{rf}])^{-1} [\mathbf{M}_{rf}]^T$$

  Flexible variables $\mathbf{q}_f$ are governed by

$$\ddot{\mathbf{q}}_f + [\mathbf{M}_{ff}]^{-1}(\mathbf{C}_f + \mathbf{G}_f) + ([\Omega] - [\mathscr{M}][\Delta\ \Omega])\mathbf{q}_f = -[\mathbf{M}_{ff}]^{-1}[\mathbf{M}_{rf}]\tau'_{\mathbf{q}_r}$$

  where $[\mathscr{M}] = [\mathbf{M}_{ff}]^{-1}[\mathbf{M}_{rf}](\ [\mathbf{M}_{rr}] - [\mathbf{M}_{rf}]^T[\mathbf{M}_{ff}]^{-1}[\mathbf{M}_{rf}]\ )^{-1}[\mathbf{M}_{rf}]^T$ and $[\Delta\Omega] = \widehat{[\Omega]} - [\Omega]$.

ROBUSTNESS OF TRAJECTORY FOLLOWING CONTROLLER

EFFECT OF OVERESTIMATION OF NATURAL FREQUENCY

- For $\mathbf{q}_f$ to be stable, the closed-loop *frequency matrix* ($[\Omega] - [\mathscr{M}]\Delta[\Omega]$) must be positive definite (Inman 1989).
- Intuitive justification:
  - Spring-mass-damper system $\ddot{x} + \omega^2 x = u(t)$ – $\omega^2 < 0 \rightarrow x(t) \rightarrow \infty$.
  - ($[\Omega] - [\mathscr{M}][\Delta\ \Omega]$) is like an equivalent closed-loop natural frequency matrix for the multi-link flexible manipulator – positive definite for $\mathbf{q}_f(t)$ to be bounded.
- $[\Delta\ \Omega] < 0 \rightarrow$ Closed-loop frequency matrix is positive definite and $\mathbf{q}_f$ will be stable.
- $[\Delta\ \Omega] > 0 \rightarrow$ Closed-loop frequency matrix may not be positive definite and $\mathbf{q}_f$ may be unstable.
- Bounds on uncertainty in natural frequency for stable $\mathbf{q}_f$ can be derived (see Theodore (1995), Theodore and Ghosal (1995, 2003)).

Robustness of Trajectory Following Controller

Effect of overestimation of natural frequency

- For $\mathbf{q}_f$ to be stable, the closed-loop *frequency matrix* $([\Omega] - [\mathscr{M}]\Delta[\Omega])$ must be positive definite (Inman 1989).
- Intuitive justification:
  - Spring-mass-damper system $\ddot{x} + \omega^2 x = u(t)$ – $\omega^2 < 0 \rightarrow x(t) \rightarrow \infty$.
  - $([\Omega] - [\mathscr{M}][\Delta\ \Omega])$ is like an equivalent closed-loop natural frequency matrix for the multi-link flexible manipulator – positive definite for $\mathbf{q}_f(t)$ to be bounded.
- $[\Delta\ \Omega] < 0 \rightarrow$ Closed-loop frequency matrix is positive definite and $\mathbf{q}_f$ will be stable.
- $[\Delta\ \Omega] > 0 \rightarrow$ Closed-loop frequency matrix may not be positive definite and $\mathbf{q}_f$ may be unstable.
- Bounds on uncertainty in natural frequency for stable $\mathbf{q}_f$ can be derived (see Theodore (1995), Theodore and Ghosal (1995, 2003)).

Robustness of Trajectory Following Controller

Effect of overestimation of natural frequency

- For $\mathbf{q}_f$ to be stable, the closed-loop *frequency matrix* $([\Omega] - [\mathscr{M}]\Delta[\Omega])$ must be positive definite (Inman 1989).
- Intuitive justification:
    - Spring-mass-damper system $\ddot{x} + \omega^2 x = u(t)$ – $\omega^2 < 0 \rightarrow x(t) \rightarrow \infty$.
    - $([\Omega] - [\mathscr{M}][\Delta\ \Omega])$ is like an equivalent closed-loop natural frequency matrix for the multi-link flexible manipulator – positive definite for $\mathbf{q}_f(t)$ to be bounded.
- $[\Delta\ \Omega] < 0 \rightarrow$ Closed-loop frequency matrix is positive definite and $\mathbf{q}_f$ will be stable.
- $[\Delta\ \Omega] > 0 \rightarrow$ Closed-loop frequency matrix may not be positive definite and $\mathbf{q}_f$ may be unstable.
- Bounds on uncertainty in natural frequency for stable $\mathbf{q}_f$ can be derived (see Theodore (1995), Theodore and Ghosal (1995, 2003)).

Robustness of Trajectory Following Controller

Effect of overestimation of natural frequency

- For $\mathbf{q}_f$ to be stable, the closed-loop *frequency matrix* $([\Omega]-[\mathscr{M}]\Delta[\Omega])$ must be positive definite (Inman 1989).
- Intuitive justification:
  - Spring-mass-damper system $\ddot{x}+\omega^2 x = u(t)$ – $\omega^2 < 0 \rightarrow x(t) \rightarrow \infty$.
  - $([\Omega]-[\mathscr{M}][\Delta\ \Omega])$ is like an equivalent closed-loop natural frequency matrix for the multi-link flexible manipulator – positive definite for $\mathbf{q}_f(t)$ to be bounded.
- $[\Delta\ \Omega] < 0 \rightarrow$ Closed-loop frequency matrix is positive definite and $\mathbf{q}_f$ will be stable.
- $[\Delta\ \Omega] > 0 \rightarrow$ Closed-loop frequency matrix may not be positive definite and $\mathbf{q}_f$ may be unstable.
- Bounds on uncertainty in natural frequency for stable $\mathbf{q}_f$ can be derived (see Theodore (1995), Theodore and Ghosal (1995, 2003)).

ROBUSTNESS OF TRAJECTORY FOLLOWING CONTROLLER

EFFECT OF OVERESTIMATION OF NATURAL FREQUENCY

- For $\mathbf{q}_f$ to be stable, the closed-loop *frequency matrix* $([\Omega] - [\mathscr{M}]\Delta[\Omega])$ must be positive definite (Inman 1989).
- Intuitive justification:
  - Spring-mass-damper system $\ddot{x} + \omega^2 x = u(t)$ – $\omega^2 < 0 \rightarrow x(t) \rightarrow \infty$.
  - $([\Omega] - [\mathscr{M}][\Delta\ \Omega])$ is like an equivalent closed-loop natural frequency matrix for the multi-link flexible manipulator – positive definite for $\mathbf{q}_f(t)$ to be bounded.
- $[\Delta\ \Omega] < 0 \rightarrow$ Closed-loop frequency matrix is positive definite and $\mathbf{q}_f$ will be stable.
- $[\Delta\ \Omega] > 0 \rightarrow$ Closed-loop frequency matrix may not be positive definite and $\mathbf{q}_f$ may be unstable.
- Bounds on uncertainty in natural frequency for stable $\mathbf{q}_f$ can be derived (see Theodore (1995), Theodore and Ghosal (1995, 2003)).

Numerical Simulation of a Flexible Link Manipulator

- Three DOF manipulator with two flexible links – Parameters.

Physical system parameters	Value
mass of link 1 (m_1)	3.66 kg
linear mass density of link 2 ($\rho_2 A_2$)	0.331 $kg\,m^{-1}$
linear mass density of link 3 ($\rho_3 A_3$)	0.331 $kg\,m^{-1}$
mass of payload (m_p)	0.1 kg
length of link 1	0.12 m
length of link 2	1.0 m
length of link 3	1.0 m
rotary inertia of joint 1 (I_{joint_1})	0.4 $kg\,m^2$
rotary inertia of joint 2 (I_{joint_2})	3.275 $kg\,m^2$
rotary inertia of joint 3 (I_{joint_3})	3.275 $kg\,m^2$
flexural rigidity of link 2 ($(EI)_2$)	1165.4916 $N m^2$
flexural rigidity of link 3 ($(EI)_3$)	1165.4916 $N m^2$

NUMERICAL SIMULATION OF A FLEXIBLE LINK MANIPULATOR

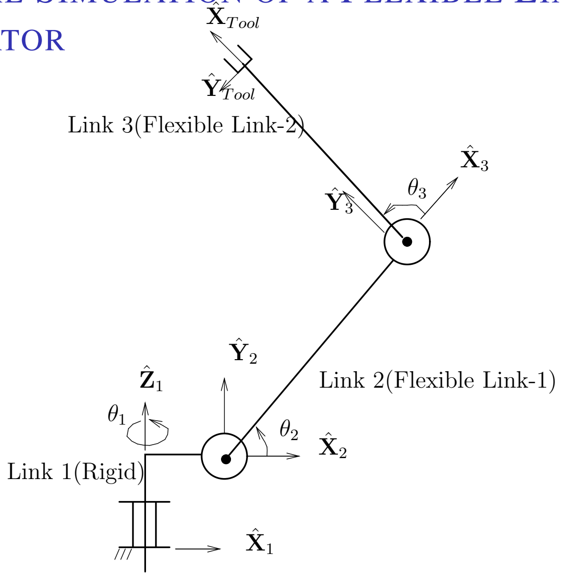

Figure 17: Schematic of a 3R flexible manipulator

Numerical Simulation of a Flexible Link Manipulator

- Desired trajectory is smooth sine profile with zero velocity and acceleration at the start and end – represents a right-circular helix of radius 25 cm, pitch 2.5 cm, and 3π rotations about the helix axis.
- Total time is 1.0 seconds – chosen 'fast' to excite vibrations!
- After 1.0 seconds, $\dot{\mathscr{X}}_d = 0$ is chosen to be zero & 1.0 seconds to damp vibrations.
- Controller gains:
  - I-stage – $[K_p]_{\mathbf{q}_r}$ and $[K_v]_{\mathbf{q}_r}$ are diagonal matrices with equal diagonal elements of 64.0 and 32.0.
  - II-stage – $[K_p]_{\mathscr{X}}$ and $[K_v]_{\mathscr{X}}$ are chosen as diagonal matrices with elements $\{100.0, 100.0, 400.0\}$ and $\{40.0, 40.0, 80.0\}$, respectively.
- Mass parameters underestimated by 25% and stiffness parameters overestimated by 25%.

Numerical Simulation of a Flexible Link Manipulator

- Desired trajectory is smooth sine profile with zero velocity and acceleration at the start and end – represents a right-circular helix of radius 25 cm, pitch 2.5 cm, and 3π rotations about the helix axis.
- Total time is 1.0 seconds – chosen 'fast' to excite vibrations!
- After 1.0 seconds, $\dot{\mathscr{X}}_d = 0$ is chosen to be zero & 1.0 seconds to damp vibrations.
- Controller gains:
  - I-stage – $[K_p]_{\mathbf{q}_r}$ and $[K_v]_{\mathbf{q}_r}$ are diagonal matrices with equal diagonal elements of 64.0 and 32.0.
  - II-stage – $[K_p]_{\mathscr{X}}$ and $[K_v]_{\mathscr{X}}$ are chosen as diagonal matrices with elements $\{100.0, 100.0, 400.0\}$ and $\{40.0, 40.0, 80.0\}$, respectively.
- Mass parameters underestimated by 25% and stiffness parameters overestimated by 25%.

Numerical Simulation of a Flexible Link Manipulator

- Desired trajectory is smooth sine profile with zero velocity and acceleration at the start and end – represents a right-circular helix of radius 25 cm, pitch 2.5 cm, and 3π rotations about the helix axis.
- Total time is 1.0 seconds – chosen 'fast' to excite vibrations!
- After 1.0 seconds, $\dot{\mathscr{X}}_d = 0$ is chosen to be zero & 1.0 seconds to damp vibrations.
- Controller gains:
  - I-stage – $[K_p]_{\mathbf{q}_r}$ and $[K_v]_{\mathbf{q}_r}$ are diagonal matrices with equal diagonal elements of 64.0 and 32.0.
  - II-stage – $[K_p]_{\mathscr{X}}$ and $[K_v]_{\mathscr{X}}$ are chosen as diagonal matrices with elements $\{100.0, 100.0, 400.0\}$ and $\{40.0, 40.0, 80.0\}$, respectively.
- Mass parameters underestimated by 25% and stiffness parameters overestimated by 25%.

Numerical Simulation of a Flexible Link Manipulator

- Desired trajectory is smooth sine profile with zero velocity and acceleration at the start and end – represents a right-circular helix of radius 25 cm, pitch 2.5 cm, and 3π rotations about the helix axis.
- Total time is 1.0 seconds – chosen 'fast' to excite vibrations!
- After 1.0 seconds, $\dot{\mathscr{X}}_d = 0$ is chosen to be zero & 1.0 seconds to damp vibrations.
- Controller gains:
  - I-stage – $[K_p]_{\mathbf{q}_r}$ and $[K_v]_{\mathbf{q}_r}$ are diagonal matrices with equal diagonal elements of 64.0 and 32.0.
  - II-stage – $[K_p]_{\mathscr{X}}$ and $[K_v]_{\mathscr{X}}$ are chosen as diagonal matrices with elements $\{100.0, 100.0, 400.0\}$ and $\{40.0, 40.0, 80.0\}$, respectively.
- Mass parameters underestimated by 25% and stiffness parameters overestimated by 25%.

Numerical Simulation of a Flexible Link Manipulator

- Desired trajectory is smooth sine profile with zero velocity and acceleration at the start and end – represents a right-circular helix of radius 25 cm, pitch 2.5 cm, and 3π rotations about the helix axis.
- Total time is 1.0 seconds – chosen 'fast' to excite vibrations!
- After 1.0 seconds, $\dot{\mathscr{X}}_d = 0$ is chosen to be zero & 1.0 seconds to damp vibrations.
- Controller gains:
    - I-stage – $[K_p]_{\mathbf{q}_r}$ and $[K_v]_{\mathbf{q}_r}$ are diagonal matrices with equal diagonal elements of 64.0 and 32.0.
    - II-stage – $[K_p]_{\mathscr{X}}$ and $[K_v]_{\mathscr{X}}$ are chosen as diagonal matrices with elements $\{100.0, 100.0, 400.0\}$ and $\{40.0, 40.0, 80.0\}$, respectively.
- Mass parameters underestimated by 25% and stiffness parameters overestimated by 25%.

Numerical Simulation of a Flexible Link Manipulator

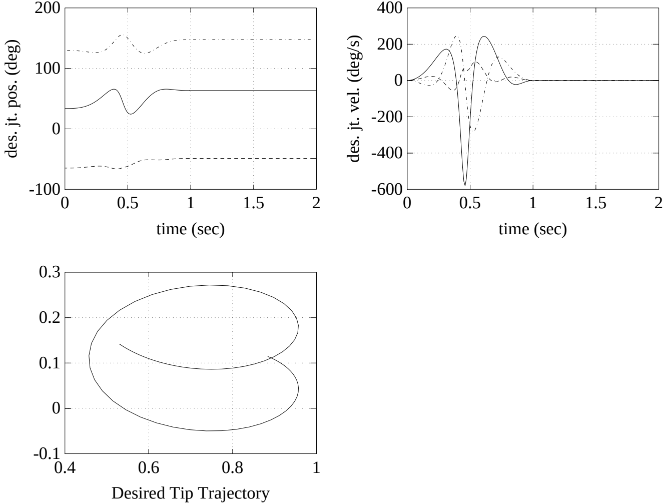

Figure 18: Desired trajectories (— : $q^d_{r_1}(\dot{q}^d_{r_1})$, - - - : $q^d_{r_2}(\dot{q}^d_{r_2})$, -·-·- : $q^d_{r_3}(\dot{q}^d_{r_3})$)

NUMERICAL SIMULATION OF A FLEXIBLE LINK MANIPULATOR

- Two simulation result cases:

  CASE 1: Two-stage control algorithm with no uncertainties in model parameters – $\tau_{\mathbf{q}_r} = [\alpha]\tau'_{\mathbf{q}_r} + \beta$ and

$$
\begin{aligned}
[\alpha] &= [\mathbf{M}_{rr}] - [\mathbf{M}_{rf}]^T[\mathbf{M}_{ff}]^{-1}[\mathbf{M}_{rf}] \\
\beta &= \mathbf{C}_r + \mathbf{G}_r - [\mathbf{M}_{rf}]^T\ [\mathbf{M}_{ff}]^{-1}(\mathbf{C}_f + \mathbf{G}_f + [\mathbf{K}]\mathbf{q}_f) \\
\tau'_{\mathbf{q}_r} &= \ddot{\mathbf{q}}_{r_d}(t) + [K_p]_{\mathbf{q}_r}\mathbf{e}(t) + [K_v]_{\mathbf{q}_r}\dot{\mathbf{e}}(t)
\end{aligned}
$$

  CASE 2: Two-stage control algorithm with uncertainty in model parameters

$$
\begin{aligned}
\tau_{\mathbf{q}_r} &= ([\mathbf{M}_{rr}] - [\mathbf{M}_{rf}]^T[\mathbf{M}_{ff}]^{-1}[\mathbf{M}_{rf}])\tau'_{\mathbf{q}_r} \\
&\quad +(\mathbf{C}_r + \mathbf{G}_r - [\mathbf{M}_{rf}]^T([\mathbf{M}_{ff}]^{-1}(\mathbf{C}_f + \mathbf{G}_f) + [\widehat{\Omega}]\mathbf{q}_f)) \\
\tau'_{\mathbf{q}_r} &= \ddot{\mathbf{q}}_{r_d}(t) + [K_p]_{\mathbf{q}_r}\mathbf{e}(t) + [K_v]_{\mathbf{q}_r}\dot{\mathbf{e}}(t)
\end{aligned}
$$

Numerical Simulation of a Flexible Link Manipulator

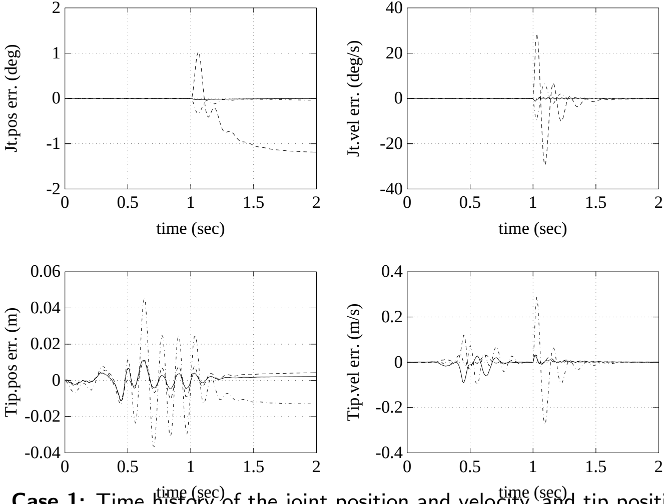

Figure 19: Case 1: Time history of the joint position and velocity, and tip position and velocity errors for two-stage controller (joint error: — : $e_1(\dot{e}_1)$, - - - : $e_2(\dot{e}_2)$, -·-·- : $e_3(\dot{e}_3)$; tip error: — : $e_x(\dot{e}_x)$, - - - : $e_y(\dot{e}_y)$, -·-·- : $e_z(\dot{e}_z)$)

Numerical Simulation of a Flexible Link Manipulator

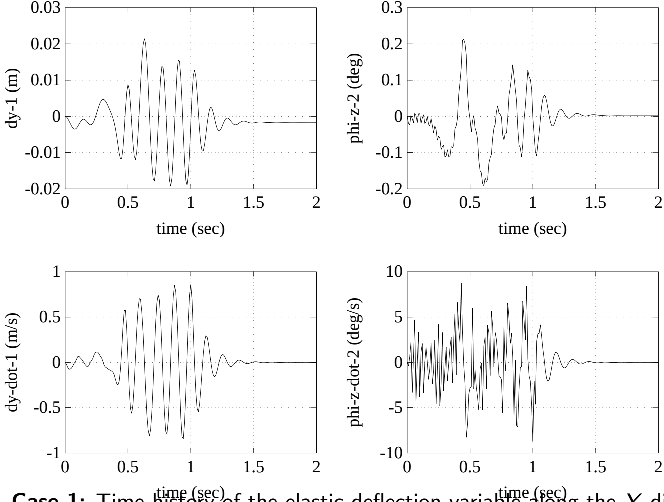

Figure 20: Case 1: Time history of the elastic deflection variable along the Y direction, at the tip of flexible link 1, and its rate; time history of the elastic rotation variable about the Z direction, at the tip of flexible link 2, and its rate

Numerical Simulation of a Flexible Link Manipulator

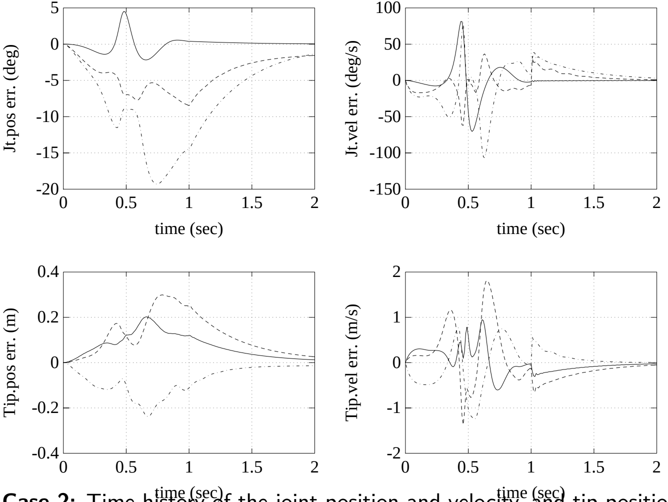

Figure 21: Case 2: Time history of the joint position and velocity, and tip position and velocity errors for two-stage controller (joint error: — : $e_1(\dot{e}_1)$, - - - : $e_2(\dot{e}_2)$, -·-·- : $e_3(\dot{e}_3)$; tip error: — : $e_x(\dot{e}_x)$, - - - : $e_y(\dot{e}_y)$, -·-·- : $e_z(\dot{e}_z)$)

Numerical Simulation of a Flexible Link Manipulator

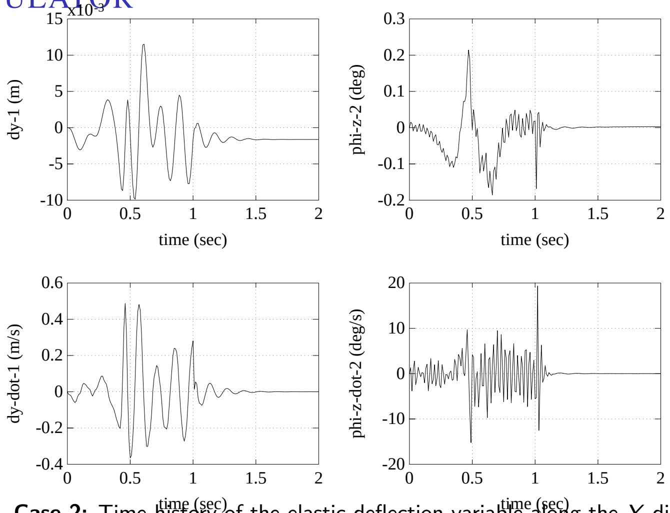

Figure 22: Case 2: Time history of the elastic deflection variable along the Y direction, at the tip of flexible link 1, and its rate; time history of the elastic rotation variable about the Z direction, at the tip of flexible link 2, and its rate

Numerical Simulation of a Flexible Link Manipulator

Summary of simulation results

- Without any uncertainty (Case 1), joint trajectory errors (between 0 and 1 sec) are quite small.
- Even in Case 1, the tip errors at the the end of trajectory following ($t = 1$ sec) are ≈ 5 cm – quite large!
- With the end-position controller (between 1 and 2 sec), the tip vibration errors are reduced to ≈ 1 cm.
- In presence of uncertainties in model parameters (Case 2), joint and tip errors are much larger – $\approx 20^\circ$ & ≈ 30 cm.
- Due to end position vibration controller (between 1 and 2 sec), the joint and tip position errors are again driven to lower levels of about 2° and 3 cm.
- To reduce errors further, robust compensator is required (See Theodore and Ghosal (2003)).

Numerical Simulation of a Flexible Link Manipulator

Summary of simulation results

- Without any uncertainty (Case 1), joint trajectory errors (between 0 and 1 sec) are quite small.
- Even in Case 1, the tip errors at the the end of trajectory following ($t = 1$ sec) are ≈ 5 cm – quite large!
- With the end-position controller (between 1 and 2 sec), the tip vibration errors are reduced to ≈ 1 cm.
- In presence of uncertainties in model parameters (Case 2), joint and tip errors are much larger – $\approx 20^\circ$ & ≈ 30 cm.
- Due to end position vibration controller (between 1 and 2 sec), the joint and tip position errors are again driven to lower levels of about 2° and 3 cm.
- To reduce errors further, robust compensator is required (See Theodore and Ghosal (2003)).

Summary of simulation results

- Without any uncertainty (Case 1), joint trajectory errors (between 0 and 1 sec) are quite small.
- Even in Case 1, the tip errors at the the end of trajectory following ($t = 1$ sec) are ≈ 5 cm – quite large!
- With the end-position controller (between 1 and 2 sec), the tip vibration errors are reduced to ≈ 1 cm.
- In presence of uncertainties in model parameters (Case 2), joint and tip errors are much larger – $\approx 20°$ & ≈ 30 cm.
- Due to end position vibration controller (between 1 and 2 sec), the joint and tip position errors are again driven to lower levels of about 2° and 3 cm.
- To reduce errors further, robust compensator is required (See Theodore and Ghosal (2003)).

Numerical Simulation of a Flexible Link Manipulator

Summary of simulation results

- Without any uncertainty (Case 1), joint trajectory errors (between 0 and 1 sec) are quite small.
- Even in Case 1, the tip errors at the the end of trajectory following ($t = 1$ sec) are ≈ 5 cm – quite large!
- With the end-position controller (between 1 and 2 sec), the tip vibration errors are reduced to ≈ 1 cm.
- In presence of uncertainties in model parameters (Case 2), joint and tip errors are much larger – $\approx 20^\circ$ & ≈ 30 cm.
- Due to end position vibration controller (between 1 and 2 sec), the joint and tip position errors are again driven to lower levels of about 2° and 3 cm.
- To reduce errors further, robust compensator is required (See Theodore and Ghosal (2003)).

Numerical Simulation of a Flexible Link Manipulator

Summary of simulation results

- Without any uncertainty (Case 1), joint trajectory errors (between 0 and 1 sec) are quite small.
- Even in Case 1, the tip errors at the the end of trajectory following ($t = 1$ sec) are ≈ 5 cm – quite large!
- With the end-position controller (between 1 and 2 sec), the tip vibration errors are reduced to ≈ 1 cm.
- In presence of uncertainties in model parameters (Case 2), joint and tip errors are much larger – $\approx 20^\circ$ & ≈ 30 cm.
- Due to end position vibration controller (between 1 and 2 sec), the joint and tip position errors are again driven to lower levels of about 2° and 3 cm.
- To reduce errors further, robust compensator is required (See Theodore and Ghosal (2003)).

Numerical Simulation of a Flexible Link Manipulator

Summary of simulation results

- Without any uncertainty (Case 1), joint trajectory errors (between 0 and 1 sec) are quite small.
- Even in Case 1, the tip errors at the the end of trajectory following ($t = 1$ sec) are ≈ 5 cm – quite large!
- With the end-position controller (between 1 and 2 sec), the tip vibration errors are reduced to ≈ 1 cm.
- In presence of uncertainties in model parameters (Case 2), joint and tip errors are much larger – $\approx 20^\circ$ & ≈ 30 cm.
- Due to end position vibration controller (between 1 and 2 sec), the joint and tip position errors are again driven to lower levels of about 2° and 3 cm.
- To reduce errors further, robust compensator is required (See Theodore and Ghosal (2003)).

SUMMARY

- Kinematic modeling → Dynamic equations of motion using Lagrangian formulation.
- Equations of motion can be done using computer algebra software such as Maple® or Mathematica®.
- Two-way coupling between rigid joint variables and flexible vibration variables!
- Number of ODE's in 3D with n_f flexible links and N_j modes or elements for each flexible link – $2\sum_{j=1}^{n_f} N_j$ in AMM and $4\sum_{j=1}^{n_f} N_j$ in FEM.
- Trajectory and end-position vibration control using *only* rigid joint variable.
- Overestimation of natural frequency → unstable behaviour!
- Numerical simulation results for 2-stage controller.

SUMMARY

- Kinematic modeling $\rightarrow$ Dynamic equations of motion using Lagrangian formulation.
- Equations of motion can be done using computer algebra software such as Maple® or Mathematica®.
- Two-way coupling between rigid joint variables and flexible vibration variables!
- Number of ODE's in 3D with n_f flexible links and N_j modes or elements for each flexible link – $2\sum_{j=1}^{n_f} N_j$ in AMM and $4\sum_{j=1}^{n_f} N_j$ in FEM.
- Trajectory and end-position vibration control using *only* rigid joint variable.
- Overestimation of natural frequency $\rightarrow$ unstable behaviour!
- Numerical simulation results for 2-stage controller.

SUMMARY

- Kinematic modeling $\rightarrow$ Dynamic equations of motion using Lagrangian formulation.
- Equations of motion can be done using computer algebra software such as Maple® or Mathematica®.
- Two-way coupling between rigid joint variables and flexible vibration variables!
- Number of ODE's in 3D with n_f flexible links and N_j modes or elements for each flexible link – $2\sum_{j=1}^{n_f} N_j$ in AMM and $4\sum_{j=1}^{n_f} N_j$ in FEM.
- Trajectory and end-position vibration control using *only* rigid joint variable.
- Overestimation of natural frequency $\rightarrow$ unstable behaviour!
- Numerical simulation results for 2-stage controller.

SUMMARY

- Kinematic modeling $\rightarrow$ Dynamic equations of motion using Lagrangian formulation.
- Equations of motion can be done using computer algebra software such as Maple® or Mathematica®.
- Two-way coupling between rigid joint variables and flexible vibration variables!
- Number of ODE's in 3D with n_f flexible links and N_j modes or elements for each flexible link – $2\sum_{j=1}^{n_f} N_j$ in AMM and $4\sum_{j=1}^{n_f} N_j$ in FEM.
- Trajectory and end-position vibration control using *only* rigid joint variable.
- Overestimation of natural frequency $\rightarrow$ unstable behaviour!
- Numerical simulation results for 2-stage controller.

Summary

- Kinematic modeling $\rightarrow$ Dynamic equations of motion using Lagrangian formulation.
- Equations of motion can be done using computer algebra software such as Maple® or Mathematica®.
- Two-way coupling between rigid joint variables and flexible vibration variables!
- Number of ODE's in 3D with n_f flexible links and N_j modes or elements for each flexible link – $2\sum_{j=1}^{n_f} N_j$ in AMM and $4\sum_{j=1}^{n_f} N_j$ in FEM.
- Trajectory and end-position vibration control using *only* rigid joint variable.
- Overestimation of natural frequency $\rightarrow$ unstable behaviour!
- Numerical simulation results for 2-stage controller.

SUMMARY

- Kinematic modeling $\rightarrow$ Dynamic equations of motion using Lagrangian formulation.
- Equations of motion can be done using computer algebra software such as Maple® or Mathematica®.
- Two-way coupling between rigid joint variables and flexible vibration variables!
- Number of ODE's in 3D with n_f flexible links and N_j modes or elements for each flexible link – $2\sum_{j=1}^{n_f} N_j$ in AMM and $4\sum_{j=1}^{n_f} N_j$ in FEM.
- Trajectory and end-position vibration control using *only* rigid joint variable.
- Overestimation of natural frequency $\rightarrow$ unstable behaviour!
- Numerical simulation results for 2-stage controller.

Summary

- Kinematic modeling $\rightarrow$ Dynamic equations of motion using Lagrangian formulation.
- Equations of motion can be done using computer algebra software such as Maple® or Mathematica®.
- Two-way coupling between rigid joint variables and flexible vibration variables!
- Number of ODE's in 3D with n_f flexible links and N_j modes or elements for each flexible link – $2\sum_{j=1}^{n_f} N_j$ in AMM and $4\sum_{j=1}^{n_f} N_j$ in FEM.
- Trajectory and end-position vibration control using *only* rigid joint variable.
- Overestimation of natural frequency $\rightarrow$ unstable behaviour!
- Numerical simulation results for 2-stage controller.

Outline

INTRODUCTION

- A planar 2R flexible link system moving on a horizontal table on air bearings.
- Simulate deployment of a two element solar panel in zero gravity environment.
- Added complication: Locking at the end of motion induces flexible vibration.
- Modeled as flexible beams (made of Aluminum), actuated by two springs and locking mechanism.
- Instrumented with potentiometer (to measure joint rotation) and strain gages (to estimate vibration).
- Goal is to do modeling and numerical simulation & compare with experimental data.
- See details in Nagaraj et al.(1997) & Nagaraj et al. (2003).

INTRODUCTION

- A planar 2R flexible link system moving on a horizontal table on air bearings.
- Simulate deployment of a two element solar panel in zero gravity environment.
- Added complication: Locking at the end of motion induces flexible vibration.
- Modeled as flexible beams (made of Aluminum), actuated by two springs and locking mechanism.
- Instrumented with potentiometer (to measure joint rotation) and strain gages (to estimate vibration).
- Goal is to do modeling and numerical simulation & compare with experimental data.
- See details in Nagaraj et al.(1997) & Nagaraj et al. (2003).

INTRODUCTION

- A planar 2R flexible link system moving on a horizontal table on air bearings.
- Simulate deployment of a two element solar panel in zero gravity environment.
- Added complication: Locking at the end of motion induces flexible vibration.
- Modeled as flexible beams (made of Aluminum), actuated by two springs and locking mechanism.
- Instrumented with potentiometer (to measure joint rotation) and strain gages (to estimate vibration).
- Goal is to do modeling and numerical simulation & compare with experimental data.
- See details in Nagaraj et al.(1997) & Nagaraj et al. (2003).

INTRODUCTION

- A planar 2R flexible link system moving on a horizontal table on air bearings.
- Simulate deployment of a two element solar panel in zero gravity environment.
- Added complication: Locking at the end of motion induces flexible vibration.
- Modeled as flexible beams (made of Aluminum), actuated by two springs and locking mechanism.
- Instrumented with potentiometer (to measure joint rotation) and strain gages (to estimate vibration).
- Goal is to do modeling and numerical simulation & compare with experimental data.
- See details in Nagaraj et al.(1997) & Nagaraj et al. (2003).

INTRODUCTION

- A planar 2R flexible link system moving on a horizontal table on air bearings.
- Simulate deployment of a two element solar panel in zero gravity environment.
- Added complication: Locking at the end of motion induces flexible vibration.
- Modeled as flexible beams (made of Aluminum), actuated by two springs and locking mechanism.
- Instrumented with potentiometer (to measure joint rotation) and strain gages (to estimate vibration).
- Goal is to do modeling and numerical simulation & compare with experimental data.
- See details in Nagaraj et al.(1997) & Nagaraj et al. (2003).

INTRODUCTION

- A planar 2R flexible link system moving on a horizontal table on air bearings.
- Simulate deployment of a two element solar panel in zero gravity environment.
- Added complication: Locking at the end of motion induces flexible vibration.
- Modeled as flexible beams (made of Aluminum), actuated by two springs and locking mechanism.
- Instrumented with potentiometer (to measure joint rotation) and strain gages (to estimate vibration).
- Goal is to do modeling and numerical simulation & compare with experimental data.
- See details in Nagaraj et al.(1997) & Nagaraj et al. (2003).

INTRODUCTION

- A planar 2R flexible link system moving on a horizontal table on air bearings.
- Simulate deployment of a two element solar panel in zero gravity environment.
- Added complication: Locking at the end of motion induces flexible vibration.
- Modeled as flexible beams (made of Aluminum), actuated by two springs and locking mechanism.
- Instrumented with potentiometer (to measure joint rotation) and strain gages (to estimate vibration).
- Goal is to do modeling and numerical simulation & compare with experimental data.
- See details in Nagaraj et al.(1997) & Nagaraj et al. (2003).

Motion Stages of a Planar 2R System

- Initially both links are folded – shown in (a).
- Both joints are actuated by torsional springs with link 1 rotating counter-clockwise (CCW) and link 2 rotating clock-wise (CW) – Stage 1 motion shown in (b).
- The second joint locks first when $\theta_2 = 0$ – shown as (c).
- Both links rotate as one in a CCW manner – Stage 2 motion shown as (d).
- At $\theta_1 = 90^\circ$, the first joint locks – shown as (e).
- Both links together vibrate as a cantilever – Stage 3.

Motion Stages of a Planar 2R System

- Initially both links are folded – shown in (a).
- Both joints are actuated by torsional springs with link 1 rotating counter-clockwise (CCW) and link 2 rotating clock-wise (CW) – Stage 1 motion shown in (b).
- The second joint locks first when $\theta_2 = 0$ – shown as (c).
- Both links rotate as one in a CCW manner – Stage 2 motion shown as (d).
- At $\theta_1 = 90^\circ$, the first joint locks – shown as (e).
- Both links together vibrate as a cantilever – Stage 3.

Motion Stages of a Planar 2R System

- Initially both links are folded – shown in (a).
- Both joints are actuated by torsional springs with link 1 rotating counter-clockwise (CCW) and link 2 rotating clock-wise (CW) – Stage 1 motion shown in (b).
- The second joint locks first when $\theta_2 = 0$ – shown as (c).
- Both links rotate as one in a CCW manner – Stage 2 motion shown as (d).
- At $\theta_1 = 90^\circ$, the first joint locks – shown as (e).
- Both links together vibrate as a cantilever – Stage 3.

Motion Stages of a Planar 2R System

- Initially both links are folded – shown in (a).
- Both joints are actuated by torsional springs with link 1 rotating counter-clockwise (CCW) and link 2 rotating clock-wise (CW) – Stage 1 motion shown in (b).
- The second joint locks first when $\theta_2 = 0$ – shown as (c).
- Both links rotate as one in a CCW manner – Stage 2 motion shown as (d).
- At $\theta_1 = 90^\circ$, the first joint locks – shown as (e).
- Both links together vibrate as a cantilever – Stage 3.

Motion Stages of a Planar 2R System

- Initially both links are folded – shown in (a).
- Both joints are actuated by torsional springs with link 1 rotating counter-clockwise (CCW) and link 2 rotating clock-wise (CW) – Stage 1 motion shown in (b).
- The second joint locks first when $\theta_2 = 0$ – shown as (c).
- Both links rotate as one in a CCW manner – Stage 2 motion shown as (d).
- At $\theta_1 = 90^\circ$, the first joint locks – shown as (e).
- Both links together vibrate as a cantilever – Stage 3.

Motion Stages of a Planar 2R System

- Initially both links are folded – shown in (a).
- Both joints are actuated by torsional springs with link 1 rotating counter-clockwise (CCW) and link 2 rotating clock-wise (CW) – Stage 1 motion shown in (b).
- The second joint locks first when $\theta_2 = 0$ – shown as (c).
- Both links rotate as one in a CCW manner – Stage 2 motion shown as (d).
- At $\theta_1 = 90^\circ$, the first joint locks – shown as (e).
- Both links together vibrate as a cantilever – Stage 3.

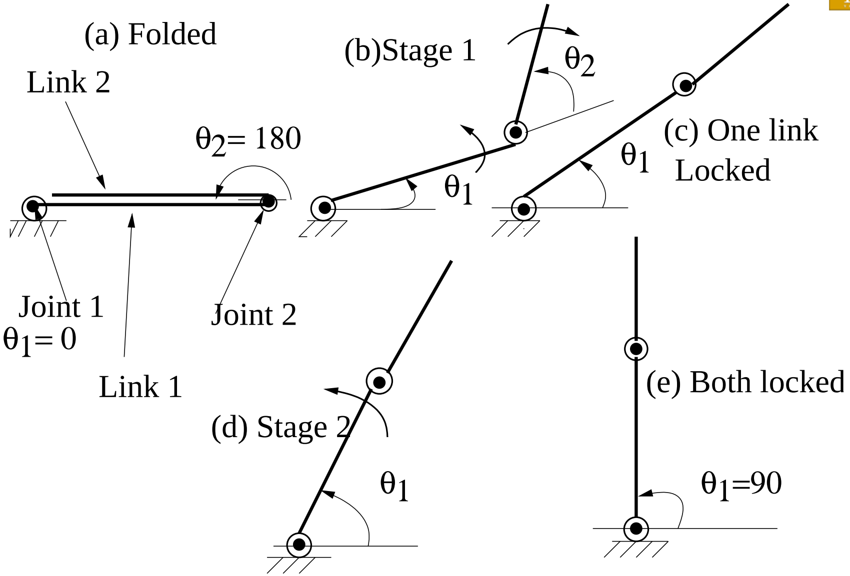

Figure 23: Planar 2R system in different stages of motion

Modeling of Stage 1

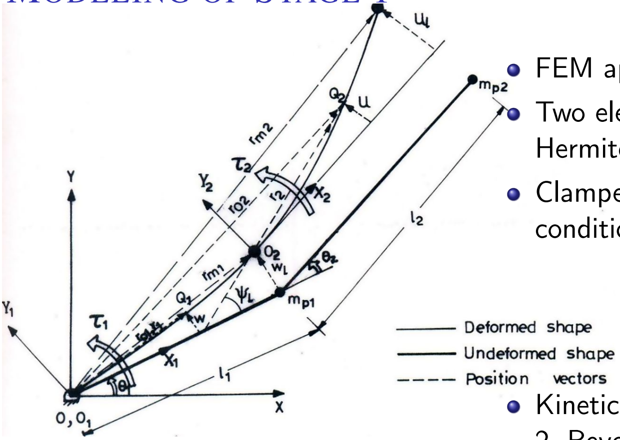

Figure 24: Flexible 2R system in Stage 1 – τ_2 is *actually* CW

- FEM approach for modeling.
- Two elements in each link and Hermite cubic shape functions.
- Clamped-mass boundary conditions for both links.
- Kinetic energy from Links 1 and 2, Revolute joints 1 and 2m and tip mass at end of both links.
- Potential energy from strain energy of both links and torsion springs.
- Torque due to rocker arm in the locking mechanism.
- Dynamic equations of motion obtained using Lagrangian formulation.

- Equations of motion for Stage 1 motion (see Lecture 3)

$$\begin{pmatrix} [\mathbf{M}_{rr}] & [\mathbf{M}_{rf}]^T \\ [\mathbf{M}_{rf}] & [\mathbf{M}_{ff}] \end{pmatrix} \begin{pmatrix} \ddot{\mathbf{q}}_r \\ \ddot{\mathbf{q}}_f \end{pmatrix} + \begin{pmatrix} \mathbf{C}_r(\mathbf{q}, \dot{\mathbf{q}}) \\ \mathbf{C}_f(\mathbf{q}, \dot{\mathbf{q}}) \end{pmatrix} + \begin{pmatrix} [\mathbf{K}_j] & \mathbf{0} \\ \mathbf{0} & [\mathbf{K}_f] \end{pmatrix} \begin{pmatrix} \mathbf{q}_r \\ \mathbf{q}_f \end{pmatrix} = \begin{pmatrix} \tau \\ \mathbf{0} \end{pmatrix}$$

  Note: the gravity term is not present, the stiffness due to torsional springs is $[\mathbf{K}_j]$ and τ is due to the rocker-arm force.

- After θ_2 rotates by π (CW direction), the joint locks $\rightarrow$ 2R system changes to 1R system.
- Initial conditions for motion just after locking (Stage 2 motion) obtained using *momentum balance*.
- Assumptions:
  - Time duration of impact during locking is neglected.
  - Generalised coordinates before and after locking is same $\rightarrow \mathbf{q}_+ = \mathbf{q}_-$
  - Velocities are bounded during impact.

- Equations of motion for Stage 1 motion (see Lecture 3)

$$\begin{pmatrix} [\mathbf{M}_{rr}] & [\mathbf{M}_{rf}]^T \\ [\mathbf{M}_{rf}] & [\mathbf{M}_{ff}] \end{pmatrix} \begin{pmatrix} \ddot{\mathbf{q}}_r \\ \ddot{\mathbf{q}}_f \end{pmatrix} + \begin{pmatrix} \mathbf{C}_r(\mathbf{q}, \dot{\mathbf{q}}) \\ \mathbf{C}_f(\mathbf{q}, \dot{\mathbf{q}}) \end{pmatrix} + \begin{pmatrix} [\mathbf{K}_j] & \mathbf{0} \\ \mathbf{0} & [\mathbf{K}_f] \end{pmatrix} \begin{pmatrix} \mathbf{q}_r \\ \mathbf{q}_f \end{pmatrix} = \begin{pmatrix} \tau \\ \mathbf{0} \end{pmatrix}$$

  Note: the gravity term is not present, the stiffness due to torsional springs is $[\mathbf{K}_j]$ and τ is due to the rocker-arm force.
- After θ_2 rotates by π (CW direction), the joint locks $\rightarrow$ 2R system changes to 1R system.
- Initial conditions for motion just after locking (Stage 2 motion) obtained using *momentum balance*.
- Assumptions:
  - Time duration of impact during locking is neglected.
  - Generalised coordinates before and after locking is same $\rightarrow$ $\mathbf{q}_+ = \mathbf{q}_-$
  - Velocities are bounded during impact.

- Equations of motion for Stage 1 motion (see Lecture 3)

$$\begin{pmatrix} [\mathbf{M}_{rr}] & [\mathbf{M}_{rf}]^T \\ [\mathbf{M}_{rf}] & [\mathbf{M}_{ff}] \end{pmatrix} \begin{pmatrix} \ddot{\mathbf{q}}_r \\ \ddot{\mathbf{q}}_f \end{pmatrix} + \begin{pmatrix} \mathbf{C}_r(\mathbf{q}, \dot{\mathbf{q}}) \\ \mathbf{C}_f(\mathbf{q}, \dot{\mathbf{q}}) \end{pmatrix} + \begin{pmatrix} [\mathbf{K}_j] & \mathbf{0} \\ \mathbf{0} & [\mathbf{K}_f] \end{pmatrix} \begin{pmatrix} \mathbf{q}_r \\ \mathbf{q}_f \end{pmatrix} = \begin{pmatrix} \tau \\ \mathbf{0} \end{pmatrix}$$

Note: the gravity term is not present, the stiffness due to torsional springs is $[\mathbf{K}_j]$ and τ is due to the rocker-arm force.

- After θ_2 rotates by π (CW direction), the joint locks $\rightarrow$ 2R system changes to 1R system.
- Initial conditions for motion just after locking (Stage 2 motion) obtained using *momentum balance*.
- Assumptions:
  - Time duration of impact during locking is neglected.
  - Generalised coordinates before and after locking is same $\rightarrow \mathbf{q}_+ = \mathbf{q}_-$
  - Velocities are bounded during impact.

Modeling of Stage 1

Modeling of Locking

- Equations of motion for Stage 1 motion (see Lecture 3)

$$\begin{pmatrix} [\mathbf{M}_{rr}] & [\mathbf{M}_{rf}]^T \\ [\mathbf{M}_{rf}] & [\mathbf{M}_{ff}] \end{pmatrix} \begin{pmatrix} \ddot{\mathbf{q}}_r \\ \ddot{\mathbf{q}}_f \end{pmatrix} + \begin{pmatrix} \mathbf{C}_r(\mathbf{q}, \dot{\mathbf{q}}) \\ \mathbf{C}_f(\mathbf{q}, \dot{\mathbf{q}}) \end{pmatrix} + \begin{pmatrix} [\mathbf{K}_j] & \mathbf{0} \\ \mathbf{0} & [\mathbf{K}_f] \end{pmatrix} \begin{pmatrix} \mathbf{q}_r \\ \mathbf{q}_f \end{pmatrix} = \begin{pmatrix} \tau \\ \mathbf{0} \end{pmatrix}$$

  Note: the gravity term is not present, the stiffness due to torsional springs is $[\mathbf{K}_j]$ and τ is due to the rocker-arm force.
- After θ_2 rotates by π (CW direction), the joint locks $\rightarrow$ 2R system changes to 1R system.
- Initial conditions for motion just after locking (Stage 2 motion) obtained using *momentum balance*.
- Assumptions:
  - Time duration of impact during locking is neglected.
  - Generalised coordinates before and after locking is same $\rightarrow$ $\mathbf{q}_+ = \mathbf{q}_-$
  - Velocities are bounded during impact.

- Momentum balance equation, with **H** denoting generalised impulse,

$$[\mathbf{M}(\mathbf{q})]\Delta\dot{\mathbf{q}} = \mathbf{H}$$

- The velocity after locking is $\dot{\mathbf{q}}_+ = \dot{\mathbf{q}}_- + \Delta\dot{\mathbf{q}}, \quad \dot{\theta}_{2+} = 0$
- Momentum balance, for this case, is given by (see Nagaraj et al. 1997)

$$\begin{pmatrix} M_{rr_{11}} & M_{rf_{11}} & \ldots & M_{rf_{14}} & 0 \\ M_{rr_{21}} & M_{rf_{21}} & \ldots & M_{rf_{24}} & -1 \\ M_{rf_{11}} & M_{ff_{11}} & \ldots & M_{ff_{14}} & 0 \\ .. & .. & \ldots & .. & .. \\ M_{rf_{14}} & M_{ff_{41}} & \ldots & M_{ff_{44}} & 0 \end{pmatrix} \begin{pmatrix} \Delta\dot{\theta}_1 \\ \Delta\dot{q}_{11} \\ .. \\ .. \\ .. \\ H_1 \end{pmatrix} = \dot{\theta}_{2-} \begin{pmatrix} M_{rr_{12}} \\ M_{rr_{22}} \\ M_{rf_{21}} \\ .. \\ .. \\ M_{rf_{24}} \end{pmatrix}$$

where H_1 is the impulse acting on joint 2 and $M_{rf_{ij}}$ is computed assuming 2 elements in each link.

- The velocities after locking are

$$\dot{\theta}_{1+} = \dot{\theta}_{1-} + \Delta\dot{\theta}_1, \quad \dot{\mathbf{q}}_{f+} = \dot{\mathbf{q}}_{f-} + \Delta\dot{\mathbf{q}}_f$$

Modeling of Stage 1

Modeling of Locking (contd.)

- Momentum balance equation, with **H** denoting generalised impulse,

$$[\mathbf{M}(\mathbf{q})]\Delta\dot{\mathbf{q}} = \mathbf{H}$$

- The velocity after locking is $\dot{\mathbf{q}}_+ = \dot{\mathbf{q}}_- + \Delta\dot{\mathbf{q}}, \quad \dot{\theta}_{2+} = 0$
- Momentum balance, for this case, is given by (see Nagaraj et al. 1997)

$$\begin{pmatrix} M_{rr_{11}} & M_{rf_{11}} & \ldots & M_{rf_{14}} & 0 \\ M_{rr_{21}} & M_{rf_{21}} & \ldots & M_{rf_{24}} & -1 \\ M_{rf_{11}} & M_{ff_{11}} & \ldots & M_{ff_{14}} & 0 \\ .. & .. & \ldots & .. & .. \\ M_{rf_{14}} & M_{ff_{41}} & \ldots & M_{ff_{44}} & 0 \end{pmatrix} \begin{pmatrix} \Delta\dot{\theta}_1 \\ \Delta\dot{q}_{11} \\ .. \\ .. \\ .. \\ H_1 \end{pmatrix} = \dot{\theta}_{2-} \begin{pmatrix} M_{rr_{12}} \\ M_{rr_{22}} \\ M_{rf_{21}} \\ .. \\ .. \\ M_{rf_{24}} \end{pmatrix}$$

where H_1 is the impulse acting on joint 2 and $M_{rf_{ij}}$ is computed assuming 2 elements in each link.
- The velocities after locking are

$$\dot{\theta}_{1+} = \dot{\theta}_{1-} + \Delta\dot{\theta}_1, \quad \dot{\mathbf{q}}_{f+} = \dot{\mathbf{q}}_{f-} + \Delta\dot{\mathbf{q}}_f$$

- Momentum balance equation, with **H** denoting generalised impulse,

$$[\mathbf{M}(\mathbf{q})]\Delta\dot{\mathbf{q}} = \mathbf{H}$$

- The velocity after locking is $\dot{\mathbf{q}}_+ = \dot{\mathbf{q}}_- + \Delta\dot{\mathbf{q}}, \quad \dot{\theta}_{2+} = 0$
- Momentum balance, for this case, is given by (see Nagaraj et al. 1997)

$$\begin{pmatrix} M_{rr_{11}} & M_{rf_{11}} & \ldots & M_{rf_{14}} & 0 \\ M_{rr_{21}} & M_{rf_{21}} & \ldots & M_{rf_{24}} & -1 \\ M_{rf_{11}} & M_{ff_{11}} & \ldots & M_{ff_{14}} & 0 \\ .. & .. & \ldots & .. & .. \\ M_{rf_{14}} & M_{ff_{41}} & \ldots & M_{ff_{44}} & 0 \end{pmatrix} \begin{pmatrix} \Delta\dot{\theta}_1 \\ \Delta\dot{q}_{11} \\ .. \\ .. \\ .. \\ H_1 \end{pmatrix} = \dot{\theta}_{2-} \begin{pmatrix} M_{rr_{12}} \\ M_{rr_{22}} \\ M_{rf_{21}} \\ .. \\ .. \\ M_{rf_{24}} \end{pmatrix}$$

where H_1 is the impulse acting on joint 2 and $M_{rf_{ij}}$ is computed assuming 2 elements in each link.

- The velocities after locking are

$$\dot{\theta}_{1+} = \dot{\theta}_{1-} + \Delta\dot{\theta}_1, \quad \dot{\mathbf{q}}_{f+} = \dot{\mathbf{q}}_{f-} + \Delta\dot{\mathbf{q}}_f$$

- Momentum balance equation, with **H** denoting generalised impulse,

$$[\mathbf{M}(\mathbf{q})]\Delta\dot{\mathbf{q}} = \mathbf{H}$$

- The velocity after locking is $\dot{\mathbf{q}}_+ = \dot{\mathbf{q}}_- + \Delta\dot{\mathbf{q}}, \quad \dot{\theta}_{2+} = 0$
- Momentum balance, for this case, is given by (see Nagaraj et al. 1997)

$$\begin{pmatrix} M_{rr_{11}} & M_{rf_{11}} & \dots & M_{rf_{14}} & 0 \\ M_{rr_{21}} & M_{rf_{21}} & \dots & M_{rf_{24}} & -1 \\ M_{rf_{11}} & M_{ff_{11}} & \dots & M_{ff_{14}} & 0 \\ .. & .. & \dots & .. & .. \\ M_{rf_{14}} & M_{ff_{41}} & \dots & M_{ff_{44}} & 0 \end{pmatrix} \begin{pmatrix} \Delta\dot{\theta}_1 \\ \Delta\dot{q}_{11} \\ .. \\ .. \\ .. \\ H_1 \end{pmatrix} = \dot{\theta}_{2-} \begin{pmatrix} M_{rr_{12}} \\ M_{rr_{22}} \\ M_{rf_{21}} \\ .. \\ .. \\ M_{rf_{24}} \end{pmatrix}$$

where H_1 is the impulse acting on joint 2 and $M_{rf_{ij}}$ is computed assuming 2 elements in each link.

- The velocities after locking are

$$\dot{\theta}_{1+} = \dot{\theta}_{1-} + \Delta\dot{\theta}_1, \quad \dot{\mathbf{q}}_{f+} = \dot{\mathbf{q}}_{f-} + \Delta\dot{\mathbf{q}}_f$$

Modeling of Stage 2

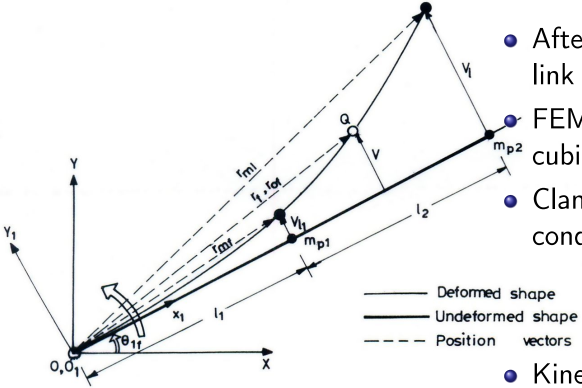

Figure 25: Flexible 1R system in Stage 2

- After locking at joint 2, single link flexible manipulator.
- FEM approach with Hermite cubic shape functions.
- Clamped-mass boundary conditions.
- Kinetic energy from link, revolute joint and payload at end of link 1 and link 2.
- Potential energy from strain energy and torsion spring.
- Torque due to rocker arm in the locking mechanism.
- Dynamic equations of motion obtained using Lagrangian formulation.

Modeling of Stage 2 (Contd.)

- Equations of motion are (see Lecture 3)

$$\begin{pmatrix} M_{rr} & [\mathbf{M}_{rf}]^T \\ [\mathbf{M}_{rf}] & [\mathbf{M}_{ff}] \end{pmatrix} \begin{pmatrix} \ddot{q}_r \\ \ddot{\mathbf{q}}_f \end{pmatrix} + \begin{pmatrix} C_r(\mathbf{q}, \dot{\mathbf{q}}) \\ \mathbf{C}_f(\mathbf{q}, \dot{\mathbf{q}}) \end{pmatrix}$$

$$+ \begin{pmatrix} K_j & \mathbf{0} \\ \mathbf{0} & [\mathbf{K}_f] \end{pmatrix} \begin{pmatrix} q_r \\ \mathbf{q}_f \end{pmatrix} = \begin{pmatrix} \tau \\ \mathbf{0} \end{pmatrix}$$

- Only one rigid body equation and scalar joint spring stiffness.
- $\mathbf{q}_f \in \Re^{2(n_1+n_2)}$, n_1 and n_2 are number of element in link 1 and 2 (both chosen equal to 2 in simulations).
- Displacement and slope at first element is set to zero.
- At $\theta_1 = \pi/2$, the first joint locks.
- After locking, system becomes a vibrating cantilever.

MODELING OF STAGE 2 (CONTD.)

- Equations of motion are (see Lecture 3)

$$\begin{pmatrix} M_{rr} & [\mathbf{M}_{rf}]^T \\ [\mathbf{M}_{rf}] & [\mathbf{M}_{ff}] \end{pmatrix} \begin{pmatrix} \ddot{q}_r \\ \ddot{\mathbf{q}}_f \end{pmatrix} + \begin{pmatrix} C_r(\mathbf{q}, \dot{\mathbf{q}}) \\ \mathbf{C}_f(\mathbf{q}, \dot{\mathbf{q}}) \end{pmatrix}$$

$$+ \begin{pmatrix} K_j & \mathbf{0} \\ \mathbf{0} & [\mathbf{K}_f] \end{pmatrix} \begin{pmatrix} q_r \\ \mathbf{q}_f \end{pmatrix} = \begin{pmatrix} \tau \\ \mathbf{0} \end{pmatrix}$$

- Only one rigid body equation and scalar joint spring stiffness.
- $\mathbf{q}_f \in \Re^{2(n_1+n_2)}$, n_1 and n_2 are number of element in link 1 and 2 (both chosen equal to 2 in simulations).
- Displacement and slope at first element is set to zero.
- At $\theta_1 = \pi/2$, the first joint locks.
- After locking, system becomes a vibrating cantilever.

Modeling of Stage 2 (Contd.)

- Equations of motion are (see Lecture 3)

$$\begin{pmatrix} M_{rr} & [\mathbf{M}_{rf}]^T \\ [\mathbf{M}_{rf}] & [\mathbf{M}_{ff}] \end{pmatrix} \begin{pmatrix} \ddot{q}_r \\ \ddot{\mathbf{q}}_f \end{pmatrix} + \begin{pmatrix} C_r(\mathbf{q}, \dot{\mathbf{q}}) \\ \mathbf{C}_f(\mathbf{q}, \dot{\mathbf{q}}) \end{pmatrix}$$
$$+ \begin{pmatrix} K_j & \mathbf{0} \\ \mathbf{0} & [\mathbf{K}_f] \end{pmatrix} \begin{pmatrix} q_r \\ \mathbf{q}_f \end{pmatrix} = \begin{pmatrix} \tau \\ \mathbf{0} \end{pmatrix}$$

- Only one rigid body equation and scalar joint spring stiffness.
- $\mathbf{q}_f \in \Re^{2(n_1+n_2)}$, n_1 and n_2 are number of element in link 1 and 2 (both chosen equal to 2 in simulations).
- Displacement and slope at first element is set to zero.
- At $\theta_1 = \pi/2$, the first joint locks.
- After locking, system becomes a vibrating cantilever.

Modeling of Stage 2 (contd.)

- Equations of motion are (see Lecture 3)

$$\begin{pmatrix} M_{rr} & [\mathbf{M}_{rf}]^T \\ [\mathbf{M}_{rf}] & [\mathbf{M}_{ff}] \end{pmatrix} \begin{pmatrix} \ddot{q}_r \\ \ddot{\mathbf{q}}_f \end{pmatrix} + \begin{pmatrix} C_r(\mathbf{q},\dot{\mathbf{q}}) \\ \mathbf{C}_f(\mathbf{q},\dot{\mathbf{q}}) \end{pmatrix}$$
$$+ \begin{pmatrix} K_j & \mathbf{0} \\ \mathbf{0} & [\mathbf{K}_f] \end{pmatrix} \begin{pmatrix} q_r \\ \mathbf{q}_f \end{pmatrix} = \begin{pmatrix} \tau \\ \mathbf{0} \end{pmatrix}$$

- Only one rigid body equation and scalar joint spring stiffness.
- $\mathbf{q}_f \in \Re^{2(n_1+n_2)}$, n_1 and n_2 are number of element in link 1 and 2 (both chosen equal to 2 in simulations).
- Displacement and slope at first element is set to zero.
- At $\theta_1 = \pi/2$, the first joint locks.
- After locking, system becomes a vibrating cantilever.

Modeling of Stage 2 (contd.)

- Equations of motion are (see Lecture 3)

$$\begin{pmatrix} M_{rr} & [\mathbf{M}_{rf}]^T \\ [\mathbf{M}_{rf}] & [\mathbf{M}_{ff}] \end{pmatrix} \begin{pmatrix} \ddot{q}_r \\ \ddot{\mathbf{q}}_f \end{pmatrix} + \begin{pmatrix} C_r(\mathbf{q}, \dot{\mathbf{q}}) \\ \mathbf{C}_f(\mathbf{q}, \dot{\mathbf{q}}) \end{pmatrix}$$

$$+ \begin{pmatrix} K_j & \mathbf{0} \\ \mathbf{0} & [\mathbf{K}_f] \end{pmatrix} \begin{pmatrix} q_r \\ \mathbf{q}_f \end{pmatrix} = \begin{pmatrix} \tau \\ \mathbf{0} \end{pmatrix}$$

- Only one rigid body equation and scalar joint spring stiffness.
- $\mathbf{q}_f \in \Re^{2(n_1+n_2)}$, n_1 and n_2 are number of element in link 1 and 2 (both chosen equal to 2 in simulations).
- Displacement and slope at first element is set to zero.
- At $\theta_1 = \pi/2$, the first joint locks.
- After locking, system becomes a vibrating cantilever.

- Equations of motion are (see Lecture 3)

$$\begin{pmatrix} M_{rr} & [\mathbf{M}_{rf}]^T \\ [\mathbf{M}_{rf}] & [\mathbf{M}_{ff}] \end{pmatrix} \begin{pmatrix} \ddot{q}_r \\ \ddot{\mathbf{q}}_f \end{pmatrix} + \begin{pmatrix} C_r(\mathbf{q}, \dot{\mathbf{q}}) \\ \mathbf{C}_f(\mathbf{q}, \dot{\mathbf{q}}) \end{pmatrix}$$
$$+ \begin{pmatrix} K_j & \mathbf{0} \\ \mathbf{0} & [\mathbf{K}_f] \end{pmatrix} \begin{pmatrix} q_r \\ \mathbf{q}_f \end{pmatrix} = \begin{pmatrix} \tau \\ \mathbf{0} \end{pmatrix}$$

- Only one rigid body equation and scalar joint spring stiffness.
- $\mathbf{q}_f \in \Re^{2(n_1+n_2)}$, n_1 and n_2 are number of element in link 1 and 2 (both chosen equal to 2 in simulations).
- Displacement and slope at first element is set to zero.
- At $\theta_1 = \pi/2$, the first joint locks.
- After locking, system becomes a vibrating cantilever.

Modeling of Stage 3

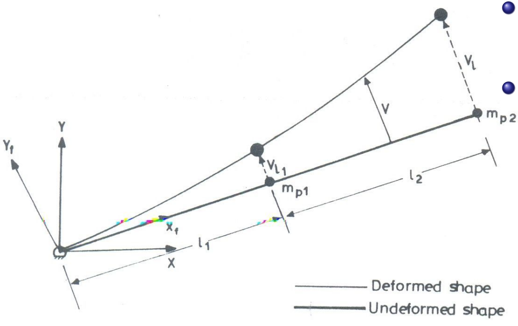

Figure 26: Vibrating flexible cantilever

- FEM with clamped-mass boundary conditions.
- Equations of motion

$$[\mathbf{M}_c]\ddot{\mathbf{q}}_f + [\mathbf{K}_c]\mathbf{q}_f = \mathbf{0}$$

  $[\mathbf{M}_c]$ and $[\mathbf{K}_c]$ are the mass and stiffness matrix and $\mathbf{q}_f$ are the flexible variables for the cantilever.
- $\dot{\theta}_{1+} = 0$.
- Velocity after locking $\dot{\mathbf{q}}_{f+} = \dot{\mathbf{q}}_{f-} + \Delta\dot{\mathbf{q}}_{f-}$, and $\Delta\dot{\mathbf{q}}_{f-}$ is obtained from

$$\begin{pmatrix} M_{rf_{11}} & .. & M_{rf_{14}} & -1 \\ & [M_{ff}] & & \mathbf{0}^T \end{pmatrix} \begin{pmatrix} \Delta\dot{\mathbf{q}}_{f-} \\ H_2 \end{pmatrix} = \dot{\theta}_{1-} \begin{pmatrix} M_{rr_{11}} \\ M_{rf_{11}} \\ .. \\ M_{rf_{14}} \end{pmatrix}$$

H_2 is the impulse acting at joint 1.

- Parameters of link 1 (from hardware)
  - Length $= 1.006423$ m
  - X-section $= 1.78076\ 10^{-4}\ \mathrm{m}^2$
  - Thickness $= 4.4519\ 10^{-3}$ m
  - Flexural Rigidity $EI = 20.5879\ \mathrm{N}-\mathrm{m}^2$
  - Link mass $= 0.52334$ Kg
  - Spring stiffness $= 0.0789\ \mathrm{N\ m/rad}$
- Parameters of link 2 (from hardware)
  - Length $= 0.9945$ m
  - X-section $= 1.77748\ 10^{-4}\ \mathrm{m}^2$
  - Thickness $= 4.437\ 10^{-3}$ m
  - Flexural Rigidity $EI = 20.3819\ \mathrm{N}-\mathrm{m}^2$
  - Link mass $= 0.42958$ Kg
  - Spring stiffness $= 0.0789\ \mathrm{N\ m/rad}$

Numerical Simulation

Rigid Body Simulation

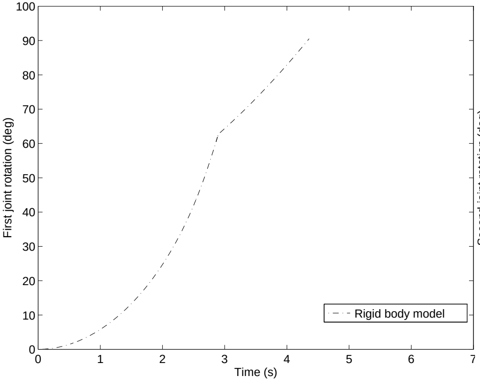

Figure 27: Motion of joint 1

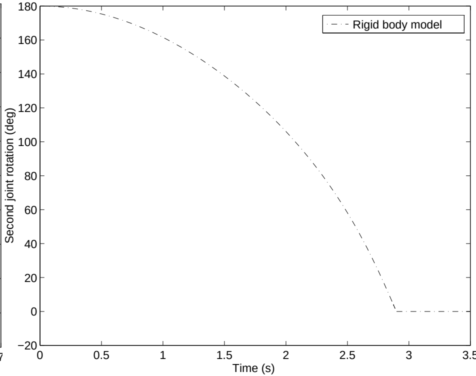

Figure 28: Motion of joint 2

- Time to first lock – 2.898 sec
- Time to second lock – 4.38 sec

Numerical Simulation

Flexible Link Simulation - Joint Motion

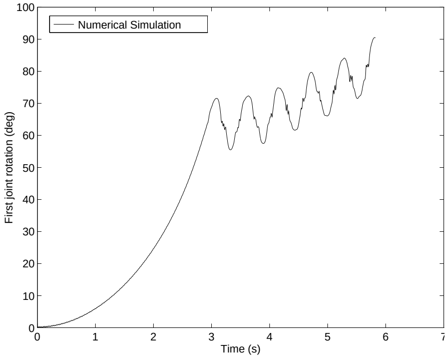

Figure 29: Motion of joint 1

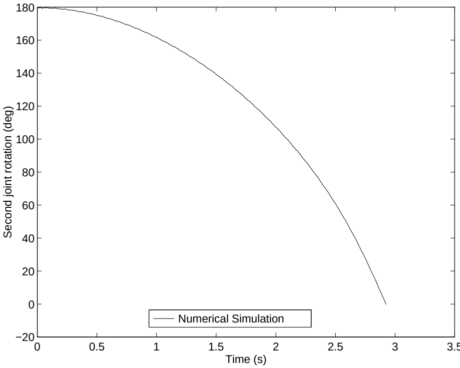

Figure 30: Motion of joint 2

- Time to first lock – 2.923 sec
- Time to second lock – 5.78 sec

Numerical Simulation

Flexible Link Simulation – Strains

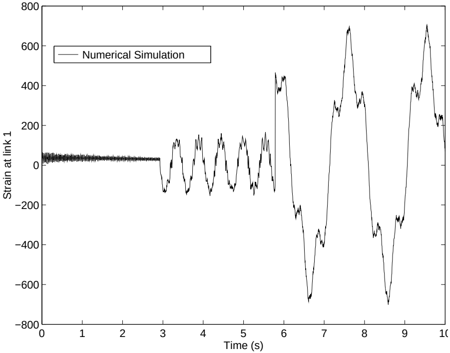

Figure 31: Strain at a location near base of link 1

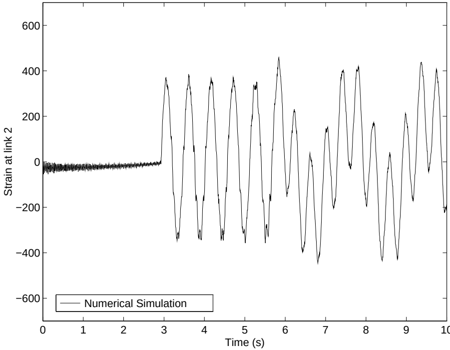

Figure 32: Strain at location near base of link 2

- Maximum strain (Stage 1): link 1 and link 2 $< 50\mu$-strains.
- Maximum strain (Stage 2): link 1 $\approx$ 150 & link 2 $\approx$ 400 μ-strains.
- Maximum strain (Stage 3): link 1 $\approx$ 700 & link 2 $\approx$ 400 μ-strains.

Experimental Set-up

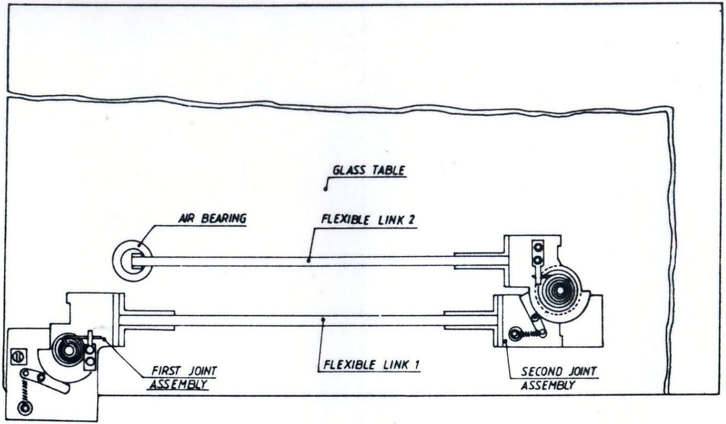

Figure 33: Experimental set-up for planar 2R motion studies

- Flexible Aluminum beams floating on air bearings on a horizontal glass table and actuated by two springs.
- Locking mechanism to lock after deployment.
- Instrumented to measure rotation and strain.

Experimental Set-up

First-joint Assembly

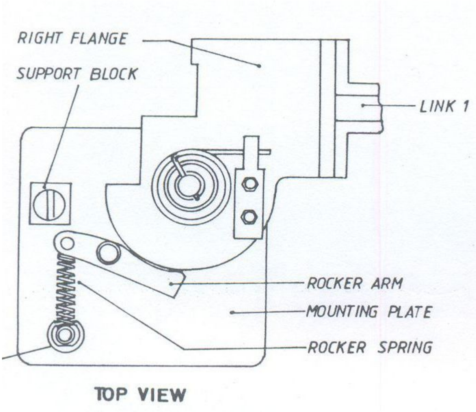

Figure 34: First joint assembly at initial configuration

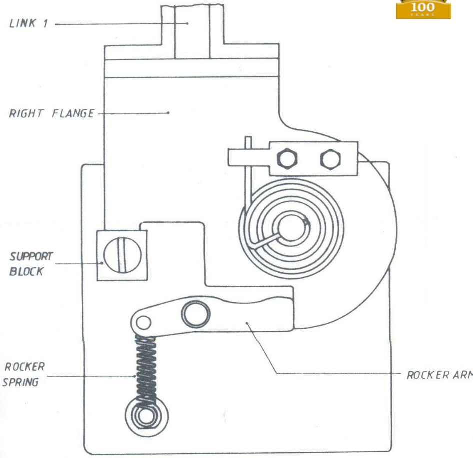

Figure 35: First joint assembly at locked configuration

- Rocker arm moves on cam and pressed by a spring.
- At $\theta_1 = \pi/2$, the joint 1 is locked.

Experimental Set-up

Instrumentation

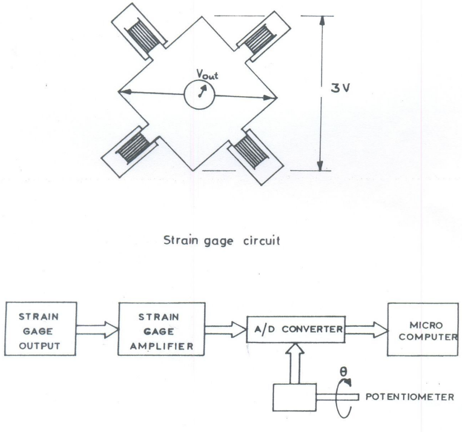

Figure 36: Instrumentation to measure rotation and strain

- Potentiometer measures joint rotation.
- Strain gages used to measure strains near the base of the links.
- All readings stored on a PC.

EXPERIMENTAL HARDWARE

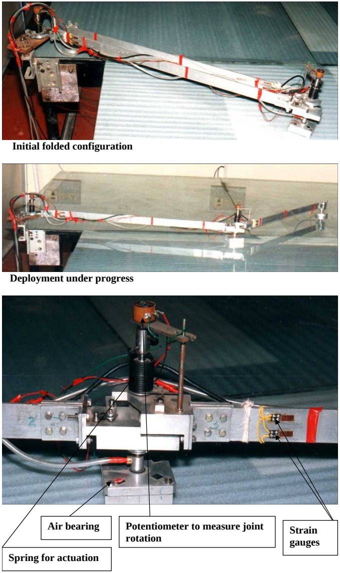

Figure 37: Experimental set-up for planar 2R motion studies

EXPERIMENTAL RESULTS

JOINT ROTATION

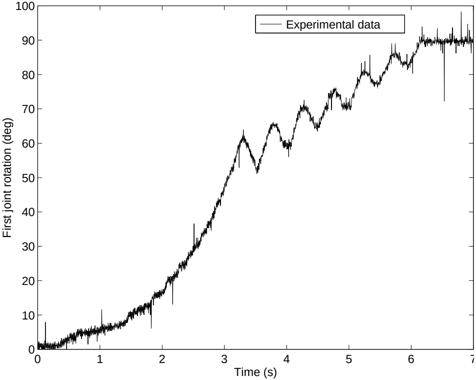

Figure 38: Rotation at joint 1 in Stage 1 and Stage 2

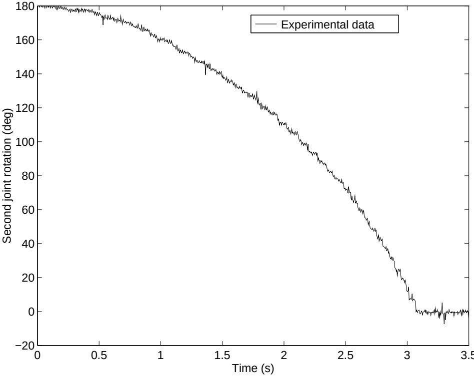

Figure 39: Rotation at joint 2

- Time to first lock – 3.07 sec
- Time to second lock – 6.13 sec

Experimental Results

Strain in Link 1 and 2

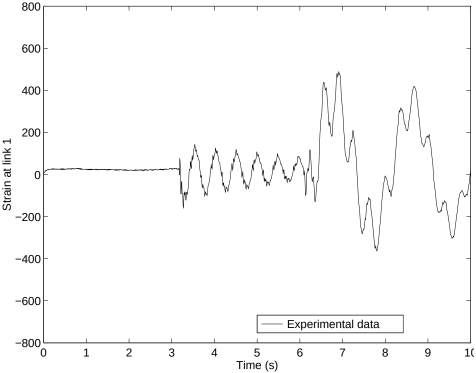

Figure 40: Strain measurement in link 1

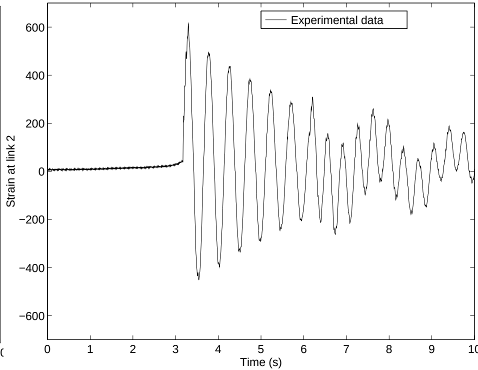

Figure 41: Strain measurement in link 2

- Maximum strain (Stage 1): link 1 and link 2 $< 50\ \mu$-strains
- Maximum strain (Stage 2): link 1 ≈ 150 and link 2 $\approx 600\ \mu$-strains.
- Maximum strain (Stage 3): link 1 ≈ 500 and link 2 $\approx 300\ \mu$-strains.

Comparison of experimental and numerical simulation

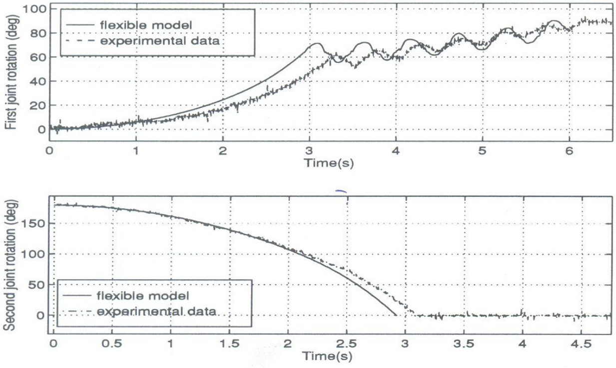

Figure 42: Comparison of joint rotations

- Time for first locking – 2.92 sec(computed) Vs. 3.07 sec(measured).
- Time for second locking – 5.87 sec(computed) Vs. 6.13 sec(measured).

Comparison of experimental and numerical simulation

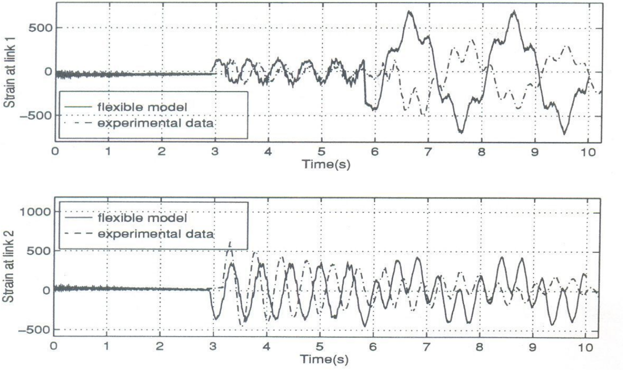

Figure 43: Comparison of strains near base of links

- Simulation $\approx$ 700 μ-strains Vs. experimental $\approx$ 500 μ-strains .
- Simulation $\approx$ 400 μ-strain Vs. experimental $\approx$ 600 μ-strains.
- Frequency after first lock: 1.95 Hz – good agreement with simulation.
- Two frequencies after second lock: 0.39 Hz and 2.73 Hz (simulation) Vs. 0.49 Hz and 2.93 Hz (experiments).

SUMMARY

- Modeling of 2 link flexible system mimicking deployment of a two element solar panel under zero gravity environment.
- Three stage motion – Stage 1: two link flexible, Stage 2: One link flexible system and Stage 3: Vibrating cantilever.
- Numerical simulation results based on finite element modeling of flexible multi-link manipulators.
- Modeling of locking to determine initial conditions in different stages of motion.
- Experimental hardware and results.
- Experimental results match reasonably well – time for locking is underestimated due to un-modeled friction.

Summary

- Modeling of 2 link flexible system mimicking deployment of a two element solar panel under zero gravity environment.
- Three stage motion – Stage 1: two link flexible, Stage 2: One link flexible system and Stage 3: Vibrating cantilever.
- Numerical simulation results based on finite element modeling of flexible multi-link manipulators.
- Modeling of locking to determine initial conditions in different stages of motion.
- Experimental hardware and results.
- Experimental results match reasonably well – time for locking is underestimated due to un-modeled friction.

SUMMARY

- Modeling of 2 link flexible system mimicking deployment of a two element solar panel under zero gravity environment.
- Three stage motion – Stage 1: two link flexible, Stage 2: One link flexible system and Stage 3: Vibrating cantilever.
- Numerical simulation results based on finite element modeling of flexible multi-link manipulators.
- Modeling of locking to determine initial conditions in different stages of motion.
- Experimental hardware and results.
- Experimental results match reasonably well – time for locking is underestimated due to un-modeled friction.

SUMMARY

- Modeling of 2 link flexible system mimicking deployment of a two element solar panel under zero gravity environment.
- Three stage motion – Stage 1: two link flexible, Stage 2: One link flexible system and Stage 3: Vibrating cantilever.
- Numerical simulation results based on finite element modeling of flexible multi-link manipulators.
- Modeling of locking to determine initial conditions in different stages of motion.
- Experimental hardware and results.
- Experimental results match reasonably well – time for locking is underestimated due to un-modeled friction.

SUMMARY

- Modeling of 2 link flexible system mimicking deployment of a two element solar panel under zero gravity environment.
- Three stage motion – Stage 1: two link flexible, Stage 2: One link flexible system and Stage 3: Vibrating cantilever.
- Numerical simulation results based on finite element modeling of flexible multi-link manipulators.
- Modeling of locking to determine initial conditions in different stages of motion.
- Experimental hardware and results.
- Experimental results match reasonably well – time for locking is underestimated due to un-modeled friction.

Summary

- Modeling of 2 link flexible system mimicking deployment of a two element solar panel under zero gravity environment.
- Three stage motion – Stage 1: two link flexible, Stage 2: One link flexible system and Stage 3: Vibrating cantilever.
- Numerical simulation results based on finite element modeling of flexible multi-link manipulators.
- Modeling of locking to determine initial conditions in different stages of motion.
- Experimental hardware and results.
- Experimental results match reasonably well – time for locking is underestimated due to un-modeled friction.

OUTLINE

1 CONTENTS

2 LECTURE 1
- Flexible Manipulators

3 LECTURE 2*
- Kinematic Modeling of Flexible Link Manipulators

4 LECTURE 3*
- Dynamic Modeling of Flexible Link Manipulators
- Control of Flexible Link Manipulators

5 LECTURE 4
- Experiments with a Planar Two Link Flexible System

6 MODULE 8 – ADDITIONAL MATERIAL
- Problems, References and Suggested Reading

Module 8 – Additional Material

- Exercise Problems
- References & Suggested Reading